EXPERIMENTAL STUDIES OF MERCURY OXIDATION BY ANAEROBIC BACTERIA

by

MATTHEW JORDAN COLOMBO

A dissertation submitted to the

Graduate School-New Brunswick

Rutgers, The State University of New Jersey

In partial fulfillment of the requirements

For the degree of

Doctor of Philosophy

Graduate Program in Environmental Sciences

Written under the direction of

Dr. Nathan Yee

And approved by

_____

_____

_____

_____

New Brunswick, New Jersey

October 2013

ABSTRACT OF THE DISSERTATION

Experimental Studies of Mercury Oxidation by Anaerobic Bacteria

By MATTHEW JORDAN COLOMBO

Dissertation Director:

Dr. Nathan Yee

Mercury is a toxic element with complex biogeochemistry. Bacteria influence mercury fate and transport in the environment by contributing to mercury sorption, reduction, and methylation. While these biogeochemical reactions have been well studied, the role of bacteria in mercury oxidation is poorly understood. In this dissertation, the oxidation of elemental mercury by anaerobic bacteria is documented in detail.

The oxidation and methylation of elemental mercury by *Desulfovibrio desulfuricans* ND132 is described in Chapter 2. Bulk chemical analyses, derivatization reactions, and X-ray absorption spectroscopy showed that *D. desulfuricans* ND132 oxidized elemental mercury to divalent mercury and produced methylmercury when provided with elemental mercury as its sole mercury source. X-ray absorption spectroscopy demonstrated that the majority of cell-associated mercury was oxidized and covalently bound to organic sulfur. This work reveals previously unrecognized

mercury transformations by anaerobic bacteria that may be important in anoxic aquatic settings.

Other phylogenetically and metabolically diverse anaerobic bacteria were then investigated for their mercury oxidation abilities in Chapter 3. *Geothrix fermentans* H5, *Shewanella oneidensis* MR-1, and *Cupriavidus metallidurans* AE104 all oxidized elemental mercury to divalent mercury. Heat-inactivation of the cells did not diminish mercury oxidation ability, indicating that the bacteria do not have to be metabolically active to oxidize mercury. X-ray absorption spectroscopy also revealed that oxidized mercury was bound to cellular thiol groups. The results of this study suggest that mercury oxidation may be widespread among bacteria and be mediated by a passive cellular mechanism.

Chapter 4 presents preliminary data demonstrating the fractionation of mercury stable isotopes during microbial mercury oxidation, in which the light isotopes preferentially accumulate in the oxidized product. Fractionation appeared to be mass dependent since no odd isotope anomalies or deviations from theoretical fractionation laws were observed. The data, considered in light of past experimental and theoretical work, suggests that isotope fractionation was the result of a kinetic isotope effect. This study provides initial insight into isotope fractionation during mercury oxidation and guides future efforts to detect this reaction in the environment.

ACKNOWLEDGEMENTS

This dissertation would not have been possible without the guidance and support of my advisor, Dr. Nathan Yee. I remember coming to his office for the first time four years ago, and can see how much I have grown as a scientist and a person since then. His passion for science and concern for my success have been inspiring and kept me going over the years. I would also like to thank the other members of my dissertation committee: Dr. Tamar Barkay, Dr. John Reinfelder, and Dr. Juyoung Ha for their guidance, helpful discussions, and co-authorship of the published and submitted chapters of this dissertation. I am thankful to Dr. Juyoung Ha for her companionship on trips to the Advanced Photon Source and for performing analysis on the X-ray absorption spectroscopy data in this dissertation. I also thank Dr. Tom Johnson and Gideon Bartov from UIUC for helpful discussions regarding mercury isotopes and Gideon for performing the mercury stable isotope analysis in Chapter 4.

I have several institutions to thank for funding my research and my life: the U.S. Department of Energy for funding my research project and one year of graduate assistantship, the Graduate School of New Brunswick for the Albert Fellows Fellowship, and the U.S. Department of Education for providing me with two years of GAANN fellowship support. Integral to the completion of this dissertation was the use of GeoSoilEnviroCARS at the Advanced Photon Source. This beamline is supported by the National Science Foundation and the Department of Energy, and use of the Advanced Photon Source was supported by the Department of Energy.

A big thank you to my lab mates Madhavi Parikh and Joanne Theisen. Madhavi patiently taught me microbiological techniques and how to be a good graduate student – without her I would not have had a companion in the lab to see the clock strike midnight on many nights. I also thank Thomas Wang for his comic relief and his helping hand(s). Thank you to the Reinfelder lab: Sarah, Laura, UD, and Phil for sharing in the ups and downs of mercury research and for their friendship. To all of my other colleagues and friends from Rutgers: Jeff, Amanda, Sarah W., Adam, Chu-Ching and Kritee.

Without the core support provided by my family and loving girlfriend, Lindsay, I would not have completed this work. I dedicate this work to them, for their unconditional support and encouragement, and always telling me to aim high.

TABLE OF CONTENTS

Abstract of the Dissertation ii

Acknowledgements iv

List of Figures viii

List of Tables x

Chapter 1 – Introduction 1

Chapter 2 – Anaerobic Oxidation of Hg(0) and Methylmercury Formation by *Desulfovibrio desulfuricans* ND132 13

Abstract 13

Introduction 15

Methods 19

Results and Discussion 26

Chapter 3 – Oxidation of Hg(0) to Hg(II) by Diverse Anaerobic Bacteria 50

Abstract 50

Introduction 52

Materials and Methods 55

Results 60

Discussion 64

Chapter 4 – A Preliminary Investigation of Hg Stable Isotope Fractionation During Hg(0) Oxidation by an Anaerobic Bacterium 77

Abstract 77

Introduction 78

Theory 80

Methods 82

Results 85

Discussion 87

Chapter 5 – Conclusion 103

References 110

LIST OF FIGURES

Figure 1.1. Rayleigh fractionation (solid black lines) and closed-system equilibrium (dotted lines) models 12

Figure 2.1. Loss of volatile Hg(0) and formation of non-purgeable Hg during Hg(0) reaction with *D. desulfuricans* ND132 cells 38

Figure 2.2. Gas-chromatography CVAFS analysis of ethylated non-purgeable Hg 39

Figure 2.3. Formation of non-purgeable Hg by *D. desulfuricans* ND132 in constant Hg(0) source experiments 40

Figure 2.4. Retention of Hg by *G. sulfurreducens* PCA 41

Figure 2.5. Hg L_{III}-edge XANES spectroscopic analysis of Hg(0)-reacted *D. desulfuricans* ND132 cells 42

Figure 2.6. MeHg production from Hg(0) 43

Figure 3.1. Non-purgeable Hg produced by bacterial cells exposed to 24.5 ± 0.5 ng of Hg(0) 68

Figure 3.2. Gas chromatography CVAFS analysis of ethylated non-purgeable Hg in bacterial suspensions 69

Figure 3.3. Non-purgeable Hg produced by metabolically active cultures exposed to a constant source of Hg(0) 70

Figure 3.4. Formation of non-purgeable Hg by heat-inactivated cells exposed to a constant source of Hg(0) for 2 h 72

Figure 3.5. Hg L_{III}-edge XANES spectroscopic analysis of Hg(0)-reacted bacterial cells ... 74

Figure 4.1. Formation of non-purgeable Hg by *D. desulfuricans* ND132 97

Figure 4.2. Concentration of Hg(0) in solution due to dissolution and sampling 98

Figure 4.3. Mass dependence of isotope fractionation 99

Figure 4.4. Non-purgeable δ^{202}Hg data with superimposed models 100

LIST OF TABLES

Table 2.1. Production of non-purgeable Hg and Hg methylation by *D. desulfuricans* ND132 45

Table 2.2. Hg L_{III}-edge first inflection points (E_1), second inflection points (E_2), and separations (ΔE) in model compounds and bacterial samples showing oxidation of Hg(0) to Hg(II) and the covalent character of the Hg-ligand bond in our samples 46

Table 2.3. Percent composition of mercury species in bacterial samples as determined by linear combination fitting of Hg L_{III}-edge XANES spectra (First Derivative)..... 47

Table 2.4. MeHg concentrations in sterile medium controls..... 48

Table 2.5. Standard potentials for the Hg(II)/Hg(0) and other relevant redox couples... 49

Table 3.1. Formation of non-purgeable Hg from Hg(0) by bacterial cell suspensions..... 75

Table 3.2. First inflection points (E_1), second inflection points (E_2), and separations (ΔE) in first derivatives of Hg L_{III}-edge XANES spectra of bacterial samples and reference compounds 76

Table 4.1. δ^{202}Hg of aqueous Hg(0) during dissolution and sampling..... 101

Table 4.2. δ^{202}Hg of non-purgeable Hg produced by *D. desulfuricans* ND132 102

CHAPTER 1

INTRODUCTION

Mercury (Hg) is a toxic element with no known biological benefits, and public health crises in Japan (Harada, 1995) and Iraq (Skerfving and Copplestone, 1976) have demonstrated the catastrophic effects that Hg can have on humans. In these incidents, thousands of people died or were severely impaired from eating mercury-contaminated aquatic organisms (Japan) and grain (Iraq). These tragedies highlighted the seriousness of Hg as a local, point source pollutant. However, elevated concentrations of Hg have also been detected in pristine settings, and evidence suggests that the atmospheric transport of mercury causes it to be a truly global pollutant (Fitzgerald et al., 1998). As a result of environmental exposures and recognition of the extent of Hg pollution, the biogeochemistry of mercury has been heavily studied for over half a century.

The three main chemical forms of mercury in aquatic systems are elemental mercury [Hg(0)], divalent mercury [Hg(II)], and methylmercury [MeHg]. Hg(0) is generally present as a volatile, dissolved gas in aquatic environments and thought to be relatively inert (Morel et al., 1998). In contrast, Hg(II) sorbs onto mineral surfaces (Lockwood and Chen, 1974; Newton et al., 1976) and organic matter (Xia et al., 1999) and reacts with sulfide to precipitate $HgS_{(s)}$ (Morel et al., 1998). Certain Hg(II) complexes are also available to anaerobic bacteria for conversion to MeHg (Hsu-Kim et al., 2013). Due to its efficient trophic transfer (Mason et al., 1995), organic MeHg biomagnifies in

the food chain and thus is concentrated in aquatic organisms that may be consumed by humans. Since the chemical form of Hg dramatically affects the element's fate and transport, an understanding of the transformation of Hg between its inorganic/organic forms and redox states in aquatic systems is critical.

The net reaction of inorganic Hg(II) methlyation and MeHg demethylation is an important control on the accumulation of MeHg in the environment (Lin et al., 2011). Methylation and demethylation processes are well studied due to human health impacts resulting from the bioaccumulative properties of MeHg. The reduction of Hg(II) and oxidation of Hg(0) also play a significant role in mercury biogeochemistry, with Hg(II) formation processes increasing the pool of mercury available for methylation and retarding Hg transport in groundwater. While the reduction of Hg(II) (particularly by bacteria (Barkay et al., 2003)) has been studied extensively, the agents of Hg(0) oxidation in the environment are poorly understood. This is particularly true in dark, anoxic environments, and the oxidation of Hg(0) to Hg(II) by anaerobic bacteria has never been demonstrated. Therefore, a key reaction may be missing from current mercury biogeochemical models, especially due to the presence of Hg(0) in many aquatic settings.

Occurrence and Production of Elemental Mercury in Aquatic Environments

Generally, elemental mercury exists in water as a dissolved gas with concentrations in the femtomolar to picomolar range (Amyot et al., 2000; Andersson et al., 2008). These aqueous concentrations are generated by the atmospheric

transport/exchange of Hg(0) (Lin and Pehkonen, 1999) and the reduction of atmospherically deposited or geologically derived Hg(II) (Fitzgerald et al., 1998; Amyot et al., 2000). Though Hg(0) usually exists in the environment at low concentrations, it has been detected at elevated concentrations in contaminated environments. For example, potable groundwater in New Jersey, USA has been shown to contain ~0.1 micromolar levels of Hg(0) (Murphy et al., 1994). The waters of East Fork Poplar Creek in Oak Ridge, Tennessee (USA) harbor similar levels of dissolved Hg(0) resulting from liquid elemental mercury deposits in the creek bed (Brooks and Southworth, 2011).

In aquatic systems where mercury enters predominantly as Hg(II), both biotic and abiotic factors cause Hg(0) formation. In oxic environments, mercury reduction by aerobic bacteria is perhaps the most studied mechanism of Hg(II) conversion to Hg(0). Some bacteria are mercury resistant due to the presence of the *mer* operon in their genomes, which is a genetic system that produces proteins specific for Hg(II) reduction to Hg(0) (Barkay et al., 2003). However, the *mer* operon is induced by nanomolar Hg concentrations and thus may only play a significant role in contaminated environments. At lower concentrations, MeHg and Hg(II) can be photoreduced to Hg(0) in the presence of light (Amyot et al., 1994; Amyot et al., 1997; Bergquist and Blum, 2007). Mercury demethylation by bacteria using the *mer* system can also produce Hg(0) (Spangler et al., 1973; Schaefer et al., 2004).

Elemental mercury may enter anoxic groundwater via transport from oxic surface water (Barringer et al., 2013), but can also be generated directly in these settings. In anoxic environments, Hg(II) can be reduced biotically by constitutively

produced enzymes in metal-reducing bacteria (Wiatrowski et al., 2006). Hg(0) can also be formed in anoxic environments by chemical reaction of Hg(II) with humic acids (Skogerboe and Wilson, 1981) and iron minerals (Charlet et al., 2002; Wiatrowski et al., 2009). The reduction of Hg(II) by dissolved organic matter depends strongly on the dissolved organic matter / Hg ratio (Gu et al., 2011).

Since water is typically supersaturated with Hg(0) with respect to atmospheric concentrations (Fitzgerald et al., 2007), the formation of elemental mercury has been thought to greatly reduce the concentration of reactive mercury in the aqueous phase through volatilization (Fitzgerald et al., 1991). However, studies examining the oxidation of elemental mercury suggest that this redox reaction may be an underappreciated process modulating the concentrations of Hg(0) in aquatic systems.

The Oxidation of Elemental Mercury

Agents oxidizing Hg(0) to Hg(II) in oxic environments include sunlight, dissolved ligands, and bacteria. Sunlight has been shown to play an important role in dissolved Hg(0) oxidation in fresh and marine surface waters (Amyot et al., 1997; Amyot et al., 2000; Lalonde et al., 2001; Lalonde et al., 2004). Chloride and thiol compounds in the presence of oxygen oxidize beads of liquid Hg(0) in water (Demagalhaes and Tubino, 1995; Yamamoto et al., 1995; Yamamoto, 1996; Amyot et al., 2005). Smith *et al.* (1998) showed that *E. coli* oxidized dissolved Hg(0) in proportion to its production of the catalase enzyme KatG. Siciliano *et al.* (2002) also discovered a positive correlation between the loss of dissolved gaseous Hg(0) and catalase activity in two lakes,

suggesting the role of bacteria in Hg(0) oxidation. However, the soil bacterium *Streptomyces venezuelae* also produced a high concentration of Hg(II), but exhibited far less catalase activity than *E. coli* (Smith et al., 1998). Furthermore, Poulain *et al.* (2007) showed that the exudates of marine algae can oxidize Hg(0). These studies demonstrate that there are other mechanisms leading to Hg oxidation by microbes that should be further explored.

The oxidation of Hg(0) in anoxic environments is poorly understood. Recent studies have demonstrated that dissolved organic matter can complex (Gu et al., 2011) and oxidize (Zheng et al., 2012) Hg(0). The authors of these studies implicate the thiol functional groups of dissolved organic matter in the oxidation reaction. The biological contributions to mercury oxidation under anoxic conditions are unknown, and the oxidation of Hg(0) by anaerobic bacteria has never been demonstrated. The overall objective of this dissertation is to study this oxidation reaction in detail.

In Chapter 2, we test if the model mercury-methylating bacterium *Desulfovibrio desulfuricans* ND132 (Gilmour et al., 2011) can oxidize dissolved Hg(0). The oxidation of elemental mercury in anoxic environments is particularly important since it produces Hg(II) complexes which are substrates for methylation by certain anaerobic bacteria (Compeau and Bartha, 1985; Fleming et al., 2006; Kerin et al., 2006; Parks et al., 2013). However, our picture of the chemical species of Hg that are bioavailable to methylating bacteria is still incomplete (Hsu-Kim et al., 2013). Currently, dissolved neutral complexes of Hg(II) are thought be the most prevalent bioavailable forms of Hg (Barkay et al., 1997; Benoit et al., 1999; Benoit et al., 2001; Drott et al., 2007). Schaefer and Morel (2009)

also demonstrated that the Hg-cysteine complex enhances mercury methylation by *Geobacter sulfurreducens* PCA. The role of nanoparticulate HgS in MeHg production is a relatively new finding (Zhang et al., 2012). Although Hg(0) is also a neutral form of mercury, its availability to anaerobic bacteria for redox and methylation reactions has not been tested. Thus, by selecting *D. desulfuricans* ND132, we seek to test if a single bacterial strain can produce MeHg when provided with Hg(0) as its sole mercury source.

In order to demonstrate the formation of oxidized Hg(II) in this study, Hg L_{III}-edge X-ray Absorption Near Edge Structure (XANES) spectroscopy is employed. Though XANES spectroscopy has been around for half a century, its use in the study of environmentally relevant Hg-containing materials has developed more recently, used initially to study the binding of Hg in soil humic matter (Xia et al., 1999). X-ray absorption spectroscopy has also been used to determine the speciation of Hg in swordfish (Harris et al., 2003) and water hyacinths (Rajan et al., 2008), and to examine the sorption of Hg(II) to various minerals (Kim et al., 2004; Brigatti et al., 2005). Recently, Mishra *et al.* (2011) used XANES to examine the speciation of Hg bound to bacterial cells following Hg(II) reduction to Hg(0). Similar to Mishra *et al.*, we use XANES spectra to determine if Hg(0) has been oxidized to Hg(II).

Once the oxidation of Hg(0) to Hg(II) is examined in one bacterium, we then test the abilities of diverse anaerobic bacteria to oxidize Hg(0) in Chapter 3. *Geothrix fermentans* H5, *Shewanella oneidensis* MR-1, and *Cupriavidus metallidurans* AE104 are selected due to their distinct metabolic capabilities and their isolation from diverse environments. If these bacteria can also oxidize Hg(0), the likelihood of Hg(0) oxidation

by bacteria occurring in the environment will increase. Currently, Hg(0) oxidation by bacteria is known only to be the result of an enzymatic process requiring active cells (Smith et al., 1998). In our study, we test the oxidation of Hg(0) by resting and heat-killed cells. Since hypoxic/anoxic environments can be nutrient poor and inhabited by slowly metabolizing bacteria, Hg(0) oxidation by inactive cells has important implications for our understanding of the role of bacteria in subsurface mercury redox processes.

The combination of XANES spectroscopy and testing live/dead cells for their Hg(0) reactivity in Chapters 2 and 3 also allows us to probe the mechanism of Hg(0) oxidation by anaerobic bacteria. XANES spectroscopy has been used in many past studies to examine the bonding environment of Hg (Xia et al., 1999; Harris et al., 2003; Rajan et al., 2008; Mishra et al., 2011). Examination of bonding environment may allow us to infer information about the oxidation mechanism. Mercury oxidation could be mediated by an enzymatic process in anaerobic bacteria as observed by Smith *et al.* (1998) for aerobic bacteria. However, if inactive, heat-treated cells can oxidize Hg(0), a passive, non-enzymatic process is responsible for Hg(0) oxidation. Oxidation by inactive cells would be unsurprising since the thiol moieties of reduced natural organic matter have been implicated in Hg(0) oxidation (Gu et al., 2011; Zheng et al., 2012). Bacterial cells consist of and contain molecules with reduced thiol functional groups (Morris et al., 1984; Fahey, 2001; Joe-Wong et al., 2012). Thus, a similar mechanism to oxidation by natural organic matter could occur with bacterial cells.

While Chapters 2 and 3 may establish that anaerobic bacteria can oxidize mercury in pure culture, the application of these findings to the environment would still

be quite limited. The objective of the last research chapter of this dissertation (Chapter 4) is to investigate mercury stable isotope fractionation during Hg(0) oxidation by *D. desulfuricans* ND132. These laboratory experiments provide a basis for tracking Hg(0) oxidation in the environment.

Mercury Stable Isotope Fractionation

Mercury has seven stable isotopes: Hg^{196}, Hg^{198}, Hg^{199}, Hg^{200}, Hg^{201}, Hg^{202}, and Hg^{204}. Mercury stable Isotope fractionation is the name given to the varying Hg stable isotope ratios in different chemical pools of Hg due to biogeochemical processes (Hoefs, 2009). Since differences in isotope ratios are small, especially with heavier elements like Hg, isotope ratios are reported as deviations from a standard in delta notation, with the ratio of ^{202}Hg to ^{198}Hg being the accepted reporting ratio (Blum and Bergquist, 2007):

$$\delta^{202}Hg = \frac{(^{202}Hg/^{198}Hg_{sample} - {}^{202}Hg/^{198}Hg_{standard})}{^{202}Hg/^{198}Hg_{standard}} \times 1000\ ‰$$

Determining the underlying isotope effects causing isotope fractionation in laboratory studies is important to applying the results of these studies to environmental observations. The causes of mass dependent stable isotope fractionation are generally divided into two categories: kinetic isotope effects and equilibrium isotope effects (Hoefs, 2009). The theory of kinetic isotope effects predicts that the lighter isotopes of an element will react faster than the heavier isotopes of that element in a chemical reaction. This behavior is due to the weaker element-ligand bonds of the lighter isotopes relative to corresponding bonds of the heavier isotopes (Bigeleisen and

Wolfsberg, 1958). For example, the mercury-chloride bonds in $^{198}HgCl_2$ are weaker than those in $^{202}HgCl_2$. A kinetic effect can be deciphered only when the reactant and product do not interact, i.e. if the reaction is unidirectional. In such a scenario, plotting the δ values of the reactant and product against the fraction of reactant remaining should result in a Rayleigh fractionation model similar to the one shown in solid black lines in Figure 1.1. This model has been drawn using an initial reactant with δ = -0.63‰ and a constant isotopic separation between reactant and product of 1.5‰ using forms of the Rayleigh equations similar to those in Hoefs (2009). The instantaneous product curve is a theoretical curve that can be approximated experimentally by collecting product in small, discrete intervals (Kritee et al., 2007). The cumulative product curve is fit experimentally by a bulk measurement of the product from the start of the reaction to the time of sampling. Data that fit a Rayleigh fractionation model typically indicate that a kinetic effect was responsible for observed isotope fractionation (Johnson et al., 2004).

In contrast, equilibrium isotope effects are driven not by differences in reaction rate between different isotopes, but instead by an intrinsic distribution of isotopes between the two chemical or physical forms of the element being reacted (Bigeleisen and Mayer, 1947; Urey, 1947). Therefore, this effect occurs only when the product and reactant are left in contact to allow for isotopic equilibration. If the δ values of the reactant and product are plotted against the fraction of product remaining in this closed system setup, two parallel lines should evolve as in Figure 1.1 (Johnson et al., 2004). Heavier isotopes of an element tend to accumulate in the reservoir with the relatively

stronger bond to the element under an equilibrium scenario (Schauble, 2004). In the case of redox reactions, the more oxidized phase tends to be enriched in the heavy isotopes relative to the reduced form. Therefore, for the schematic in Figure 1.1, if the oxidized form of an element with δ = -0.63‰ was reduced under conditions where isotopic equilbirum was maintained with the product, the δ values of the oxidized form should follow a line similar to the top dotted line whereas those for the reduced form would follow the bottom line. The distinction between equilbrium and kinetic effects in laboratory experiments is important to applying the findings of these experiments to the environment, where considerations of isotopic equilibrium must be taken into account.

Isotope fractionation during Hg redox reactions has been demonstrated in numerous studies of Hg(II) reduction. Kritee *et al.* (2007) determined the isotopic compositions of Hg(II) and Hg(0) during *mer*-dependent Hg(II) reduction in pure cultures and enrichments of natural samples. The resulting kinetic isotope effect was that product Hg(0) was enriched in the light isotope relative to reactant Hg(II). The same was shown to be true for microbes that reduce Hg(II) via different reaction pathways and degrade MeHg to Hg(0) (Kritee et al., 2008, 2009). Chemical reduction of Hg(II) by dissolved organic matter and stannous chloride has also been shown to induce similar isotope fractionation (Zheng and Hintelmann, 2010a). Photochemical Hg reduction has attracted much attention since it causes mass independent fractionation along with mass dependent fractionation (Bergquist and Blum, 2007; Zheng and Hintelmann, 2010b). No studies have been published that examine Hg fractionation during the

oxidation of Hg(0) to Hg(II). Without understanding and quantifying fractionation during mercury oxidation by anaerobic bacteria, our abilities to explain mercury biogeochemistry using stable isotope ratios in the environment are limited.

Summary: Study Goals and Objectives

While many redox transformations of mercury have been well studied, the oxidation of Hg(0) to Hg(II) by anaerobic bacteria has never been demonstrated. Therefore, a key reaction may be missing from current mercury biogeochemical models. The overall goal of this research was to examine Hg(0) oxidation by anaerobic bacteria under controlled laboratory conditions. Specific objectives for each chapter were to:

Chapter 2. Quantify the oxidation of Hg(0) by *D. desulfuricans* ND132, determine the chemical speciation of oxidized Hg, and quantify methylmercury produced from Hg(0).

Chapter 3. Examine the abilities of bacteria from different phyla and with diverse metabolic capabilities to oxidize Hg(0), determine the chemical speciation of oxidized Hg, and test whether oxidation occurs by an active or passive cellular mechanism.

Chapter 4. Investigate mercury stable isotope fractionation during Hg(0) oxidation by anaerobic bacteria.

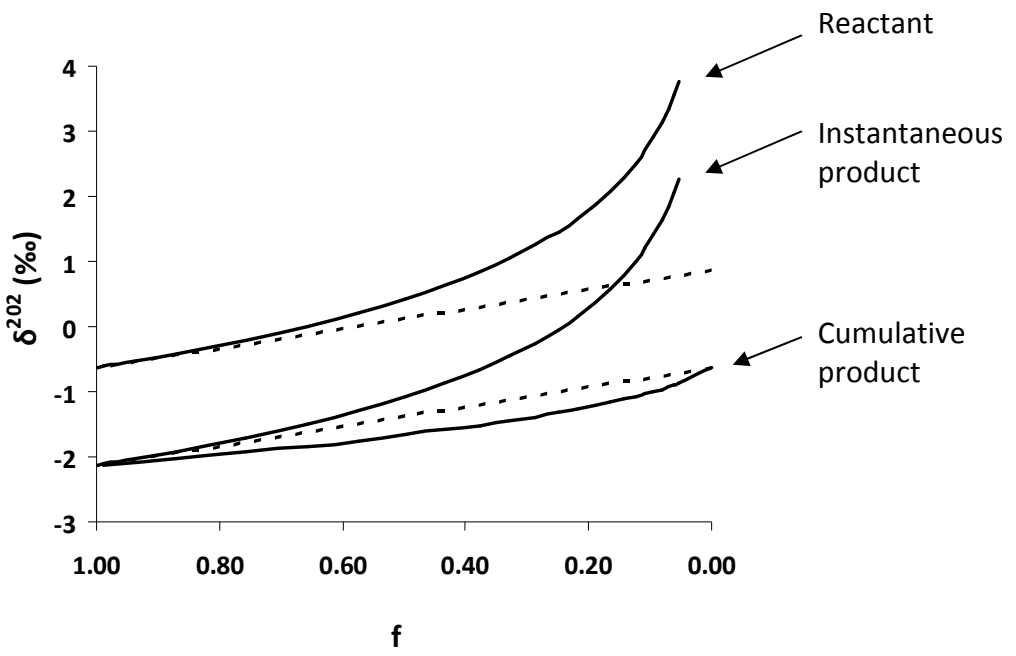

Figure 1.1. Rayleigh fractionation (solid black lines) and closed-system equilibrium (dotted lines) models. *f* is the fraction of reactant remaining in a given reaction.

CHAPTER 2

ANAEROBIC OXIDATION OF Hg(0) AND METHYLMERCURY FORMATION BY *Desulfovibrio desulfuricans* ND132

Published in *Geochimica et Cosmochimica Acta* (2013, 112:166-177)

ABSTRACT

The conversion of inorganic mercury (Hg) to methylmercury (MeHg) plays a key role in determining the amount of Hg that is bioaccumulated in aquatic food chains. An accurate knowledge of Hg methylation mechanisms is required to predict the conditions that promote MeHg production in the environment. In this study, we conducted experiments to examine the oxidation and methylation of dissolved elemental mercury [Hg(0)] by the anaerobic bacterium *Desulfovibrio desulfuricans* ND132. Anoxic cultures of *D. desulfuricans* ND132 were exposed to a constant source of Hg(0) in the dark, and samples were collected and analyzed for the formation of non-purgeable Hg and MeHg over time. We found that *D. desulfuricans* ND132 rapidly converted dissolved gaseous mercury into non-purgeable Hg, with bacterial cultures producing approximately 40 μg/L of non-purgeable Hg within 30 min, and as much as 800 μg/L of non-purgeable Hg after 36 h. Derivatization of the non-purgeable Hg in the cell suspensions to diethylmercury and analysis of Hg(0)-reacted *D. desulfuricans* ND132 cells using X-ray absorption near edge structure (XANES) spectroscopy demonstrated that cell-associated Hg was dominantly in the oxidized Hg(II) form. Spectral comparisons and linear

combination fitting of the XANES spectra indicated that the oxidized Hg(II) was covalently bonded to cellular thiol functional groups. MeHg analyses revealed that *D. desulfuricans* ND132 produced up to 118 µg/L of methylmercury after 36 h of incubation. We found that a major fraction of the methylated Hg was exported out of the cell and released into the culture medium. The results of this work demonstrate a previously unrecognized pathway in the mercury cycle, whereby anaerobic bacteria produce MeHg when provided with dissolved Hg(0) as their sole Hg source.

1. INTRODUCTION

Mercury (Hg) is a highly toxic element, and its concentration in the environment has risen significantly as a result of human activities (Selin, 2009). Anthropogenic sources of Hg typically enter the environment as inorganic mercury. Anaerobic microbial processes in anoxic sediments subsequently convert inorganic mercury into neurotoxic methylmercury (MeHg) (Compeau and Bartha, 1985; Gilmour et al., 1992). Because MeHg is bioaccumulated in fish, the transformation of inorganic Hg to MeHg is a critical step that governs the transfer of Hg to aquatic food webs and its biomagnification in higher trophic levels. In order to predict the fate and deleterious effects of mercury contaminants in the environment, a mechanistic understanding of MeHg production in aquatic ecosystems is required.

Dissolved elemental mercury [Hg(0)] is a ubiquitous form of inorganic mercury in marine and terrestrial water (Amyot et al., 2000; Andersson et al., 2008). Previous studies have shown that surface water (Siciliano et al., 2002; Poulain et al., 2007), soil (Zhang et al., 2001), and groundwater (Murphy et al., 1994; Walvoord et al., 2008) can accumulate high concentrations of Hg(0). The formation of Hg(0) in these environments primarily occurs by the reduction of mercuric Hg [Hg(II)], which is mediated by photoreactions with sunlight (Amyot et al., 1997), enzymatic reduction by mercury-resistant microorganisms (Barkay et al., 2003), and geochemical reactions with humic acids and mineral-associated ferrous iron (Skogerboe and Wilson, 1981; Charlet et al., 2002; Wiatrowski et al., 2009). In terrestrial settings, the loss of gaseous Hg(0) to the atmosphere from soils is an important process that decreases the amount of Hg

remaining in watersheds (Selvendiran et al., 2008). In saturated sediments where gas-exchange is restricted, Hg(0) can remain dissolved in water and be mobilized by groundwater advection. Hg(0) in groundwater has been found to discharge to drinking water wells (Murphy et al., 1994) and has been suggested to contribute to the unexpectedly low partition coefficient of Hg in confined aquifers due to its low affinity for sediment surfaces (Bone et al., 2007). Because Hg(0) is generally considered to be unreactive (Morel et al., 1998), its formation and transport are thought to limit the amount of Hg available for methylation (Fitzgerald et al., 1991). However, the uptake and methylation of Hg(0) by anaerobic bacteria have never been tested.

In aquatic environments, Hg(0) is oxidized to Hg(II) by both chemical and biological processes. In surficial waters exposed to sunlight, Hg(0) oxidation is controlled by photochemical reactions. Laboratory investigations of natural and artificial waters have shown that the oxidation of Hg(0) by solar UV-B radiation is linked to photochemically produced reactive compounds such as hydroxyl radicals (Lalonde et al., 2001, 2004). In the dark, Amyot et al. (1997) demonstrated that dissolved Hg(0) can also be oxidized by unfiltered seawater, with O_2 as the most likely oxidant. Furthermore, experimental studies have shown that drops of liquid Hg(0) in water can be rapidly oxidized in the presence of oxygen and chloride or thiol compounds (Demagalhaes and Tubino, 1995; Yamamoto et al., 1995; Yamamoto, 1996; Amyot et al., 2005).

The microbial oxidation of Hg(0) to Hg(II) is also known to occur. To date, aerobic and phototrophic microorganisms have been implicated as the primary microbial agents catalyzing Hg(0) oxidation reactions. Smith et al. (1998) showed that the catalase

enzymes in *Escherichia coli* can oxidize dissolved Hg(0) in water. The Hg(0) oxidation activity in *E. coli* was associated with the cytosolic catalase/hydroperoxidase proteins KatG and KatE. However, a double mutant lacking both the *katG* and *katE* genes retained the ability to oxidize Hg(0), suggesting the existence of other bacterial oxidation pathways that are currently uncharacterized. The aerobic soil bacteria *Bacillus* and *Streptomyces* exhibited high levels of Hg(0) oxidizing activity (Smith et al., 1998), illustrating the potential for microbial oxidation in the cycling of Hg in soils. In a field study at Jack's Lake and Lake Ontario, Siciliano et al. (2002) showed that a strong correlation exists between microbial Hg(0) oxidase activity and the decrease in dissolved elemental Hg concentrations in freshwater lakes. Experiments by Poulain et al. (2007) demonstrated that biogenic organic materials produced by marine algae can oxidize Hg(0). Currently, the subsurface microbial processes involved in Hg oxidation remain poorly understood, and the ability of anaerobic microorganisms to oxidize Hg(0) has not been explored.

Anaerobic bacteria play a central role in the Hg biogeochemical cycle through their catalysis of Hg methylation. Laboratory and field studies have shown that bacterial uptake of neutral Hg(II) species is an important control on the methylation process (Barkay et al., 1997; Benoit et al., 1999, 2001; Drott et al., 2007). Neutral Hg(II) complexes do not adsorb onto negatively charged bacterial cell walls, and can passively diffuse across the cell membrane into the cytoplasm. Benoit et al. (1999, 2001) proposed that dissolved mercuric sulfide [$HgS^0(aq)$] is a substrate for Hg methylation by sulfate-reducing bacteria in sulfidic sediments. Recently, Schaefer and Morel (2009)

showed that the Hg(II)-cysteine$_2$ complex is an important form of Hg for methylation in iron-reducing bacteria, and that the uptake of these Hg(II)-thiol complexes occurs by active cellular transport (Schaefer et al., 2011). Although Hg(0) is a neutral form of dissolved mercury, little is known about the interactions of anaerobic methylating bacteria with Hg(0). If dissolved Hg(0) can be converted to MeHg, then an important MeHg source may be missing in current Hg biogeochemistry models.

Previous studies have shown that X-ray Absorption Near Edge Structure (XANES) spectroscopy is a useful analytical method to determine the speciation of mercury in environmental and laboratory samples (Xia et al., 1999; Kim et al., 2004; Brigatti et al., 2005; Khwaja et al., 2006; Skyllberg et al., 2006). XANES spectroscopy has been employed successfully to identify the coordination of Hg to sulfhydryl, carboxyl, and amine groups in natural organic matter (NOM) (Xia et al., 1999; Skyllberg et al., 2006). Recently, Mishra et al. (2011) used XANES spectral analysis to demonstrate that mercury binding onto bacterial cells occurs via complexation to sulfhydryl and carboxyl functional groups in *Bacillus subtilis*, a gram positive bacterium known to sorb high concentrations of Hg(II) (Daughney et al., 2002). Other applications of Hg XANES spectroscopy in biological systems include analyses of mercury speciation in swordfish (Harris et al., 2003) and water hyacinth (Rajan et al., 2008).

In this study, we carried out Hg(0) oxidation and methylation experiments using the model anaerobic bacterium *Desulfovibrio desulfuricans* ND132. The objectives of this study were (1) to determine if anaerobic bacteria oxidize dissolved Hg(0) to non-purgeable Hg(II) and (2) to determine if anaerobic Hg-methylating bacteria produce

MeHg when provided with Hg(0) as their sole Hg source. We employed a combination of bulk chemical and XANES spectroscopic methods to investigate the anaerobic oxidation and methylation of Hg(0). The results of this work provide experimental evidence for a previously unrecognized pathway in the mercury cycle, whereby MeHg is produced from dissolved elemental mercury by anaerobic bacteria.

2. METHODS

2.1. Bacterial growth conditions. *D. desulfuricans* ND132 was grown under strict anaerobic conditions in a defined medium containing 10 mM MOPS, 1.5 mM KH_2PO_4, 4.7 mM NH_4Cl, 6.7 mM KCl, 3.2 mM $MgCl_2$, 1.4 mM $CaCl_2$, 257 mM NaCl, 10 mL/L Wolfe's vitamins (Balch et al., 1979), 5 mL/L Wolfe's minerals (contributing 75 µM sulfate as a sulfur source), and ~10 mM NaOH to adjust the pH to ~7.3. The medium was amended with 25 mM pyruvate as the electron donor and 30 mM fumarate as the electron acceptor, and deoxygenated by purging with ultra-high purity N_2 gas. Additional sulfate was not supplied to the medium to limit the formation of biogenic sulfide by this sulfate-reducing bacterium. All media were sealed with butyl rubber stoppers in acid-cleaned serum bottles and autoclaved. *D. desulfuricans* cultures were inoculated at a 1:10 (v:v) dilution of an active culture, incubated at 28°C, and grown to mid-exponential phase for experiments.

2.2. Hg(0) oxidation and methylation experiments. Cells were harvested by centrifugation at 10000 RPM for 7 min in anaerobic centrifuge tubes. After washing in

anoxic 0.5 mM phosphate buffer containing 1 mM NaCl, cells were resuspended in 20 mL of phosphate buffer. Cell suspensions were then transferred to 40 mL BrooksRand® MERX Total Hg certified autosampler bottles fitted with septum caps and wrapped in aluminum foil. A volume of Hg(0)-saturated N_2 gas containing a known amount was injected through the septum cap of the BrooksRand® vials. After the desired duration of reaction, the bottles were removed from the glove box and placed on the autosampler of a BrooksRand® MERX Total Mercury Analytical System. The remaining Hg(0) was quantified by purging samples directly through a BrooksRand® cold vapor atomic fluorescence spectroscopy (CVAFS) detector with Hg-free N_2 as a carrier gas. Samples were purged sequentially for 1 minute intervals until no further Hg(0) was detected (typically 4 to 5 rounds of purging). An aliquot of the purged sample was then collected, preserved with 5% bromine monochloride (BrCl), reduced with $SnCl_2$, and analyzed by CVAFS. A sample of non-purgeable Hg was also collected and used immediately for an ethylation experiment to directly measure the formation of Hg(II). Ethylation experiments were performed by adding sodium tetraethylborate to purged samples that were not oxidized with BrCl. Diethylmercury was then measured by gas chromatography CVAFS, as described below for methylmercury analysis.

Experiments were also carried out by reacting growing cultures of *D. desulfuricans* ND132 with a constant source of Hg(0) gas. In these experiments, Hg(0) gas was generated by placing a drop of liquid Hg(0) in an uncapped HPLC vial inside of a 30 mL serum bottle. Before the experiment, the volatilized Hg(0) gas was flushed several times by purging the bottles inside the antechamber of a Coy® glove box, and then the

serum bottle was capped with a butyl rubber stopper inside the glove box under 95% N_2 / 5% H_2. The redox potential of the chamber was monitored by Oxoid® anaerobic indicators to ensure anoxic conditions were maintained. The serum bottles were then wrapped in aluminum foil and the $Hg(0)_{(l)}$ was allowed to equilibrate with the gas phase for 24 h. The Hg(0) oxidation experiments were carried out with mid-exponential phase cultures (O.D.600 = 0.22±0.01). Reaction with Hg(0) was initiated by injecting 3 mL of either live cells, cell filtrates (mid-exponential phase culture passed through a 0.2 µm filter), or sterile medium into the serum bottle around the HPLC vial. One parent culture was used for the 0-4 h experiments, a second for the 8-24 h experiments, and five independent cultures were used to inoculate the 36 h reactors. The reactors were gently agitated at 31°C.

At periodic intervals, three independent bottles per time point were sacrificed for analysis of non-purgeable Hg. Approximately 2.5 mL of the cell suspension was removed from the reactor by needle and syringe, placed in an acid-cleaned I-Chem® vial, and then immediately purged with N_2 gas at 0.8 L/min for 5 minutes to remove the unreacted Hg(0). This method was validated by purging Hg(0)-reacted bacteria for progressively longer intervals until no further decline in Hg concentration was observed. For some samples, the N_2-purged suspensions were syringe-filtered through a 0.2 µm polycarbonate filter to determine the concentrations of non-purgeable Hg in the aqueous phase and associated with the cells. All samples were preserved with 1 mL of concentrated BrCl. For Hg analysis, samples were prepared by adding hydroxylamine hydrochloride to destroy excess free radicals. The concentration of Hg in samples was

then determined by $SnCl_2$ reduction and cold vapor atomic absorbance spectroscopy (CVAAS) using a Leeman Labs Hydra AA Mercury Analyzer.

Cell suspensions from the reactors were also collected for total, dissolved (0.2 µm filtered), and cell-associated MeHg analysis. MeHg was analyzed using distillation and ethylation-gas chromatography (Bloom, 1989; Horvat et al., 1993). Briefly, the samples were distilled with sulfuric acid, ammonium pyrrolidinedithiocarbamate (APDC), and potassium chloride followed by ethylation with sodium tetraethylborate. The MeHg derivative, methylethylmercury, was separated from other Hg species by isothermal gas chromatography, converted to Hg(0) by thermal decomposition, and analyzed by CVAFS using a Tekran 2500 detector. MeHg distillation recoveries ranged from 70% to 96% as determined by matrix spikes. The detection limit of this method was 10 pg per sample volume (0-24 h samples) or 50 pg per sample volume (36 h samples).

2.3. Cell density, microscopy, and sulfide analyses. In addition to non-purgeable Hg and MeHg analyses, aliquots from 36 h experiments were taken for more detailed analysis. Optical density (O.D. 600) was measured at the beginning and end of the incubation using a Shimadzu spectrophotometer. For epifluorescence microscopy, each 36 h sample was diluted 1:10 and stained with a LIVE/DEAD® *Bac*LightTM Bacterial Viability Kit provided by Life Technologies according to the manufacturer's instructions. Stained suspensions were vortexed and 5 µL was wet mounted on a slide and examined under the 100x oil immersion lens of a Zeiss Axioskop 20 microscope. Dissolved sulfide

was analyzed in samples passed through a 0.2 μm filter at the start of 36 h experiments by the Cline assay (Cline, 1969).

2.4. X-ray absorption spectroscopy. Hg(0)-reacted *D. desulfuricans* ND132 cells were analyzed using X-ray absorption near edge structure (XANES) spectroscopy. Cell pellets were collected by centrifuging N_2-purged cell suspensions at 10,000 RPM for 20 min. The pellets were shipped in sealed, deoxygenated containers wrapped in ice packs to Argonne National Laboratory (Illinois, USA) and analyzed at the Advanced Photon Source. Shipment of samples took 1 day, and the samples were stored at 4°C for 12-24 h at the synchrotron until analysis. Reference compounds included hydrated Hg^{2+}, Hg-cysteine$_2$, Hg-acetate, cinnabar (HgS), $HgCl_2$, CH_3Hg-acetate, CH_3Hg-glutamate, hydrated $CH3Hg^+$, and Hg(0). Hydrated Hg^{2+} and Hg-cysteine$_2$ standards were prepared using a 5 mM (1000 ppm) stock solution of $Hg(NO_3)_2$. All pH adjustments were made with HNO_3 or NaOH. Hydrated Hg^{2+} was prepared by adjusting the solution to pH 2. Hg-cysteine$_2$ was prepared by adding 0.6 mmol of cysteine to 7 mL of solution and adjusting to pH 5. The Hg-acetate standard was prepared by dissolving 40 mg of mercuric acetate powder in 4 mL of Milli-Q water and 0.25 mL glacial acetic acid and adjusting to pH 5. Cinnabar and $HgCl_2$ were analyzed in solid form. All methylmercury standards were prepared using 4 mL of a 5 mM (1000 ppm) stock solution of CH_3HgCl. CH_3Hg-acetate was prepared by adding 0.36 mmol of sodium acetate to solution and adjusting to pH 5. CH_3Hg-glutamate was prepared by adding 0.36 mmol of sodium glutamate to solution and adjusting to pH 5. Hydrated CH_3Hg^+ ion was prepared by adjusting the solution to

pH 3. Previous studies have shown that Hg(II) is reduced to Hg(0) via reaction with magnetite under anaerobic conditions (Wiatrowski et al., 2009; Mishra et al., 2011). Thus, we obtained our Hg(0) reference compound by reacting 100 mL of a 0.2 g/L anoxic magnetite suspension with Hg(II) at a Fe(II):Hg(II) molar ratio of 10 to 1. The reaction was carried out for 2 h at pH 7 in an aluminum foil-wrapped serum bottle. The suspension was centrifuged and the mineral pellet was collected for analysis.

Hg L_{III}-edge XANES spectra were collected at station 13BMD, GeoSoilEnviroCARS, which is a bending magnet station with Si(111) crystals and a 13 element Germanium detector. Standard operating conditions were 7-GeV machine energy and had a current typically around 100 mA during these measurements. Higher order harmonics were rejected by detuning the monochromator 30%. Cell pellet samples were placed between Kapton® tape and liquid standards were placed in SPEX® SamplePrep X-Cell cups for analysis. Spectra were collected at ambient temperature and pressure. Depending on signal-to-noise criteria, eighteen to twenty five spectra were collected and averaged for each sample, while three to four individual spectra were collected and averaged for each reference compound. Energy calibration was performed using $HgCl_2$ and assigning the first edge inflection point as 12284 eV. Each scan took 18 minutes to complete the collection of data. All the scans were measured from a single position on the sample during the experiments. The energy step size for XANES scans was 0.2 eV throughout the experiments. The pre-edge background of each averaged scan was subtracted, and the absorption coefficient was normalized to a unit-edge step. Although we cannot completely rule out the possibility of beam damage causing changes in the Hg XANES

spectra during the measurements, no significant shifts or changes were observed in the spectral features between the initial and last XANES measurement. Therefore, we expect that any beam damage that might have been present in our sample is likely to be insignificant.

The first derivative of the Hg L_{III}-edge XANES spectra were used for spectral comparisons and linear combination fittings. While the raw spectra of Hg L_{III}-edge XANES spectra often do not have distinctive spectral features, they generally have two large main peaks in their first derivative, due to transitions from the core level binding energy of the L_{III} electron to unoccupied orbitals mainly 6s and 6p in character. Therefore, comparing the first derivative of the Hg L_{III}-edge XANES spectra can provide significant clues to speciation. Spectra were analyzed using the SixPACK interface to IFEFFIT (Newville, 2001; Webb, 2005). For the linear combination fitting analysis, each sample spectrum was first sequentially fit with one model compound to find the best 1-component fit. A second reference compound was then systematically added to determine the 2-component fit that best explained the remaining variation. Finally, 3- and 4-component fits were tested until the residual values did not show any significant improvement in the fitting analysis. For each multi- component fit, a least squares fitting module was used to determine the percentages of all the model types in the unknown samples. Similar residual analysis has been conducted by others and successfully identified the best fits based on the comparison of residual values (Kim et al., 2000; Jew et al., 2011).

3. RESULTS AND DISCUSSION

3.1. Anaerobic oxidation of Hg(0) to Hg(II). A mass balance experiment was conducted to determine if the anaerobic bacterium *D. desulfuricans* ND132 forms non-purgeable Hg when reacted with a known amount of Hg(0). After 2.5 h of reaction with 1.7 ng of Hg(0), *D. desulfuricans* ND132 cells suspended in phosphate buffer produced 1.2 ± 0.1 ng of non-purgeable Hg, while 0.46 ± 0.04 ng of unreacted volatile Hg(0) was recovered by purging with N_2 gas (Figure 2.1). We also performed control experiments with the phosphate buffer in the absence of bacterial cells and allowed the buffer solution to react with Hg(0) for the same amount of time. In the controls, 1.68 ± 0.07 ng of Hg(0) was recovered from the phosphate buffer, and the concentration of non-purgeable Hg was below the detection limit. These data indicate that reaction of Hg(0) with *D. desulfuricans* ND132 results in the loss of volatile Hg(0) and formation of non-purgeable Hg.

To determine if the non-purgeable Hg formed by *D. desulfuricans* ND132 was Hg(II), we immediately ethylated the non-purgeable Hg samples using sodium tetraethylborate and analyzed the derivatized products for diethylmercury. Because tetraethylborate reacts specifically with Hg(II) to produce diethylmercury (Rapsomanikis et al., 1986), but does not react with Hg(0), the detection of diethylmercury in non-purgeable Hg samples is a direct indication of Hg(II) formation. The gas-chromatogram of ethylated non-purgeable Hg in the *D. desulfuricans* ND132 samples show a large peak at a retention time of 4 min, corresponding to diethylmercury (Figure 2.2). A negligible amount of diethylmercury was detected in the control experiments without cells. We

interpret the large peak for diethylmercury in the ethylated *D. desulfuricans* ND132 samples as strong evidence for the formation of Hg(II).

To investigate the chemical speciation of the oxidized Hg, *D. desulfuricans* ND132 cells were reacted with a constant Hg(0) source to attain sufficient Hg concentrations for XANES analysis. In these experiments, mid-exponential phase *D. desulfuricans* ND132 cultures growing in pyruvate media were exposed to a constant amount of Hg(0) (~70 μg/L). Quantification of the non-purgeable Hg indicated that *D. desulfuricans* ND132 reacts rapidly with Hg(0), with bacterial cultures producing ~40 μg/L of non-purgeable Hg within 30 min of exposure (Figure 2.3). The concentration of non-purgeable Hg increased with time, and a high degree of reproducibility was observed in triplicate experiments in the first 4 h. Uninoculated medium retained negligible amounts of Hg, indicating that the formation of non-purgeable Hg was biologically mediated. Reactions with extracellular compounds were not responsible for the observed Hg transformation, as the spent medium without cells also produced negligible amounts of non-purgeable Hg. After 36 h of incubation, active cultures formed as much as 800 μg/L of non-purgeable Hg (Table 2.1). By filtering Hg(0)-reacted cell suspensions at 4 h and 24 h of reaction through a 0.2 μm filter, we found that approximately 80% of the non-purgeable Hg was associated with *D. desulfuricans* ND132 cells. Experiments conducted with the anaerobic iron-reducing bacterium *Geobacter sulfurreducens* PCA showed that this bacterium also converts Hg(0) into non-purgeable Hg (Figure 2.4). About 90% of the non-purgeable Hg was associated with the *G. sulfurreducens* biomass in these experiments.

D. desulfuricans ND132 cells were collected after 30 min and 24 h of reaction time and examined using XANES spectroscopy. Hg L_{III}-edge XANES spectra of the bacterial samples and reference compounds displayed spectral characteristics that are related to the Hg coordination environment (Figure 2.5a). The XANES spectra for both 30 min and 24 h bacterial samples did not exhibit the pronounced pre-edge features observed in the Hg(II)-acetate, MeHg-acetate and MeHg-glutamate reference compounds, indicating that cell-associated Hg was not complexed to carboxyl functional groups. The aqueous Hg^{2+} reference compound spectrum displayed a distinctive peak at 12310 eV which was also absent in the *D. desulfuricans* ND132 spectra. Similarity between the XANES spectra of the bacterial samples and that of the Hg-$(cysteine)_2$ reference compound suggests that the Hg was associated with cells via coordination with thiol functional groups. Most markedly, the XANES spectra for both the Hg-$(cysteine)_2$ reference compound and bacterial samples lacked a pronounced pre-edge feature and exhibited very similar Hg L_{III}-edge positions. This Hg coordination environment is in agreement with the Hg-sulfhydryl complexation mechanism recently observed in the Gram positive bacterium *Bacillus subtilis* (Mishra et al., 2011).

The first derivative of the Hg L_{III}-edge XANES spectra for both samples exhibited two major peaks due to the transitions of the L_{III} electron from core level to unoccupied orbitals of 6s and 6p character (Figure 2.5b). Table 2.2 shows the first (E_1) and second (E_2) inflection points of the XANES spectra, which correspond to the two maximum points in the first derivative of the spectra. We used the position of the first edge inflection (E_1) as an indication of the Hg oxidation state and local coordination

environment (Aakesson et al., 1994; Huggins et al., 1998; Riddle et al., 2002; Rajan et al., 2008). The E_1 values for both 30 min and 24 h samples were positioned at 12,286.6 eV, whereas the E_1 value for the Hg(0) reference compound was 12,285.0 eV. The shift in the Hg L_{III}-edge to higher energies in the bacterial samples suggests that the non-purgeable Hg associated with *D. desulfuricans* ND132 was more oxidized than the elemental Hg. The first inflection point of the XANES spectra for bacterial samples closely resembled the E_1 values of Hg(II) complexed to cysteine and methylmercury compounds. Based on spectral comparisons of the bacterial samples with the reference compounds, we concluded that *D. desulfuricans* ND132 cells had oxidized the Hg(0) to Hg(II). Finally, we noted that the E_1 values did not change between the 30 min and 24 h samples, suggesting that oxidation of Hg(0) was rapid and had occurred within 30 min of reaction.

We used the spacing between the two main peaks (E_1 and E_2) in the first derivative of the XANES spectra to gain insight into the level of ionic or covalent bonding in the cell-associated mercury-ligand complex. For this spectral comparison, we calculated the ΔE value, which represents the difference in energy values between the first and second inflection points (Table 2.2). In general, larger ΔE values correspond to Hg-ligand complexes with ionic character whereas smaller ΔE values are found in complexes with covalent character (Powers, 1982; Huggins et al., 1998). The E_1 and the ΔE values presented in Table 2.2 agree well with previously reported studies (Riddle et al., 2002; Rajan et al., 2008), and the overall trend in the ΔE values for the reference compounds varied according to the expected increase in covalent character for Hg. For

example, the ΔE value of 7.2 eV for Hg(II)-cysteine$_2$ was significantly smaller than the value of 13.2 eV for the Hg(II)-acetate reference compound, thus indicating that the Hg–S bond was more covalent. Analyzing the first derivative of the *D. desulfuricans* ND132 XANES spectra, we found a ΔE value of 7.5 eV for the 30 min sample and 7.7 eV for the 24 h sample. These ΔE values suggest that the Hg associated with the cells was bonded to bacterial ligands via strong covalent bonds, consistent with coordination to sulfur atoms.

A linear combination fitting analysis of the XANES spectra was performed to quantify the Hg species in the *D. desulfuricans* ND132 samples. Hg(II)-cysteine$_2$ was the reference compound that provided the best 1-component fit (Table 2.3). For 2-component fitting, a linear combination using the Hg(II)-cysteine$_2$ and Hg(0) reference compounds resulted in the fit with the lowest residual values (Table 2.3). While a previous XANES study that quantified Hg(0) in mine wastes by a slow cooling crystallization process shows a different Hg(0) reference spectrum (Jew et al., 2011), our ambient temperature spectrum for elemental mercury closely resembles that of Mishra *et al.* (2011). Furthermore, our Hg(0)-magnetite spectrum lacks the edge features of Hg(II) sorbed to an iron oxyhydroxide (Al-Abed et al., 2008). This previous work, combined with the 1 eV downward shift of the edge position in our Hg(0) spectrum, indicates reduced Hg(0) in our reference compound. The best fit for both the 30 min and 24 h samples was obtained by modeling the XANES data using approximately 70% of Hg(II)-cysteine$_2$ and 30% of Hg(0). Adding an additional third component such as $HgCl_2$ or HgS did not improve the goodness of fit for either sample (see Table 2.3).

While we saw no spectroscopic evidence of HgS(s) formation in the solid phase, mercury-sulfide aqueous complexation likely occurred in solution. Approximately 20% of the Hg oxidized by *D. desulfuricans* ND132 did not associate with the cells, but instead accumulated in the dissolved phase. In the spent medium, we measured 40 to 75 µM dissolved sulfide. The high affinity of Hg(II) ions for dissolved sulfide species would have resulted in mercury-sulfide aqueous complexation. Although we found that the spent medium containing dissolved sulfide does not abiotically oxidize Hg(0) (Figure 2.3), aqueous complexation with sulfide in the presence of cells may promote microbial Hg(0) oxidation by removing oxidized Hg from the reactive sites on the cell surface. Thus, the ancillary aqueous geochemistry may play a role in affecting the rates and extent of microbial Hg(0) oxidation.

The mechanism of Hg(0) oxidation by *D. desulfuricans* ND132 remains poorly understood. While Hg(0) oxidation in aerobic bacteria has been linked to the oxidative stress proteins KatG and KatE (Smith et al., 1998), the mechanism of anaerobic Hg(0) oxidation is unknown. Inspection of the *G. sulfurreducens* PCA genome reveals a homolog of the *katG* gene, suggesting that cytosolic catalase-mediated Hg(0) oxidation in iron-reducing bacteria is possible. *D. desulfuricans* ND132 and many other obligate anaerobes do not carry such catalase/hydroperoxidase genes, suggesting that Hg(0) is being oxidized by an alternate mechanism in this organism. The absence of catalase/hydroperoxidase in *D. desulfuricans* ND132 is not surprising, as obligate anaerobes are generally not exposed to oxygen in their natural habitats and do not need to decompose damaging hydrogen peroxide by-products emitted by aerobic respiration.

Our XANES data provide evidence that the oxidized Hg is associated with cells via coordination with thiol functional groups, and it is possible that these functional groups may be involved in the formation of Hg(II) products. Recently, Gu et al. (2011) demonstrated that Hg(0) can complex with thiol groups in reduced humic acids and postulated that Hg(0) bound to organic matter becomes oxidized. Subsequently, these investigators showed that other thiol-bearing organic compounds such as glutathione can also bind and oxidize Hg(0) (Zheng et al., 2012). Interestingly, electron transfer from Hg(0) to the organic molecule occurs even though mercury is coordinated to a -SH functional group. This is somewhat surprising as sulfur in the –SH moiety is in its most reduced oxidation state. Previous potentiometric studies suggest that there is direct interaction between Hg(0) and reduced sulfur that may lead to oxidation (Cohen-Atiya and Mandler, 2003). We speculate that the reactive thiol functional groups in anaerobic bacteria, either in the cell wall or cytoplasm, may be involved in Hg(0) oxidation.

3.2. MeHg production from Hg(0). *D. desulfuricans* ND132 cells reacted with a constant source of Hg(0) were analyzed for MeHg production. MeHg analyses revealed that after 36 h of incubation, *D. desulfuricans* ND132 produced up to 118 μg/L of MeHg when provided with Hg(0) as the sole mercury source (Figure 2.6a). MeHg was not detected in the first 4 h of the experiment, even though significant Hg oxidation had already occurred (Table 2.1). The largest extent of methylation occurred at 24 and 36 h. This general trend was observed in independent replicate experiments. The concentrations of MeHg in uninoculated sterile controls were generally 100 times lower

than active cultures (Table 2.4). Although high MeHg concentrations were observed in most of the 24 and 36 h samples, 3 out of 10 independent replicate experiments did not show production of MeHg. Because of this variability, we performed a Mann-Whitney U-test to determine if MeHg production by *D. desulfuricans* ND132 was statistically significant. Using the 24 h and 36 h samples, we compared the MeHg concentrations in the sterile controls (Table 2.4) to the MeHg concentrations in the bacterial experiments (Table 2.1). The test statistic rejected the null hypothesis, and U-test results indicated that samples with *D. desulfuricans* ND132 have larger MeHg values than the sterile controls.

To better understand the microbial controls on MeHg production, we performed more detailed analyses on the bacterial samples collected at 36 h. Cell density measurements and epifluorescence microscopy showed that MeHg production was strongly correlated to microbial growth, and also possibly related to the aggregation state of the cells (Figure 2.6b and c). In samples where MeHg production was low (samples h2 and h5), the cells were not growing and predominately subsisted in a planktonic state. Conversely, in samples where MeHg production was high (samples h1, h3 and h4), significant growth was observed and cells were tightly aggregated in biofilm-like communities (Figure 2.6c). Statistically, MeHg production exhibited a linear relationship with cell density at the end of the 36 h incubation ($R^2 = 0.9669$) (Figure 2.6b). Furthermore, the relationship between cell aggregation and MeHg production is consistent with the results of (Lin and Jay, 2007), who demonstrated that *D. desulfuricans* biofilms produced an order of magnitude higher MeHg than planktonic

cultures. Interestingly, we found that when extremely high levels of non-purgeable Hg accumulated in the reactor, the cells did not grow and remained mostly planktonic, suggesting a possible toxicity effect. In both the 24 h and 36 h sample sets, reactors that contained high levels of non-purgeable Hg also showed no MeHg production (Table 2.1).

The experimental data indicate that there is a lag between Hg(0) oxidation and MeHg production by *D. desulfuricans* ND132. The delay in methylation after Hg(0) oxidation may suggest that the Hg methylation pathway in *D. desulfuricans* ND132 is activated only after cellular Hg reaches a threshold concentration, or alternatively, that the cell-associated Hg is unavailable for immediate methylation. Methylation is generally considered to be an intracellular process where Hg uptake into the cytoplasm is required for the methylation reaction to occur. The transfer of Hg into and within some bacterial cells is governed by thiol-containing molecules (Barkay et al., 2003), and our detection of molecular Hg-thiol structures in *D. desulfuricans* ND132 is consistent with Hg(II) uptake into the cell. Among sulfate-reducing bacteria that completely oxidize acetate into carbon dioxide, a cobalamin-containing methyltransferase protein in the acetyl-CoA pathway has been linked to Hg methylation (Choi et al., 1994; Ekstrom and Morel, 2008). However, *D. desulfuricans* ND132 is an incomplete oxidizer of carbon, and its Hg methylation mechanism occurs through an unknown biochemical process that is distinct and unrelated to the acetyl-CoA pathway (Ekstrom et al., 2003; Gilmour et al., 2011). The cellular reactions that catalyze Hg methylation in *D. desulfuricans* ND132, as well as the connection between Hg methylation and oxidation, merit further investigation.

While *D. desulfuricans* ND132 cells retained nearly all of the oxidized inorganic Hg, we found that that the bacterium excreted methylated Hg out of the cytoplasm. By filtering the active cultures incubated for 24 h, we found that a significant fraction of the methylated Hg was exported out of the cell and released into the dissolved phase. In three separate experiments, we recovered 17, 12, and 10 µg/L of MeHg in the filtrate of 0.2 µm filtered cell suspensions, corresponding to 50%, 43% and 87% of the total MeHg. This observation of cellular MeHg export by *D. desulfuricans* ND132 is in agreement with the recent reports by Schaefer et al. (2011) and Gilmour et al. (2011). The mechanisms and biological function of MeHg export are still poorly understood, but it is known that MeHg is more toxic to bacteria than inorganic Hg (Jonas et al., 1984). We note that *D. desulfuricans* ND132 lacks the *mer* operon that encodes for broad spectrum mercury resistance, and is therefore unable to degrade MeHg via the organomercury lyase pathway. As noted by Schaefer et al. (2011), the export of MeHg may be related to a detoxification mechanism, whereby the cell pumps cytosolic MeHg into the external environment to prevent intracellular accumulation of harmful MeHg. Indeed, efflux pumps that export toxic metals out of bacterial cells are common detoxification mechanisms in prokaryotes, and play an important role in microbe-metal interactions for many important elements, including As, Cd, Zn, and Co (Silver, 1996).

3.3. Environmental implications. In natural environments, anaerobic iron- and sulfate-reducing bacteria are expected to come into contact with Hg(0). Based on the reduction potential of their Hg(II)/Hg(0) redox couples, oxidized forms of Hg, such as

mercuric chloride [$HgCl_2$] and hydroxide [$Hg(OH)_2$] species, are thermodynamically unstable in anoxic waters. At neutral pH, the Eh values of the $HgCl_2$/Hg(0) and $Hg(OH)_2$/Hg(0) couples are +0.503 and +0.418 volts, respectively (Table 2.5). The dissolved mercuric sulfide species $Hg(SH)_2$ and $Hg(SH)S^-$ are more stable under reducing conditions, and convert to Hg(0) at Eh values below -0.170 volts. In comparison, sulfate and iron oxyhydroxide reduction extends down to -0.217 and -0.291 volts, respectively. According to these redox potentials, Hg(0) is the stable form of mercury in low potential redox zones, particularly in non-sulfidic groundwaters. The prevalence of chemical reductants in anoxic environments and the rapid reduction of Hg(II) by humic acids and ferrous iron (Skogerboe and Wilson, 1981; Charlet et al., 2002; Wiatrowski et al., 2009) would strongly favor the formation of Hg(0) in subsurface anaerobic microbial ecosystems.

The experimental set up employed in our study also closely resembles the subsurface mercury contaminant situation at the Y-12 National Security Complex in Oak Ridge, Tennessee (USA) (Turner et al., 1984; Riley and Zachara, 1992). Large amounts of elemental mercury were released into the headwaters of East Fork Poplar Creek (TN) in the 1950s and early 1960s (Southworth et al., 2002; Southworth et al., 1995; Southworth et al., 2000; Campbell et al., 1998), and currently a significant amount of the waste is retained in the subsurface sediments as liquid Hg beads (Liang et al., 2012). The dissolution and vaporization of these liquid elemental mercury beads provides a constant source of dissolved Hg(0) to groundwater, as a drop of Hg(0) provides a constant dissolved Hg(0) source in our experiments. Anaerobic bacteria, including

members of *Desulfovibrionaceae* and *Geobacteraceae*, have been found in groundwater monitoring wells at the Field Research Center of Oak Ridge National Laboratory (Hwang et al., 2009; Gihring et al., 2011). Because MeHg has been detected in the water and fish of East Fork Poplar Creek (Southworth et al., 1995, 2000), microbial methylation of the Hg waste has almost certainly occurred. The oxidation and methylation of Hg(0) by *Desulfovibrionaceae* may represent one of the pathways of MeHg production at this site.

Anaerobic oxidation of Hg(0) by mercury-methylating bacteria is hitherto an unknown process for MeHg production in the environment. Because dissolved Hg(0) becomes oxidized and bound to anaerobic bacteria, the formation of Hg(0) in anoxic waters does not necessarily decrease the amount of Hg available for methylation. The uptake and methylation of Hg(0) by anaerobic methylators may be especially important in groundwater systems, where gas-exchange is limited and Hg(0) is frequently physically confined. Hg(0) and MeHg are known to accumulate in anoxic groundwater (Murphy et al., 1994), resulting in the discharge of MeHg to surface waters (Stoor et al., 2006). To accurately predict the sources of MeHg that enter aquatic food webs, our findings advise the incorporation of anaerobic oxidation and methylation of Hg(0) into Hg biogeochemical models.

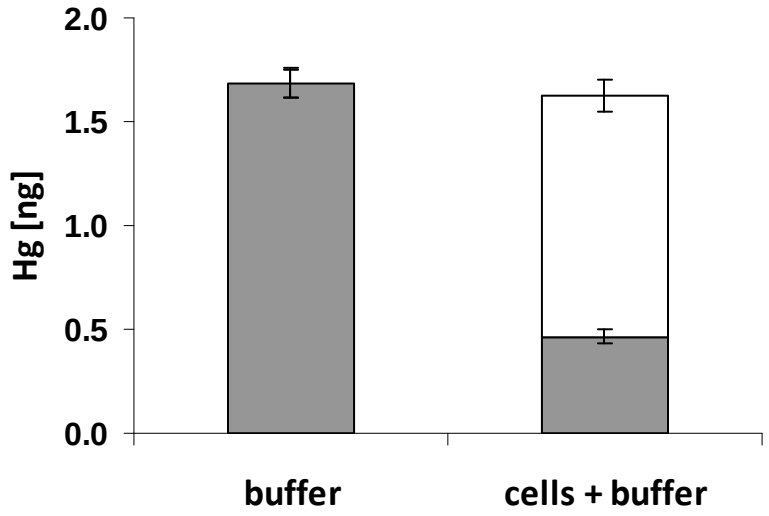

Figure 2.1. Loss of volatile Hg(0) and formation of non-purgeable Hg during Hg(0) reaction with *D. desulfuricans* ND132 cells. Non-purgeable Hg shown in white, and gaseous Hg(0) shown in gray. Experiments were conducted with an initial Hg(0) mass of 1.7 ng, and reactions were carried out for 2.5 h. Sterile controls were composed of deoxygenated 0.5 mM phosphate buffer containing 1 mM NaCl. Bars and error bars represent the means and standard deviations of triplicate experiments, respectively.

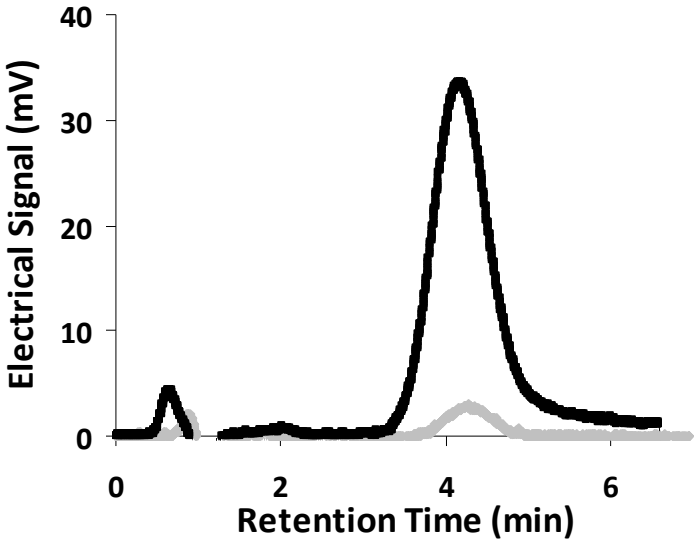

Figure 2.2. Gas-chromatography CVAFS analysis of ethylated non-purgeable Hg. Hg(0) reacted with *D. desulfuricans* ND132 cells suspended in phosphate buffer (black) and sterile phosphate buffer solution (gray). After reaction with Hg(0), samples were purged with N_2 gas and then immediately ethylated with sodium tetraethylborate. The peak at a retention time of ~4 min corresponds to diethylmercury.

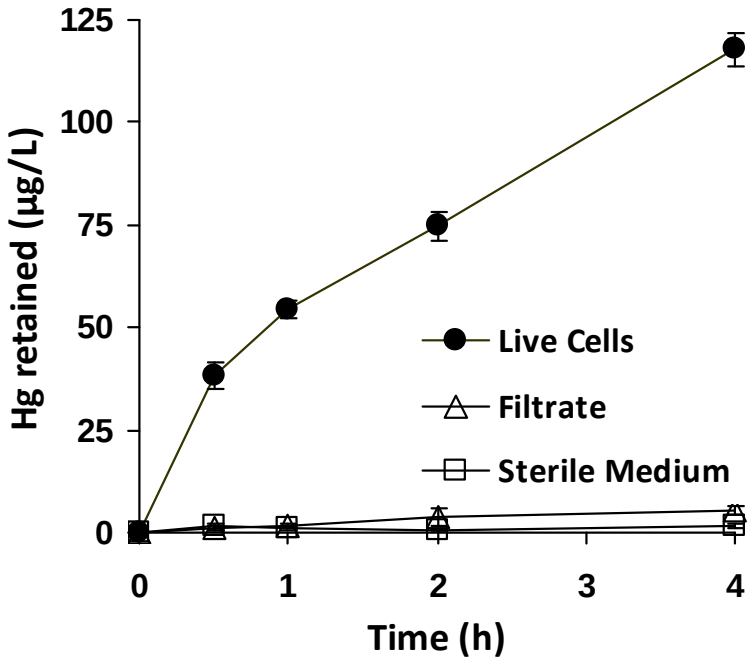

Figure 2.3. Formation of non-purgeable Hg by *D. desulfuricans* ND132 in constant Hg(0) source experiments. Hg retained is the concentration of non-purgeable Hg remaining in the reaction vessel after exposing live cultures, culture filtrate, and sterile medium to a constant source of Hg(0). The initial cell density for the live cultures experiments was 1.7 x 10^8 cells/mL. Points and error bars represent the means and standard deviations of triplicate cultures, respectively.

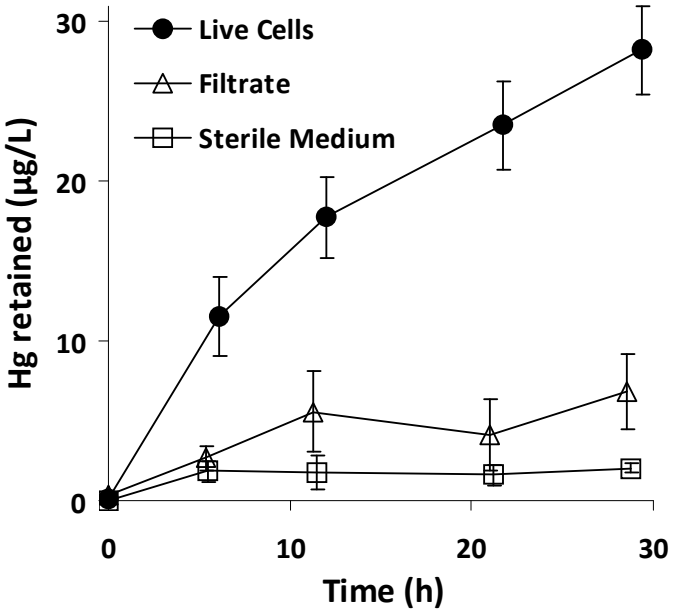

Figure 2.4. Retention of Hg by *G. sulfurreducens* PCA. Hg retained is the Hg remaining after exposing live cultures, culture filtrate, and sterile medium to a constant source of Hg(0) and purging the samples with N_2 gas at 0.8 L/min for 5 min. Points and error bars represent the means and standard deviations of triplicate cultures, respectively.

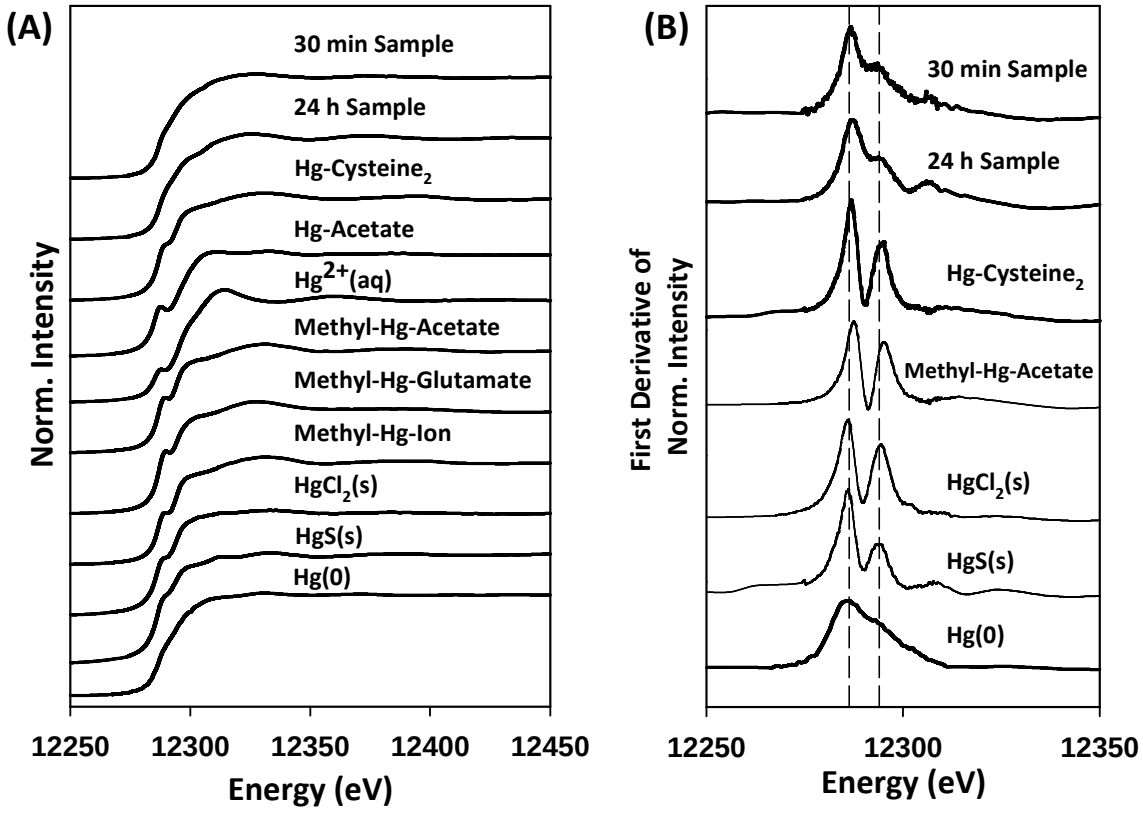

Figure 2.5. Hg L_{III}-edge XANES spectroscopic analysis of Hg(0)-reacted *D. desulfuricans* ND132 cells. (A) XANES spectra of bacterial samples collected at 30 min and 24 h, and reference compounds; (B) First derivatives of the XANES spectra of bacterial samples and reference compounds. Dashed lines are at 12,286.3 and 12,294.0 eV. See Table 2.2 for corresponding peak positions for spectra.

(A)

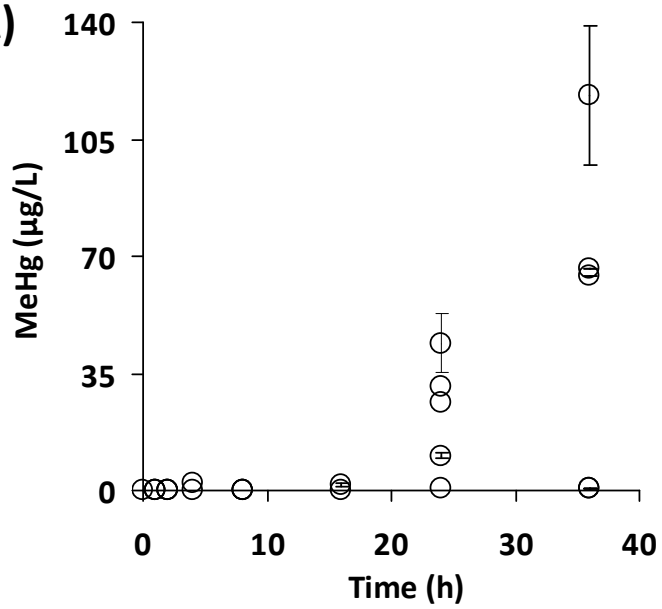
140
105
70
35
0
MeHg (µg/L)
0
10
20
30
40
Time (h)

(B)

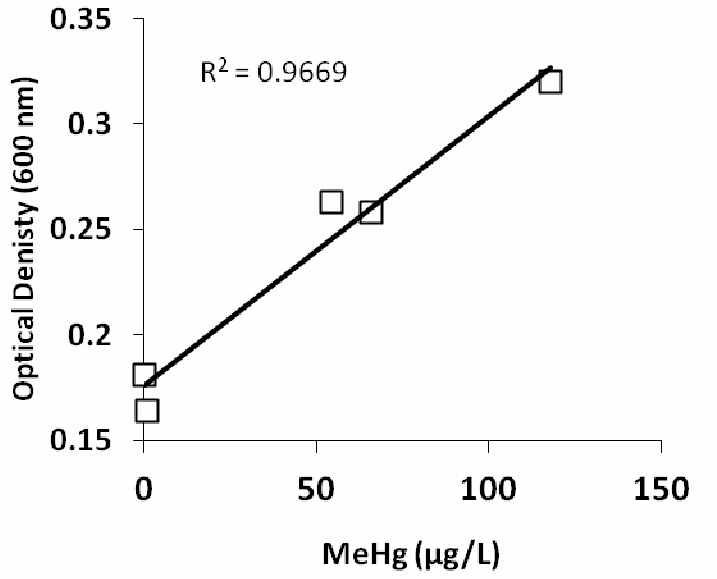
0.35
0.3
0.25
0.2
0.15
Optical Denisty (600 nm)
R2 = 0.9669
0
50
100
150
MeHg (µg/L)

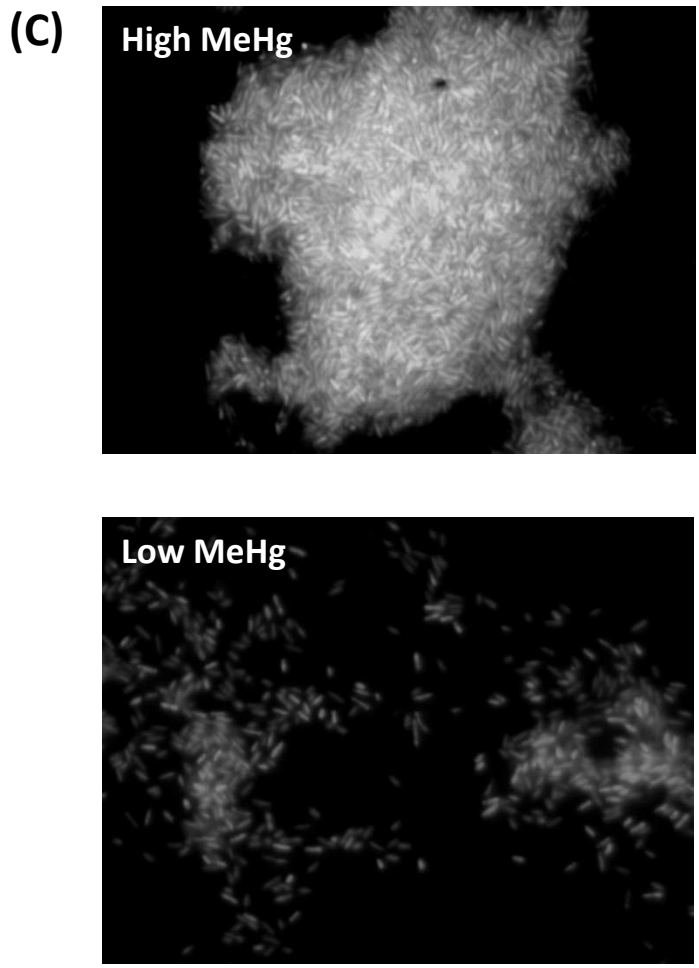

Figure 2.6. MeHg production from Hg(0). (A) MeHg concentrations in *D. desulfuricans* ND132 cultures determined at periodic intervals up to 36 h of incubation. Data points represent individual experiments and error bars are analytical replicates of a single sample. (B) Relationship between cell density and MeHg production in samples collected at 36 h (C) Representative microscopic images of samples collected at 36 h; (top) a culture of ND132 that produced a high MeHg concentration and (bottom) a culture of ND132 that produced low MeHg concentration.

Table 2.1. Production of non-purgeable Hg and Hg methylation by *D. desulfuricans* ND132. Each sample represents an independent bottle analyzed for non-purgeable Hg and MeHg. A less than sign (<) indicates samples that were below detection limit (10 pg/sample volume for samples a1 to g5, 50 pg/sample volume for h1 to h5). Standard deviations are of replicate analyses. Time points that were not analyzed are represented by a dash (-).

Sample ID	Incubation time (h)	Hg retained (µg/L)	MeHg (µg/L)	Analytical replicates (MeHg)
a1	0	0.0	-	-
a2	0	0.1	-	-
a3	0	0.0	< 1	1
b1	1	55	< 0.05	1
b2	1	57	< 0.5	1
b3	1	52	< 0.5	2
c1	2	78	< 0.05	2
c2	2	75	< 0.05	2
c3	2	71	< 0.1	1
d1	4	115	< 0.05	1
d2	4	123	-	-
d3	4	116	< 0.04	2
d4	4	-	2	1
d5	4	-	< 0.05	1
e1	8	211	< 0.03	1
e2	8	192	< 0.2	2
e3	8	257	0.02	1
f1	16	552	1.5 ± 0.4	2
f2	16	306	< 0.1	2
f3	16	354	< 0.04	1
g1	24	100	10 ± 0.8	2
g2	24	774	0.6	2
g3	24	108	44 ± 8.8	4
g4	24	-	31	1
g5	24	-	26	1
h1	36	143	54 ± 14	2
h2	36	818	< 0.7	1
h3	36	189	66	1
h4	36	172	118 ± 21	2
h5	36	693	< 0.8	2

Table 2.2. Hg L_{III}-edge first inflection points (E_1), second inflection points (E_2), and separations (ΔE) in model compounds and bacterial samples showing oxidation of Hg(0) to Hg(II) and the covalent character of the Hg-ligand bond in our samples.

ID	E_1 (eV)	E_2 (eV)	ΔE (eV)
Hg(II)-cysteine$_2$	12286.3	12293.5	7.2
Hg(II)-acetate	12285.2	12298.4	13.2
Hg(II)	12284.6	12294.1	9.5
Methylmercury acetate	12286.4	12294.9	8.5
Methylmercury glutamate	12286.7	12294.8	8.1
Methylmercury	12286.1	12295.2	9.1
HgS	12285.6	12293.6	8.0
$HgCl_2$	12285.5	12294.3	8.8
Hg(0)	12285.0	-	-
30 min sample	12286.6	12294.1	7.5
24 h sample	12286.6	12294.3	7.7

Table 2.3. Percent composition of mercury species in bacterial samples as determined by linear combination fitting of Hg L_{III}-edge XANES spectra (First Derivative). The best overall fit was ~70% of Hg(II)-cysteine$_2$ and ~30% of Hg(0). Adding additional components did not improve the fit.

Components	**30 min sample**		**24 h sample**	
	Fraction	**Residual**	**Fraction**	**Residual**
Hg(II)-cysteine$_2$	100	0.0887	100	0.1110
Hg(II)-cysteine$_2$ HgS(s)	94.0 ± 4.5 6 ± 3.4	0.0755	83.2 ± 1.2 16.8 ± 3.4	0.1013
Hg(II)-cysteine$_2$ $HgCl_2$(s)	88.1 ± 5.7 11.9 ± 4.2	0.0880	100 ---	0.1110
Hg(II)-cysteine$_2$ Methyl-Hg-Acetate	96.0 ± 6.5 4 ± 2.8	0.0802	100 ---	0.1110
Hg(II)-cysteine$_2$ Hg(0)	64.4 ± 1.2 35.6 ± 2.5	0.0350	68.2 ± 3.8 31.8 ± 3.8	0.0519
Hg(II)-cysteine$_2$ Hg(0) HgS(s)	59.6 ± 5.9 39.1 ± 1.1 1.3 ± 2.1	0.0350	67.8 ± 2.1 32.2 ± 6.1 ---	0.0591

Table 2.4. MeHg concentrations in sterile medium controls. Each sample represents an independent experiment. A less than sign indicates samples that were below detection limit (10 pg/sample volume for samples up to 36 h, 50 pg/sample volume for 36 h samples). Standard deviations are of replicate analyses.

Incubation time (h)	MeHg (μg/L)	Analytical replicates
0.5	< 0.5	1
1	< 0.05	1
2	< 0.01	1
4	< 0.5	1
16	< 0.03	1
16	0.4 ± 0.3	2
24	< 0.1	2
24	0.04	1
36	< 0.2	1
36	< 0.1	1
36	< 0.1	1
36	< 0.1	1
36	< 0.1	1

Table 2.5. Standard potentials for the Hg(II)/Hg(0) and other relevant redox couples.

Reaction	E^o (volts) [a]	E^a (volts) [b]
$HgCl_2 + 2e^- \rightarrow Hg(0)_{(aq)} + 2Cl^-$	+0.234	+0.503 [c]
$Hg(OH)_2 + 2H^+ + 2e^- \rightarrow Hg(0)_{(aq)} + 2H_2O$	+0.832	+0.418 [c]
$Fe(OH)_{3(s)} + 3H^+ + e^- \rightarrow Fe^{2+} + 3H_2O$	+0.880	-0.081
$Hg(SH)_2 + 2e^- \rightarrow Hg(0)_{(aq)} + 2HS^-$	-0.434	-0.150 [c,d]
$Hg(SH)S^- + 2e- + 2H^+ \rightarrow Hg(0)_{(aq)} + 2HS^-$	-0.246	-0.170 [c,d]
$SO_4^{2-} + 10H^+ + 8e^- \rightarrow H_2S + 4H_2O$	+0.301	-0.217 [e]
$FeOOH_{(s)} + 3H^+ + e^- \rightarrow Fe^{2+} + 2H_2O$	+0.770	-0.291

[a] Calculated using the relationship $E = -\Delta G/nF$ where n is the number of electrons and F is Faraday's constant. Values for G^o were taken or calculated from Stumm and Morgan 1996 (Stumm and Morgan, 1996), Morel et al. 1998 (Morel et al., 1998), and Pecora 1970 (Pecora, 1970).

[b] Calculated at pH = 7 and species concentrations were assumed to be 1 ppm unless otherwise stated

[c] Assuming $[HgX_n^m] = [Hg(0)_{(aq)}]$

[d] $[HS^-] = 1.6 \times 10^{-5}$ M, determined at total sulfide = 1 ppm at pH 7

[e] Assuming $[SO4^{2-}] = [H_2S]$

CHAPTER 3

OXIDATION OF Hg(0) TO Hg(II) BY DIVERSE ANAEROBIC BACTERIA

Submitted to *Chemical Geology*

ABSTRACT

Redox cycling between elemental [Hg(0)] and divalent [Hg(II)] mercury is a key control on the fate and transport of Hg in groundwater systems. In this study, we tested the ability of anaerobic bacteria to oxidize dissolved Hg(0) to Hg(II). Controlled laboratory experiments were carried out with the obligate anaerobic bacterium *Geothrix fermentans* H5, and the facultative anaerobic bacteria *Shewanella oneidensis* MR-1 and *Cupriavidus metallidurans* AE104. Under anoxic conditions, all three bacterial strains reacted with dissolved gaseous Hg(0) to form non-purgeable Hg. In mass balance experiments, the formation of non-purgeable Hg corresponded to the loss of volatile Hg. To determine if the non-purgeable Hg was oxidized, we performed ethylation experiments on Hg(0)-reacted cell suspensions and X-ray absorption near edge structure (XANES) spectroscopy on Hg(0)-reacted cells. Derivatization of non-purgeable Hg to diethylmercury and the Hg L_{III}-edge position of the XANES spectra demonstrated that the reacted bacterial samples contained Hg(II). XANES analysis also revealed that cell-associated Hg(II) was covalently bound to bacterial functional groups, most likely to thiol moieties. Finally, experiments with metabolically active and heat-inactivated cells indicated that both live and dead cells oxidized Hg(0) to Hg(II). The results of this study

suggest that reactivity towards Hg(0) is widespread among diverse anaerobic bacteria, and passive microbial oxidation of Hg(0) may play an important role in the redox transformation of mercury contaminants in subsurface environments.

1. INTRODUCTION

The disposal of mercury (Hg) containing wastes has contaminated large areas of sediment and groundwater in the United States (Suchanek et al., 1995; Craft et al., 2005; Brooks and Southworth, 2011) and around the world (Biester et al., 2000; Gray et al., 2004; Rimondi et al., 2012). When discharged in groundwater, Hg undergoes redox transformations that strongly affect its solubility and sorption characteristics (Barringer et al., 2013). Whereas dissolved gaseous elemental mercury [Hg(0)] is mobile in groundwater, oxidized mercuric mercury [Hg(II)] forms strong complexes with sulfide to precipitate insoluble mineral phases, such as $HgS_{(s)}$ (Morel et al., 1998), and also readily sorbs onto mineral surfaces and organic matter (Lockwood and Chen, 1974; MacNaughton and James, 1974; Newton et al., 1976; Mierle and Ingram, 1991; Schuster, 1991; Xia et al., 1999; Lamborg et al., 2003; Kim et al., 2004a,b). In subsurface environments, Hg(0) has been shown to migrate away from buried wastes (Walvoord et al., 2008), accumulate in potable groundwater (Murphy et al., 1994), and can contribute to submarine mercury discharge (Bone et al, 2007). The oxidation of Hg(0) to Hg(II) alters the mobility of mercury contaminants and retards their subsurface transport in aquifers. Furthermore, the formation of bioavailable Hg(II) promotes the production of neurotoxic methylmercury by anaerobic methylating bacteria in anoxic waters (Barkay and Wagner-Dobler, 2005). This methylmercury can subsequently enter aquatic food webs and be biomagnified at higher trophic levels (Mason et al., 1995). Therefore, understanding the biogeochemical processes that control Hg(0) oxidation is important for predicting the fate and transport of mercury contaminants in terrestrial ecosystems.

While photochemical processes govern the oxidation of Hg(0) in the photic zone of surface waters (Amyot et al., 1997; Amyot et al., 2000; Lalonde et al., 2001; Lalonde et al., 2004), the oxidation of mercury in the subsurface is driven by dark reactions. In the absence of light, organic matter and microorganisms are known to oxidize Hg(0) (Smith et al., 1998; Gu et al., 2011; Zheng et al., 2012; Colombo et al., 2013). In a recent study, Gu *et al.* (2011) showed that reduced dissolved organic matter converts dissolved Hg(0) to non-purgeable Hg(II). Thiol functional groups in the organic matter were implicated in the oxidation reaction after demonstrating that simple organic molecules containing sulfhydryl moieties oxidized Hg(0) (Zheng et al., 2012). Aerobic bacteria can also biologically oxidize Hg(0) using catalase enzymes that degrade harmful hydrogen peroxide intermediates produced during aerobic respiration (Smith et al., 1998). A field study by Siciliano *et al.* (2002) in two lake settings showed a correlation between microbial catalase activity and decreasing dissolved gaseous mercury, suggesting that the biological oxidation of Hg(0) by aerobic bacteria is an important natural process in surface waters. Previously, we examined Hg(0) oxidation by *Desulfovibrio desulfuricans* ND132 (Colombo et al., 2013), but the abilities of other anaerobic bacteria to oxidize mercury are unknown and the metabolic factors affecting oxidation are poorly understood.

In subsurface environments, anaerobic bacteria are the principal agents mediating the redox transformation of inorganic elements (Lovley and Chapelle, 1995). Anaerobes isolated from soils and sediments have been shown to catalyze the oxidation of redox-active elements such as Fe(II), As(III), and U(IV) (Osborne and Ehrlich, 1976;

Widdel et al., 1993; Finneran et al., 2002). Because of the relatively high redox potential of the Hg(II)/Hg(0) couple (E^o = +0.8 V), Hg(0) is expected to be the stable oxidation state of mercury in suboxic redox zones. In these subsurface ecosystems, dissolved Hg(0) is frequently physically confined and gas exchange with surroundings is limited. Thus, Hg(0) can potentially interact with metabolically diverse microorganisms including nitrate-reducing, iron-reducing and fermentative bacteria. Because many anaerobes lack catalase enzymes, the mechanism of Hg(0) oxidation by subsurface anaerobic bacteria may be fundamentally different from that of aerobes.

In this study, we examined Hg(0) oxidation by the obligate anaerobe *Geothrix fermentans* H5 (Acidobacterium), and facultative anaerobic bacteria *Shewanella oneidensis* MR-1 (Gammaproteobacterium) and *Cupriavidus metallidurans* AE104 (Betaproteobacterium). These three bacterial strains were selected because they represent distinct metabolic groups of anaerobic bacteria and were isolated from different geochemical and engineered environments. Using these microorganisms, we conducted experiments to investigate the conversion of dissolved gaseous Hg(0) to non-purgeable Hg under anaerobic conditions. Derivatization of the non-purgeable Hg in cell suspensions to diethylmercury and analysis of Hg(0)-reacted bacterial cells using X-ray absorption near edge structure (XANES) spectroscopy were employed to characterize the reaction products. The results of this study demonstrate that diverse anaerobic bacterial species oxidize Hg(0) to Hg(II) and suggest that passive microbial oxidation of Hg(0) is an important process that may immobilize dissolved gaseous mercury in sediments and groundwater.

2. MATERIALS AND METHODS

2.1. Bacterial strains and growth conditions

G. fermentans H5 is an obligate anaerobe derived from a petroleum-contaminated aquifer that grows by fermenting organic acids (Coates et al., 1999). *S. oneidensis* MR-1 is a facultative anaerobe isolated from lake sediments that grows anaerobically by respiring a range of alternate electron acceptors including fumarate, Mn(VI), Fe(III), and $S_2O_3^{2-}$ (Myers and Nealson, 1988). *C. metallidurans* grows by reducing nitrate, and strain AE104 is a plasmid-free mutant of wild type strain CH34 (formerly *Ralstonia metallidurans*), which was originally cultivated from a zinc factory's decantation tank (Mergeay et al., 1985).

All three bacterial species were grown under strict anaerobic conditions in a defined medium (pH ~7) modified from Myers and Nealson (1988). All media contained 9 mM $(NH_4)_2SO_4$, 1 mM $MgSO_4$, 0.49 mM $CaCl_2 \cdot H_2O$, 1.5 mM KH_2PO_4, and 10 mM PIPES as a buffer. Media were supplemented with trace element and amino acid solutions modified from Myers and Nealson (1988). The trace elements solution was added to a final concentration of 67.2 µM disodium EDTA, 56.6 µM H_3BO_3, 10 µM NaCl, 5.4 µM $FeSO_4$, 5 µM $CoCl_2$, 5 µM $NiSO_4$, 3.9 µM Na_2MoO_4, 1.5 µM Na_2SeO_4, 1.3 µM $MnSO_4$, 1 µM $ZnSO_4$, 0.2 µM $CuSO_4$. The amino acid mix was added to the media at a final concentration of 20 mg/L L-arginine hydrochloride, 20 mg/L L-glutamate, 20 mg/L L-serine, and 100 mg/L casamino acids. The *G. fermentans* H5 medium also contained 30 mM fumarate and Wolfe's vitamins and minerals prepared as in ATCC medium 1957. The *S. oneidensis* MR-1 medium was amended with 20 mM lactate as the electron donor

and 30 mM fumarate as the electron acceptor, while *C. metallidurans* AE104 medium was amended with 20 mM acetate and 30 mM nitrate. The incubation temperature was 35°C for *G. fermentans* H5, and 28°C for *S. oneidensis* MR-1 and *C. metallidurans* AE104. All strains were harvested under anaerobic conditions at exponential phase for the Hg(0) oxidation experiments.

2.2. Hg(0) oxidation experiments

Initial Hg(0) oxidation experiments were conducted with live, non-growing, resting cells. Bacterial cultures were centrifuged at 10,000 RPM for 7 min and the cells were washed in 0.5 mM anoxic phosphate buffer (0.38 mM Na_2HPO_4 and 0.12 mM NaH_2PO_4) containing 1 mM NaCl inside an anaerobic glove box under 95% N_2 / 5% H_2. The cells were then suspended in 20 mL of the buffer solution and transferred to BrooksRand® MERX Total Hg certified autosampler bottles. These reaction vessels were sealed with air-tight septum caps and covered in aluminum foil to prevent exposure to light. To initiate reaction, gaseous Hg(0) was introduced to the bottles by injecting a known volume of Hg(0)-saturated N_2 gas through the septa. After 15 h of reaction, the bottles were placed on the autosampler of a BrooksRand® MERX Total Mercury Analytical System. The unreacted Hg(0) in the vials was removed by purging with N_2, and the mass of the volatile Hg(0) purged from the reactors was quantified using cold vapor atomic fluorescence spectroscopy (CVAFS). Complete removal of purgeable Hg(0) was confirmed when no further Hg was detectable by CVAFS. The samples containing non-purgeable Hg were then digested overnight with 1 mL of concentrated bromine

monochloride (BrCl). Prior to analysis, the samples were treated with hydroxylamine hydrochloride to destroy excess free radicals. The Hg in the samples was then reduced with $SnCl_2$ and quantified by CVAFS. A sample of non-purgeable Hg was also collected and used immediately for an ethylation experiment to directly determine the presence of Hg(II) using the method of Bloom (1989). Ethylation experiments were performed by adding sodium tetraethylborate to samples that were not pre-oxidized with BrCl. The ethylated derivatives were collected on a Tenax trap, separated from other Hg species by isothermal gas chromatography, and detected by CVAFS.

Experiments were also performed with growing cultures that were exposed to a constant source of Hg(0) gas. In these experiments, gaseous Hg(0) was generated by placing an uncapped HPLC vial containing a drop of $Hg(0)_{(l)}$ inside of a 30 mL serum bottle. The serum bottles were then vacuum-purged in the antechamber of a glove box and capped with butyl rubber stoppers. The bottles were wrapped in aluminum foil and the drop of $Hg(0)_{(l)}$ was allowed to evaporate into the gas phase and equilibrate with the headspace for 24 h. To initiate the Hg(0) oxidation reaction, 3 mL of either live cells, heat-treated cells (80°C for 30 min and cooled to ambient temperature before addition), cell exudates (exponential phase cultures filtered through a 0.2 μm filter), or sterile media were injected into the serum bottles around the HPLC vial. The reactors were gently agitated at 31°C, and a constant amount of Hg(0) (~70 μg/L) was maintained in solution. At periodic intervals, three independent bottles were sacrificed by removing the liquid sample by needle and syringe. The samples were transferred to acid cleaned vials and purged at 0.8 L/min with N_2 gas for 5 min to remove unreacted Hg(0). Removal

of unreacted Hg(0) was validated by purging Hg(0)-reacted bacteria for progressively longer intervals until no further decline in Hg concentration was observed. Samples were digested overnight with 1 mL of concentrated BrCl and the Hg in samples was quantified by CVAFS.

Cell-specific initial Hg(0) oxidation rates were calculated for the three bacterial species. Cell numbers were determined using an Influx Mariner 209S Flow Cytometer at varying optical densities (600 nm) as measured on a Shimadzu spectrophotometer. Regression analysis was performed on optical densities and cells counted at 4 cell concentrations. The resulting calibration curve was used to convert $O.D._{600}$ to cells/mL.

2.3. X-ray absorption spectroscopy (XAS)

Cell pellets were collected for XAS analysis from purged cell suspensions in 9-12 h constant Hg(0) source experiments. Procedures for *G. fermentans* H5 and *S. oneidensis* MR-1 were modified by increasing the volumes of growing bacterial cultures from 3 to 70 mL in a larger reactor to obtain sufficient biomass for XAS experiments. Cell pellets were collected from purged cell suspensions by centrifugation at 10,000 RPM for 10 min and decanted. The pellets were then sealed in deoxygenated centrifuge tubes and shipped overnight on ice to the Advanced Photon Source at Argonne National Laboratory (Illinois, USA) for XAS analysis.

Reference compounds for the XAS analysis included hydrated Hg^{2+}, Hg(II)-$cysteine_2$, Hg(II)-acetate, Hg(II)-citrate, HgS, $HgCl_2$, and Hg(0). The hydrated Hg^{2+} standard was a stock solution of $Hg(NO_3)_2$ (1000 ppm) adjusted to pH 2 using

concentrated NaOH and HNO_3. The Hg-cysteine$_2$ reference compound was prepared by adding 0.6 mmol of cysteine to 7 mL of mercuric nitrate stock solution and adjusting to pH 5 using concentrated NaOH. For the Hg-acetate standard, 40 mg of mercuric acetate powder was dissolved in 4 mL of Milli-Q water and 0.25 mL glacial acetic acid and adjusted to pH 5. Hg(II)-citrate reference solution was prepared by adding 250 mM $C_6H_7NaO_7 \cdot 2H_2O$ to the $Hg(NO_3)_2$ stock and adjusting the solution to pH 4. Cinnabar (Acros Organics) and $HgCl_2$ (Fisher Scientific) were analyzed in solid form. The Hg(0) reference compound was prepared by reacting 100 mL of a 0.2 g/L anoxic magnetite suspension with Hg(II) at a Fe(II):Hg(II) molar ratio of 10 to 1 (Mishra et al., 2011). After 2 h of reaction at pH 7 in an aluminum foil-wrapped serum bottle, the suspension containing Hg(0) was centrifuged and the mineral pellet was collected for analysis.

Hg L_{III}-edge X-ray absorption near edge structure (XANES) spectra were collected for reference compounds and cell pellets at station 13BMD, GeoSoilEnviroCARS, with Si (111) crystals with a 13 element germanium detector. Spectra were collected under ambient temperature, pressure, and an N_2 atmosphere. Cell pellets were placed in Teflon holders sealed with Kapton® tape while liquid standards were placed in SPEX® SamplePrep X-Cell cups for analysis. For each bacterial sample, 18 to 25 spectra were collected and averaged. Scans were taken at a single point on the sample at a step size of 0.2 eV throughout the experiments. We expect beam damage to the samples to be minimal since there were no significant changes in the spectra over the duration of sample collection.

The SixPACK interface to IFEFFIT (Newville, 2001; Webb, 2005) was used analyze the XANES spectra. The pre-edge background of each averaged scan was subtracted, and the absorption coefficient was normalized to a unit-edge step. In addition to the edge-positions and spectral features of XANES spectra, the first derivatives of the measured XANES spectra were used for further analysis. While the raw spectra of Hg L_{III}-edge XANES spectra often do not display distinctive spectral features, their first derivatives have more pronounced characteristics that are useful for data analysis (Huggins et al., 1998; Riddle et al., 2002; Rajan et al., 2008; Mishra et al., 2011).

3. RESULTS

All three bacterial strains converted dissolved gaseous Hg(0) to non-purgeable Hg. After reaction with 24.5 ± 0.5 ng of Hg(0) for 15 h, resting cells of *G. fermentans* H5, *S. oneidensis* MR-1, and *C. metallidurans* AE104 formed 6.4 ± 1.7, 5.5 ± 2.4, and 5.7 ± 0.8 ng of non-purgeable Hg, respectively (Figure 3.1). The formation of non-purgeable Hg was concurrent with the loss of gaseous Hg(0) from the cell suspensions (Table 3.1). Mass balance indicated that up to ~30% of the injected Hg(0) was retained as non-purgeable Hg by the cells after 15 h. Negligible loss of gaseous Hg(0) was observed in cell-free phosphate buffer controls, indicating that the non-purgeable Hg in the bacterial experiments was formed by reaction with the cells.

Because the loss of Hg(0) in the bacterial cell suspensions could be attributed to either Hg(0) sorption onto the biomass or the formation of non-volatile Hg(II), we conducted ethylation experiments to determine if the non-purgeable Hg formed by the

three bacterial strains was oxidized Hg(II). In these experiments, the unreacted Hg(0) was purged from solution and the remaining non-purgeable Hg was immediately ethylated with sodium tetraethylborate. Tetraethylborate reacts with Hg(II), but not Hg(0), to form diethylmercury (Rapsomanikis et al., 1986). Therefore, the detection of diethylmercury in the derivatized products is direct evidence for the formation of Hg(II). Gas chromatograms of ethylated non-purgeable Hg in the bacterial samples each showed a large peak at a retention time of approximately 140 seconds, indicating substantial amounts of diethylmercury were present in the ethylated samples (Figure 3.2). Gaseous Hg(0) was not present in the samples as indicated by the absence of Hg(0) peaks (75 seconds) in the chromatograms. These results demonstrate that all three bacterial strains oxidized Hg(0) to non-purgeable Hg(II).

Experiments were performed to determine if metabolically active cells growing under anaerobic conditions and heat-killed cells can oxidize Hg(0). First, exponential phase cultures containing initial cell densities of 1.3×10^8, 2.8×10^8, and 2.1×10^8 cells/mL of *G. fermentans* H5, *S. oneidensis* MR-1, and *C. metallidurans* AE104 respectively, were incubated in anaerobic growth media and exposed to a continuous supply of Hg(0). Metabolically active cells of all three bacterial strains rapidly oxidized the Hg(0) and formed high concentrations of non-purgeable Hg when grown under anaerobic conditions (Figure 3.3). After 4 h of reaction with Hg(0), growing cells of *G. fermentans* H5, *S. oneidensis* MR-1, and *C. metallidurans* AE104 formed 21.9 ± 6.5, 15.1 ± 5.5, and 12.5 ± 4.4 µg/L of non-purgeable Hg, respectively. Although it had the lowest initial cell density, *G. fermentans* H5 oxidized more Hg per cell than the other strains.

The calculated cell-specific initial oxidation rates for these strains were 23.1 x 10^{-4} fg/cell/min (*G. fermentans* H5), 1.6 x 10^{-4} fg/cell/min (*S. oneidensis* MR-1), and 2.5 x 10^{-4} fg/cell/min (*C. metallidurans* AE104). Thus *G. fermentans* H5 formed non-purgeable Hg at an initial rate 10 fold faster than the other two bacteria. Second, we conducted Hg(0) oxidation experiments with heat-inactivated cells (80^{o}C for 30 min). For all three strains, heat- treatment did not diminish reactivity towards Hg(0), and all heat-killed experiments showed the formation of non-purgeable Hg (Figure 3.4). Finally, experiments with spent media in the absence of cells produced only small amounts of non-purgeable Hg, confirming that reactions with extracellular compounds were not responsible for the formation of Hg(II).

The high concentrations of non-purgeable Hg formed in the constant source Hg(0) experiments allowed us to further examine the chemical speciation of cell-associated non-purgeable Hg by X-ray absorption spectroscopy. The Hg L_{III}-edge XANES spectra of the Hg(0)-reacted bacterial cells are presented in Figure 3.5. The spectra of *G. fermentans* H5, *S. oneidensis* MR-1, and *C. metallidurans* AE104 were very similar to each other, and all three samples lacked the pronounced XANES pre-edge feature displayed by the Hg(II)-acetate, Hg(II)-citrate, $HgCl_2$, and Hg^{2+} reference spectra (Figure 3.5a). Hg(II) coordinated with oxygen in the carboxyl-containing standards Hg(II)-acetate and Hg(II)-citrate exhibited a pre-edge peak at 12,287 eV and 12,282 eV, respectively. The absence of this peak in the spectra of the bacterial samples suggests that cell-associated Hg was not complexed to carboxyl functional groups.

The first derivatives of the XANES spectra were used to obtain more detailed information about the cell-associated Hg (Figure 3.5B). We used the energy position of the first peak (E_1) as an indicator of the oxidation state of Hg in the bacterial samples. The E_1 values of *G. fermentans* H5, *S. oneidensis* MR-1, and *C. metallidurans* AE104 spectra were positioned at approximately 12,286 eV (Table 3.2). In comparison, the E_1 value of Hg(0) was positioned at a lower energy of 12,285 eV. The E_1 values of the XANES spectra for all three bacterial samples closely resemble the E_1 value of Hg(II)-cysteine$_2$ (12286.3 eV), suggesting similarity in the Hg oxidation state. Analysis of the E_1 values of the bacterial samples and reference compounds supports the conclusion that all three strains of bacteria had oxidized Hg(0) to Hg(II).

The first derivative of the Hg(II) XANES spectra exhibited two main peaks (Figure 3.5B), and the difference between E_1 and E_2 was used to calculate the ΔE value. Because a larger ΔE corresponds to Hg-ligand complexes with ionic character and a smaller ΔE to complexes with more covalent character (Powers, 1982), we used this value to infer the local Hg(II) bonding environment of the reference compounds and the bacterial biomass. The ΔE value of 7.2 eV for Hg(II)-cysteine$_2$ was significantly smaller than the value of 9.9 eV for the Hg(II)-citrate reference compound, consistent with the stronger covalent Hg-S bond in Hg(II)-cysteine$_2$ compared to Hg-O bond in Hg(II)-citrate (Table 3.2). The ΔE values for *G. fermentans* H5, *S. oneidensis* MR-1, and *C. metallidurans* AE104 spectra were approximately 7.0 eV. The ΔE values of the three bacterial samples indicate that the oxidized Hg(II) was associated with cellular ligands via strong covalent bonds. Comparison of the ΔE values for the reference compounds and the bacterial

samples suggest that the local bonding environment of cell-associated Hg(II) was similar to that of Hg coordination with sulfur atoms in the Hg(II)-cysteine$_2$ reference compound.

4. DISCUSSION

Resting and heat-inactivated cells of *G. fermentans* H5, *S. oneidensis* MR-1, and *C. metallidurans* AE104 oxidized Hg(0) to Hg(II) (Figures 3.3 and 3.4). While the catalase enzymes KatE and KatG have been shown to play a role in mercury oxidation by certain aerobic bacteria (Smith et al., 1998), our experimental data suggest that Hg(0) oxidation by these three bacterial strains is catalase-independent. Past work shows that the heat treatment of cells (65-80^{o}C) completely destroys the catalase enzyme (Eyster, 1950). Although both *S. oneidensis* MR-1 and *C. metallidurans* AE104 carry genes for the heat-sensitive monofunctional catalase HPII and bifunctional catalase HPI, the cultures were grown anaerobically and heat-treated cells oxidize Hg(0) at similar rates to metabolizing cells (Figures 3.3 and 3.4). Furthermore, *G. fermentans* H5, an obligate anaerobe that lacks *katG* and *katE* gene homologs in its genome, oxidized Hg(0) to Hg(II) at very fast rates (Figure 3.3). Importantly, the oxidation of Hg(0) to Hg(II) by all three bacterial strains did not require metabolic activity. The reactivity of resting and heat-inactivated cells toward Hg(0) indicate that the Hg(0) oxidation reaction is mediated by a passive mechanism.

XANES data indicate that oxidized Hg is covalently bound to the bacterial cells (Table 3.2). The covalent association of Hg(II) to functional groups closely resembles Hg(II)-cysteine$_2$ complexes, suggesting that oxidized Hg is bound to cellular thiols.

Although no specific information exists on the cellular distribution of sulfur moieties in *G. fermentans* H5, *S. oneidensis* MR-1, and *C. metallidurans* AE104, microorganisms are known to harbor a network of complex organic molecules containing thiol functional groups. A previous study by Mishra et al. (2011) demonstrated spectroscopically that Hg(II) can be bound to sulfhydryl groups on the surfaces of bacterial cells. The presence of sulfhydryl groups on bacterial membranes is well known (Morris et al., 1984), and cell-surface thiol concentrations are beginning to be quantified by novel fluorescence techniques (Joe-Wong et al., 2012). Thiol-containing molecules, such as glutathione, occur at mM concentrations in the bacterial cytoplasm (Fahey, 2001) and may also contribute to Hg(II) binding.

Cellular thiol functional groups may play a role in the passive oxidation of Hg(0) by *G. fermentans* H5, *S. oneidensis* MR-1, and *C. metallidurans* AE104. Gu *et al.* (2011) postulated that oxidative complexation by thiol functional groups mediates Hg(0) oxidation in natural organic matter. It was suggested that physicochemical sorption of Hg(0) to –SH reactive sites is the first step in Hg(0) oxidation by dissolved organic matter. Further investigation revealed that organic compounds containing reduced thiol functional groups, such as glutathione and mercaptoacetic acid, oxidize Hg(0) under anoxic conditions (Zheng et al., 2012). We postulate that Hg(0) interaction with cellular molecules in bacteria containing thiol functional groups would undergo similar chemical reactions.

An important implication of our findings is that subsurface microorganisms may play a dual role in the Hg redox cycle by both oxidizing Hg(0) and reducing Hg(II). *S.*

oneidensis MR-1 has been shown to reduce Hg(II) to Hg(0) constitutively and independent of the *mer* system, and thus induction is not required for Hg(II) reduction (Wiatrowski et al., 2006). Interestingly, in our experiments with actively metabolizing cultures, *S. oneidensis* MR-1 either did not reduce Hg(II) or was a net oxidizer of Hg(0) when provided with Hg(0) as the reactant (Figure 3.3). This is also the case with actively growing cultures of *C. metallidurans* AE104, which leads to intriguing questions about the wild type strain CH34. While *C. metallidurans* AE104 is a mutant strain that lacks the wild type's mercury-resistance conferring plasmids (Mergeay et al., 1985), the parental strain CH34 carries the *mer* operon which encodes for proteins that reduce Hg(II) to Hg(0). *C. metallidurans* CH34 exhibits remarkable metal resistance, and the Mer proteins enable this bacterium to detoxify mercury by catalyzing the reduction of Hg(II). The competition between mercury reduction and oxidation by various microbial pathways and its effect on the fate of inorganic Hg is an interesting topic for further study.

Both metabolizing and inactive *G. fermentans* H5, *S. oneidensis* MR-1, and *C. metallidurans* AE104 cells oxidized Hg(0), and thus passive microbial Hg(0) oxidation could occur in the environment regardless of the physiological state of the microorganism. In contrast, the Hg(II) reduction mechanisms of *S. oneidensis* MR-1 (Wiatrowski et al., 2006) and *C. metallidurans* CH34 (Barkay et al., 2003) are energy-dependent processes that require metabolic activity for bacterial cells to reduce Hg(II) to Hg(0). We proposed that the dual role of Hg reduction and oxidation would be present only in metabolically active cells, while Hg(0) oxidation may be the dominant reaction in resting and inactive bacterial cells. Because many subsurface microbial

ecosystems are oligotrophic and populated by inactive or slowly metabolizing bacteria, the passive Hg(0) oxidation pathway may represent the prevailing mercury transformation process in nutrient-limited aquifer systems.

The results of this study add to the list of microorganisms that exhibit Hg(0) oxidation activity, which, besides *E. coli*, also includes the aerobic Gram-positive *Bacillus* (Firmicutes) and *Streptomyces* (Actinobacteria) (Smith et al., 1998). The strictly anaerobic bacteria *Desulfovibrio desulfuricans* ND132 and *Geobacter sulfurreducens* PCA (Deltaproteobacteria) have also been shown to oxidize Hg(0) (Colombo et al., 2013). Together, these data suggest that the reactivity towards Hg(0) is widespread among phylogenetically diverse bacteria. Because passive microbial Hg(0) oxidation occurs with metabolically-active and inactive cells, and Hg-oxidizing bacteria have been isolated from both natural and engineered systems, the impact of these microorganisms is likely to be important in many different Hg-bearing microbial environments. In subsurface environments, Hg(0) oxidation by anaerobic bacteria can affect the levels of Hg(0) in water distribution systems as well as the availability of inorganic Hg to methylating organisms. Future investigations aimed at quantifying the in situ dynamics of Hg redox cycling by aquifer microbes will aid in predicting the fate and transport of mercury in contaminated groundwater.

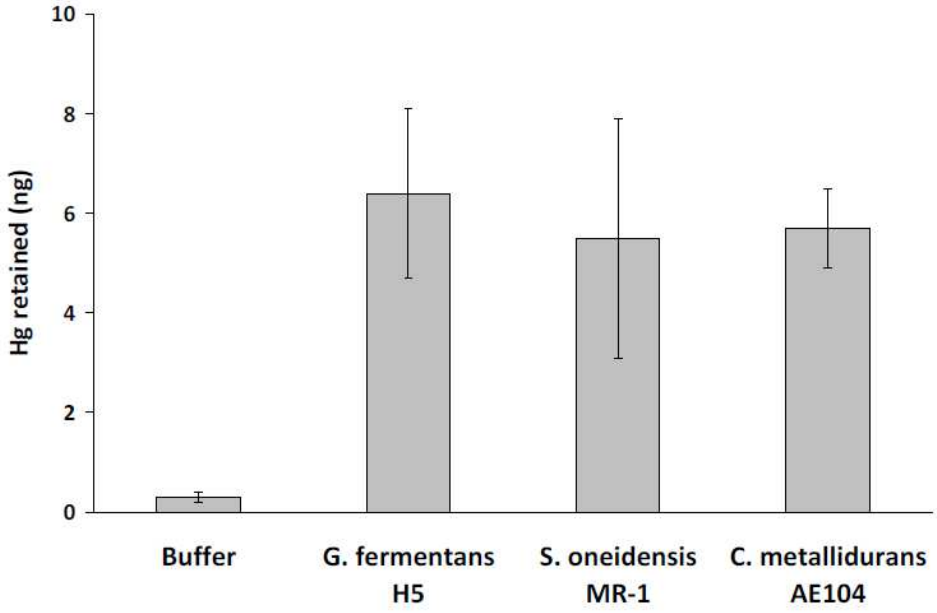

Figure 3.1. Non-purgeable Hg produced by bacterial cells exposed to 24.5 ± 0.5 ng of Hg(0). Experiments were conducted under anoxic conditions with resting cells suspended in phosphate buffer. Cell suspensions were allowed to react with Hg(0) for 15 h and then purged with N_2 gas. Values are means ± 1 SD of triplicate experiments.

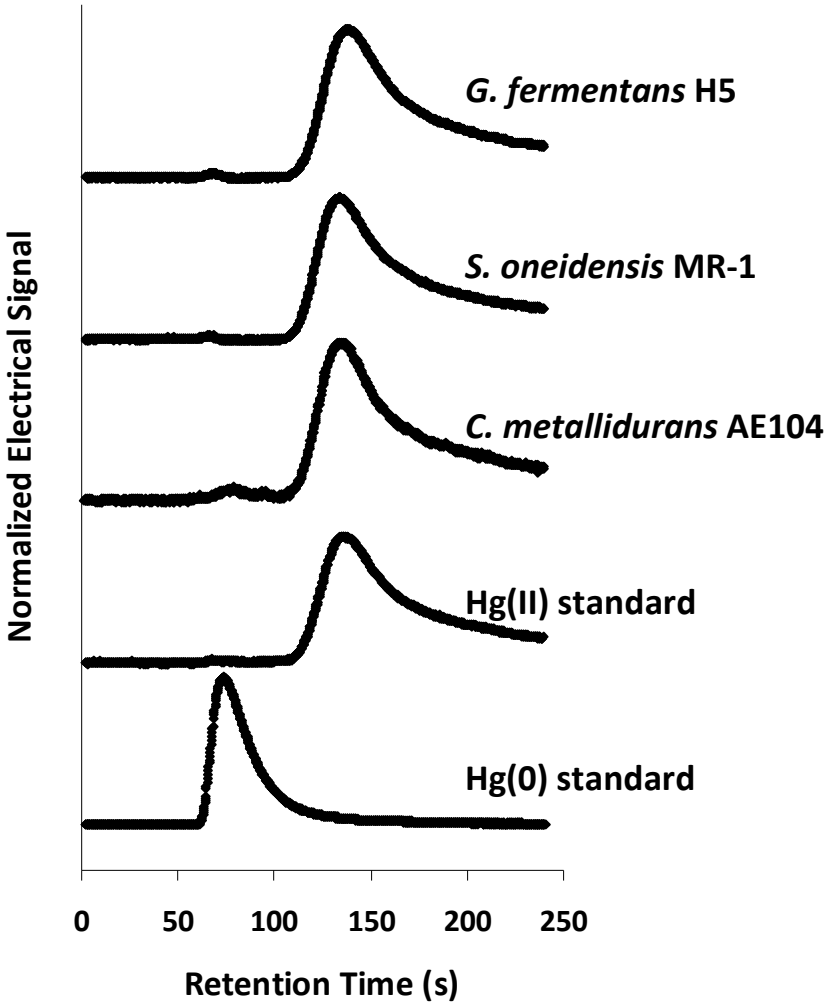

Figure 3.2. Gas chromatography CVAFS analysis of ethylated non-purgeable Hg in bacterial suspensions. The retention times for the Hg(0) and diethylmercury are 75 s and 140 s, respectively. Diethylmercury peaks indicate the presence of Hg(II) in representative bacterial chromatograms.

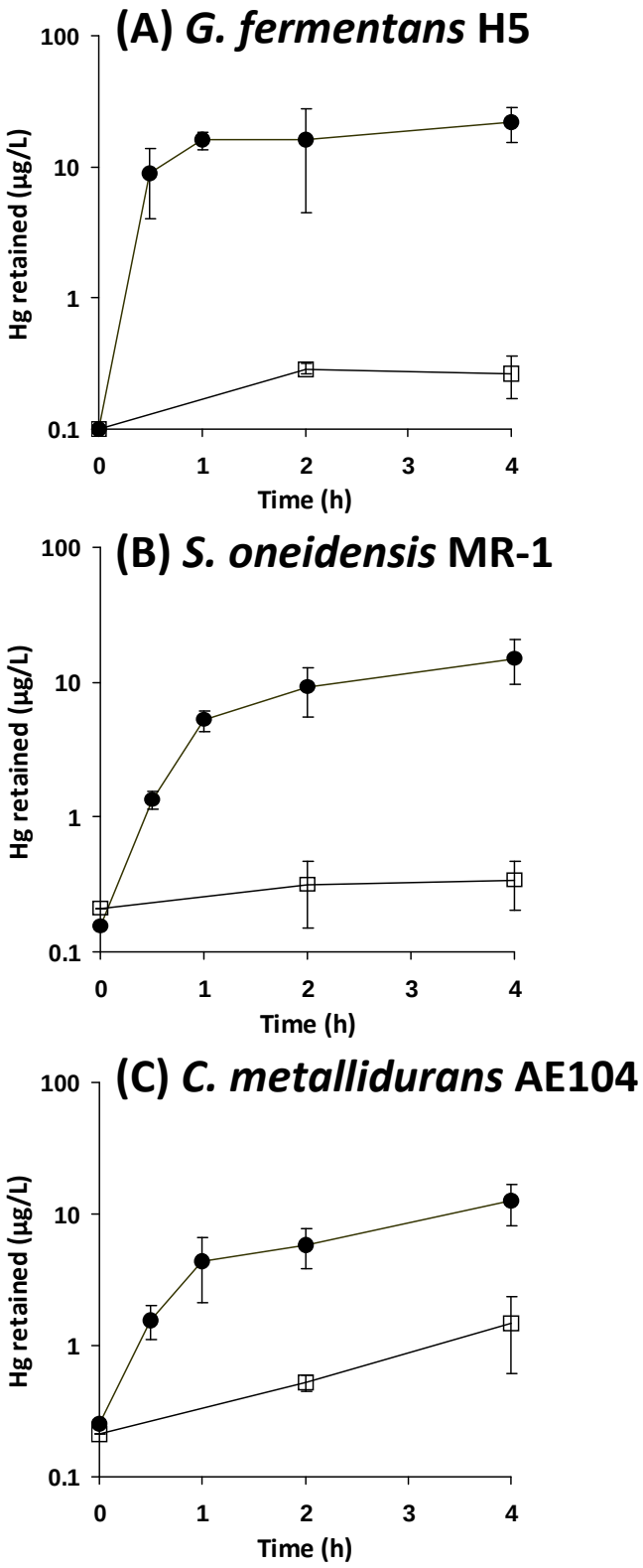

Figure 3.3. Non-purgeable Hg produced by metabolically active cultures exposed to a

constant source of Hg(0). (A) *G. fermentans* H5; (B) *S. oneidensis* MR-1; (C) *C. metallidurans* AE104. Non-purgeable Hg produced by live cells (●) and sterile medium (□). Three independent bottles per time point were sacrificed and analyzed for non-purgeable Hg. Points and error bars are the means and standard deviations of three independent experiments.

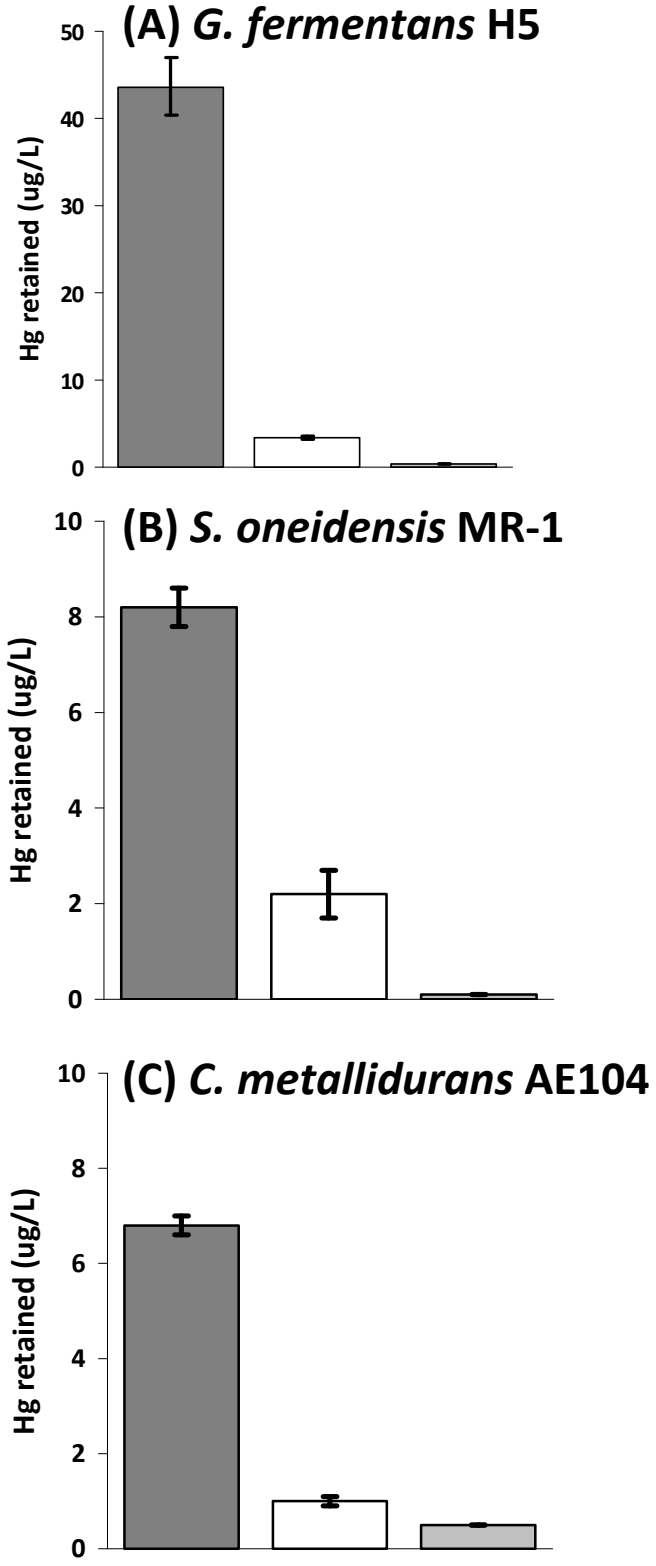

Figure 3.4. Formation of non-purgeable Hg by heat-inactivated cells exposed to a constant source of Hg(0) for 2 h. (A) *G. fermentans* H5; (B) *S. oneidensis* MR-1; (C) *C.*

metallidurans AE104. Heat-treat cultures (dark gray), cell-free exudates (white), and sterile medium (light gray). Values and error bars are the means and standard deviations of three independent experiments.

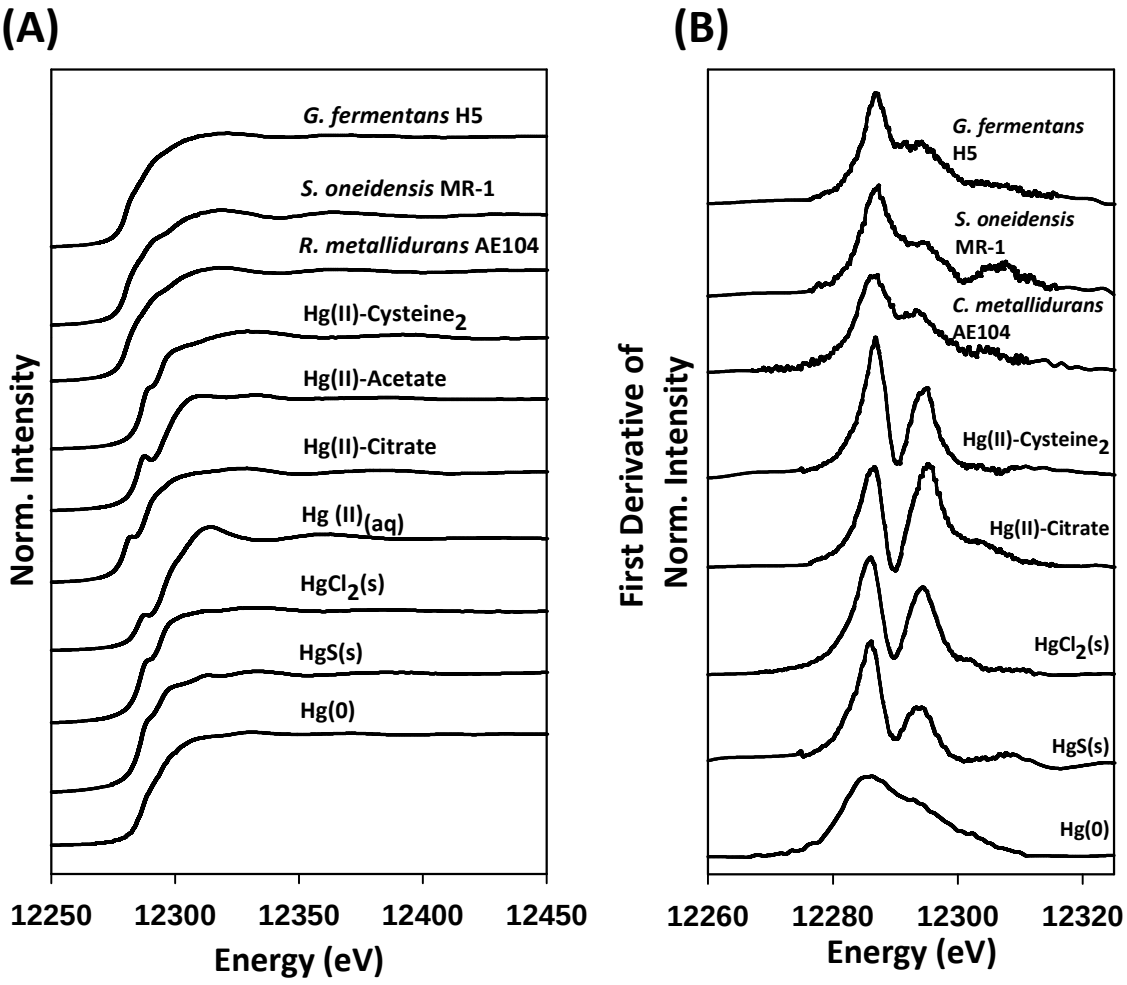

Figure 3.5. Hg L_{III}-edge XANES spectroscopic analysis of Hg(0)-reacted bacterial cells. (A) XANES spectra of *G. fermentans* H5, *S. oneidensis* MR-1, and *C. metallidurans* AE104 and reference compounds; (B) First derivatives of the XANES spectra of the bacterial samples and reference compounds.

Table 3.1. Formation of non-purgeable Hg from Hg(0) by bacterial cell suspensions. Experimental systems were provided with 24.5 ± 0.5 ng of Hg(0) and allowed to react for 15 h. Values are the means ± 1 SD of triplicate experiments.

	Hg(0) (ng)	**Non-purgeable Hg (ng)**
Buffer	24.9 ± 2.6	0.3 ± 0.1
***Geothrix fermentans* H5**	18.0 ± 2.8	6.4 ± 1.7
***Shewanella oneidensis* MR-1**	18.8 ± 1.8	5.5 ± 2.4
***Cupriavidus metallidurans* AE104**	18.5 ± 1.8	5.7 ± 0.8

Table 3.2. First inflection points (E_1), second inflection points (E_2), and separations (ΔE) in first derivatives of Hg L_{III}-edge XANES spectra of bacterial samples and reference compounds.

ID	E_1 (eV)	E_2 (eV)	ΔE (eV)
Hg(II)-cysteine$_2$	12286.3	12293.5	7.2
Hg(II)	12284.6	12294.1	9.5
Hg(II)-citrate	12286.2	12296.1	9.9
HgS	12285.6	12293.6	8.0
$HgCl_2$	12285.5	12294.3	8.8
Hg(0)	12285.0	-	-
G. fermentans H5	12286.6	12293.9	7.3
S. oneidensis MR-1	12286.8	12294.0	7.2
C. metallidurans AE104	12286.1	12293.1	7.0

CHAPTER 4

A PRELIMINARY INVESTIGATION OF Hg STABLE ISOTOPE FRACTIONATION DURING Hg(0) OXIDATION BY AN ANAEROBIC BACTERIUM

ABSTRACT

Environmental mercury stable isotope ratios are powerful tools for tracking mercury biogeochemical transformations, but it is currently unknown whether mercury oxidation causes isotope fractionation. Here we investigate mercury stable isotope fractionation during the oxidation of elemental mercury by the anaerobic bacterium *Desulfovibrio desulfuricans* ND132. The results of our experiments demonstrate that product divalent mercury is enriched in the light isotopes relative to the elemental mercury reactant. Fractionation appears to be mass dependent and the result of a kinetic isotope effect, consistent with other dark microbial reactions. Possible isotope fractionating steps in the oxidation pathway are discussed. Ultimately, these results provide a framework for future studies of mercury oxidation and allow for more accurate interpretations of mercury stable isotope signatures in the environment.

1. INTRODUCTION

Mercury (Hg) stable isotopes provide a promising tool for tracking the sources and biogeochemical transformations of Hg in the environment (Sonke and Blum, 2013). Several studies have used Hg stable isotopes for source apportionment of Hg in soil and sediment, often assuming that the isotopic composition of the Hg in these environmental media stays constant over time (Foucher et al., 2009; Feng et al., 2010; Estrade et al., 2011; Gehrke et al., 2011a; Liu et al., 2011; Bartov et al., 2013). While such an assumption applies in certain settings, an understanding of Hg biogeochemical dynamics is critical since redox changes and organic-inorganic cycling largely control the fate and transport of Hg. Few studies have attempted to explain Hg transformations in sedimentary and aquatic settings using Hg stable isotopes (Jackson et al., 2008; Gehrke et al., 2011b; Point et al., 2011; Foucher et al., 2013), especially in dark environments, owing in part to an incomplete catalogue of the isotope fractionation factors for Hg biogeochemical transformations.

Experimental fractionation factors have been determined for divalent Hg [Hg(II)] reduction by bacteria (Kritee et al., 2007, 2008), chemical reductants (Zheng and Hintelmann, 2010a), and light (Bergquist and Blum, 2007). In all instances, a mass dependent kinetic isotope effect was observed which enriched the product elemental mercury [Hg(0)] in the light isotopes relative to the reactant. Bergquist and Blum (2007) also found that Hg isotopes were fractionated by a mass-independent mechanism during photochemical reduction. Mass independent fractionation has provided a useful tool for Hg biogeochemical studies since it has been shown to occur to a large extent

only during photochemical reactions (Kritee et al., 2013). Other isotope fractionating processes that reduce Hg(II) to Hg(0) include Hg demethylation by bacteria (Kritee et al., 2009) and light (Bergquist and Blum, 2007). Fractionation factors that have been determined for non-redox reactions of Hg include methylation (Rodriguez-Gonzalez et al., 2009), changes in speciation and sorption (Wiederhold et al., 2010; Jiskra et al., 2012), evaporation (Estrade et al., 2009), and volatilization (Zheng et al., 2007). Conspicuously absent from our understanding of Hg stable isotope fractionation is that which occurs during the oxidation of Hg(0) to Hg(II).

It has become increasingly apparent that Hg(0) oxidation by bacteria may play an important role in Hg biogeochemistry (Smith et al., 1998; Siciliano et al., 2002; Colombo et al., 2013, submitted). While Smith *et al.* (1998) and Colombo *et al.* (2013, submitted) showed that aerobic and anaerobic bacteria oxidize mercury in pure culture, Siciliano *et al.* (2002) demonstrated a correlation between the loss of Hg(0) and bacterial catalase activity in two lake settings. There are many other natural and human-impacted settings containing substantial quantities of elemental mercury in which Hg oxidation has not been studied. Hydrothermal vent systems (Stoffers et al., 1999), mining areas (Dominique et al., 2007), and industrial complexes (Liang et al., 2012) contain large amounts of liquid elemental mercury which can volatilize, dissolve in water, and become available for oxidation. Dissolved elemental mercury [$Hg(0)_{(aq)}$] has also been detected at elevated levels in potable groundwater (Murphy et al., 1994) and creeks (Brooks and Southworth, 2011). In the anoxic zones of these aquatic settings, Hg(0)-oxidizing anaerobic bacteria (Colombo et al., 2013, submitted) may play a particularly crucial role

in the Hg biogeochemical cycle since Hg(II) complexes are substrates for methylmercury production by anaerobic methylating bacteria (Compeau and Bartha, 1985; Fleming et al., 2006; Kerin et al., 2006; Parks et al., 2013). Thus, understanding Hg isotope fractionation during Hg(0) oxidation by anaerobic bacteria is necessary to unraveling the biogeochemical dynamics of mercury in dark, anoxic environments.

Here we present data from a preliminary investigation of mercury isotope fractionation during Hg(0) oxidation by *Desulfovibrio desulfuricans* ND132 under anoxic conditions. We used stable isotope fractionation theory and past experiments to explain our data and evaluate whether fractionation is caused by a kinetic or equilibrium isotope effect. The results of this study provide initial insight into this oxidation process and guidance for future studies of Hg(0) oxidation.

2. THEORY

To explain the isotope fractionation observed during Hg(0) oxidation by *Desulfovibrio desulfuricans* ND132, we must partially rely on past theoretical work and experimental validations of theory. Mass dependent isotope fractionation can result from kinetic and/or equilibrium isotope effects. Kinetic isotope effect theory predicts that lighter isotopes of an element will react more rapidly than heavier isotopes in a reaction, since bonds with lighter isotopes of an element are weaker than corresponding bonds with heavier isotopes (Bigeleisen and Wolfsberg, 1958). For a kinetic isotope effect to be observed, the reaction must be unidirectional. This theory has been extensively validated for Hg in many different experimental systems, where

the lighter isotopes of mercury preferentially accumulate in the Hg reaction products (Bergquist and Blum, 2007; Kritee et al., 2007; Zheng et al., 2007; Kritee et al., 2008; Estrade et al., 2009; Kritee et al., 2009 Rodriguez-Gonzalez et al., 2009; Zheng and Hintelmann, 2010a). The fractionation data resulting from a kinetic isotope effect typically fits a Rayleigh fractionation model (Johnson et al., 2004). In this study, theoretical curves were drawn for the reactant (eq 1) and cumulative product (eq 2) using forms of the Rayleigh distillation equations from Hoefs (2009) adjusted to δ^{202} notation.

$$\delta^{202}_{react} = (\delta^{202}_{init} + 1000) f^{(\frac{1}{\alpha}-1)} - 1000 \quad (1)$$

$$\delta^{202}_{prod} = (\delta^{202}_{init} + 1000)\left(\frac{1 - f^{\frac{1}{\alpha}}}{1 - f}\right) - 1000 \quad (2)$$

where δ^{202}_{react} = δ^{202}Hg of the reactant; δ^{202}_{init} = initial δ^{202}Hg of the Hg(0) reactant; δ^{202}_{prod} = δ^{202}Hg of the cumulative product; f = fraction of added Hg(0) remaining; α = fractionation factor = $(^{202}Hg/^{198}Hg)_{reactant}$ / $(^{202}Hg/^{198}Hg)_{instantaneous\ product}$.

Equilibrium isotope effect theory predicts that if reactant and product are left in contact to allow for back reaction, heavier isotopes preferentially accumulate in the stiffer bond (Schauble, 2004). In a mercury redox reaction, the stiffer bonds would be in an oxidized Hg(II)-ligand form rather than in the weak interactions that stabilize Hg(0) in water (Schauble, 2007). Thus, if aqueous Hg(0) and Hg(II) with the same δ^{202}Hg were mixed, theory would predict that the Hg(II) would become enriched in the heavy isotopes of Hg, as has been validated for the Fe(II)/Fe(III) system (Johnson et al., 2002;

Welch et al., 2003). However, equilibrium isotope theory has not been experimentally validated for Hg, where reduced Hg(0) and oxidized Hg(II) remain in contact for a period long enough to allow back reaction. Thus, isotope exchange kinetics and the effect of isotope equilibration on environmental mercury isotope fractionation are unknown. Fractionation due to isotopic equilibration fits a closed system equilibrium model (Johnson et al., 2004). This model is simply two parallel lines (eq 3 and 4) constrained by δ^{202}_{init} and α.

$$\delta^{202}_{A} = (1-\alpha)f + \delta^{202}_{init} \quad (3)$$

$$\delta^{202}_{B} = (1-\alpha)f + (\delta^{202}_{init} + \alpha) \quad (4)$$

where δ^{202}_{A} = δ^{202}Hg of substance A and δ^{202}_{B} = δ^{202}Hg of substance B.

3. METHODS

3.1. Bacterial growth conditions

Desulfovibrio desulfuricans ND132 was grown under strict anaerobic conditions in a defined medium as described by (Colombo et al., 2013). Briefly, the medium was adjusted to pH ~7.3 and sealed in serum bottles with butyl rubber stoppers. The bottles were deoxygenated with ultra high-purity N_2 gas, autoclaved, and supplemented with 20 mM pyruvate as the electron donor and 30 mM fumarate as the electron acceptor. Cultures were inoculated at a 1:10 dilution of a growing culture to fresh medium,

incubated at 28°C, and the cells were harvested at exponential phase for use in Hg(0) oxidation experiments.

3.2. Hg(0) oxidation experiments

Cultures were centrifuged at 10,000 RPM for 10 min and washed in anoxic 0.5 mM phosphate buffer containing 1 mM NaCl. 50 mL of the reconstituted cells or 50 mL of buffer were each added to duplicate acid-cleaned 150 mL serum bottles in a Coy® anaerobic chamber. The reaction bottles were sealed with butyl rubber stoppers. A stock of Hg(0)-saturated N_2 gas was generated by placing a bead of liquid Hg(0) in a 1 L glass bottle, sealing the bottle with a thick rubber stopper, purging the air out with high-purity N_2, and allowing the metallic mercury to evaporate and equilibrate with the headspace for at least 1 day prior to use. Replicate injections of this gaseous elemental mercury [$Hg(0)_{(g)}$] into strongly oxidizing bromine monochloride (BrCl) were made to determine the isotope composition of source $Hg(0)_{(g)}$. To initiate the oxidation reactions with cells or buffer, 585 ng (30 mL) of $Hg(0)_{(g)}$ was injected into the headspace of the reaction bottles immediately after removing 30 mL of headspace gas from the reaction bottles to avoid pressurization. The bottles were then removed from the anaerobic chamber and placed on a rotary shaker on their sides at 30°C and 160 RPM.

Reactors containing bacterial cells were sampled at periodic intervals by injecting 5 mL of high purity N_2 gas into the headspace of the bottle and immediately inverting the bottle to remove 5 mL of the liquid phase. The liquid sample was transferred to an acid cleaned vial and purged with high-purity N_2 gas at 0.8 L/min for 5 min to remove

unreacted Hg(0). The complete removal of purgeable Hg(0) was validated by purging cell suspensions for progressively longer intervals until no further decline in Hg concentration was observed. The remaining non-purgeable Hg produced by *D. desulfuricans* ND132 was previously shown to be ~70% oxidized Hg(II) and ~30% Hg(0) (Colombo et al., 2013). After purging, the sample was digested with 1 mL of concentrated BrCl. One of the reaction bottles containing buffer in the absence of cells was sampled and digested identically, with and without purging samples. The other 'buffer only' bottle was not sampled, but was instead injected with BrCl by needle and syringe through the stopper of the bottle, thus oxidizing the Hg(0) completely. The concentration of Hg in this bottle was used to quantify the mass of reactant Hg(0) added to the reactors.

3.3. Hg concentration and isotope analyses

An aliquot of each sample was used to quantify Hg concentration by cold vapor atomic fluorescence spectroscopy (CVAFS) using a BrooksRand® MERX Total Mercury Analytical system. BrCl digested samples were pretreated with hydroxylamine hydrochloride to destroy excess free radicals. Hg in samples was then reduced to $Hg(0)_{(g)}$ using $SnCl_2$, and the $Hg(0)_{(g)}$ was quantified by CVAFS.

Once Hg concentrations were determined, the remaining sample volumes were sent to the University of Illinois at Urbana-Champaign for stable isotope analysis on a Nu Plasma HR multi-collector inductively coupled plasma mass spectrometer. Prior to analysis, all samples were spiked with tracer ^{196}Hg and ^{204}Hg to correct for instrumental

mass bias and isotope fractionation due to sample preparation and analysis. Mercury was introduced to the mass spectrometer as a vapor by reducing the Hg in the sample with $SnCl_2$ without the addition of hydroxylamine hydrochloride. $^{194}Pt^+$, $^{203}Tl^+$, $^{206}Pb^+$, and $^{196}HgH^+$ were measured to check for isobaric interference during analysis, and corrections were made for $^{196}HgH^+$. Hg isotope compositions are reported using accepted notation (Blum and Bergquist, 2007). $\delta^{202}Hg$ is used to express mercury isotope ratios relative to NIST Standard Reference Material 3133 and is calculated using the following formula:

$$\delta^{202}Hg = \frac{(^{202}Hg/^{198}Hg_{sample} - {}^{202}Hg/^{198}Hg_{standard})}{^{202}Hg/^{198}Hg_{standard}} \times 1000$$

We also use other delta values in this study to check the mass dependency of fractionation. Calculation of this value requires a simple change in the ^{202}Hg in the formula to ^{xxx}Hg.

4. RESULTS

In duplicate experiments, resting *D. desulfuricans* ND132 cells produced non-purgeable Hg at a rapid rate that slowed significantly after 5 h (Figure 4.1). The replicate cell suspensions displayed highly reproducible Hg(0) reactivity. The initial rate of reaction and the concentration at the 24 h time point indicate that the reaction reached completion shortly after 5 h. Phosphate buffer controls produced an order of magnitude less non-purgeable Hg than the cell suspensions, indicating that the formation of non-purgeable Hg was caused by the bacteria.

We used the earliest possible time point in our replicate bacterial experiments to determine if there was any isotope fractionation between the initial $Hg(0)_{(g)}$ reactant and the non-purgeable Hg produced by the cells. Due to the limitations of concentration/sample size, we were unable to reliably analyze the first (12 min) time point for Hg isotope composition. Instead, we measured an average $\delta^{202}Hg$ of -2.14‰ for the 45 min time point, which was still in the early phase of non-purgeable Hg formation (Figure 4.1). In contrast, the initial $\delta^{202}Hg$ of the injected Hg(0) gas was -0.63 ± 0.08‰ (n=4). These data show that, after 45 min. of reaction, the product non-purgeable Hg was significantly enriched in the light isotopes relative to the initial reactant by ~1.5‰.

To determine if the observed fractionation was due to Hg(0) dissolution/ volatilization or conversion of Hg(0) to non-purgeable Hg by the cells, we performed a parallel experiment to the *D. desulfuricans* ND132 experiments in the absence of cells. These experiments were conducted identically to those with cells except that the samples were not purged. Hg(0) dissolution into the phosphate buffer was rapid, with 9.45 ng/mL (~80%) of added Hg dissolving in the aqueous phase after 12 min (Figure 4.2). As expected, Hg(0) concentration in the liquid phase declined due to headspace dilution with N_2 and liquid sample removal. Aqueous Hg(0) had a $\delta^{202}Hg$ of -0.91‰ at the 12 and 45 min time points (Table 4.1), only ~0.3‰ lighter than the initial injected Hg(0) ($\delta^{202}Hg$ = -0.63‰). As the solution was periodically sampled, the $\delta^{202}Hg$ of $Hg(0)_{(aq)}$ remained nearly constant, becoming gradually isotopically heavier with sampling (Table 4.1). Since Hg(0) dissolution kinetics were fast relative to non-purgeable Hg formation

(Figures 4.1 and 4.2), we assume that $Hg(0)_{(aq)}$ of constant isotopic composition was available for conversion to non-purgeable Hg up to 45 min of reaction. The fractionation imparted by volatilization/dissolution alone (0.3‰) at the 45 min time point was small relative to the difference between the Hg(0) source and non-purgeable Hg (~1.5‰). Thus, formation of non-purgeable Hg by *D. desulfuricans* ND132 was the dominant cause of Hg isotope fractionation in this system.

In duplicate experiments, the δ^{202}Hg of product non-purgeable Hg generally increased as the reaction proceeded, as would be expected during the approach to reaction completion (Table 4.2). Importantly, all of the δ^{202}Hg values were lower than the initial -0.63‰ value of the Hg(0) source, confirming that non-purgeable Hg production resulted in the preferential accumulation of light Hg isotopes in the reaction product. A plot of all δ^{202}Hg values against delta values for other Hg isotopes reveals that fractionation was mass dependent, since the data follow lines predicted from theory (Figure 4.3). Values of Δ^{199} and Δ^{201} are negligible (≤0.11‰) compared to those observed in photochemical reactions causing large mass independent fractionation (Bergquist and Blum, 2009) and similar to other microbial studies which show the lack of mass-independent fractionation (Kritee et al., 2009; Rodriguez-Gonzalez et al., 2009).

5. DISCUSSION

5.1. Environmental implications

These results demonstrate that the formation of non-purgeable Hg from Hg(0) by *Desulfovibrio desulfuricans* ND132 results in Hg stable isotope fractionation in which

the light isotopes preferentially accumulate in the non-purgeable Hg product. This finding has important implications for the interpretation of Hg isotope signatures in the environment. For example, Foucher et al. (2013) have observed a spatial trend in aqueous mercury concentrations that decrease with distance from the source in a creek. When the isotope values of the mercury are plotted against the fraction of mercury remaining (calculated by dividing concentrations by the source concentration), the data appears to follow a Rayleigh fractionation model. The authors interpret the fractionation factor as a signature of reduction to Hg(0) and volatilization of the reduced Hg. However, the fractionation factor they observed (1.00038) is significantly smaller than even the most conservative combinations of chemical/bacterial reduction (1.0008 (Zheng and Hintelmann, 2010a) – 1.0020 (Kritee et al., 2007)) and volatilization (1.0004 (Zheng et al., 2007)). Since our study shows that non-purgeable Hg formation results in the preferential accumulation of light isotopes in the non-volatile Hg, a consistent conversion of recently reduced, volatile Hg(0) back to non-volatile Hg may result in a depressed signal for reduction and volatilization in this and other natural systems.

Isotopic trends potentially explained by the formation of non-purgeable Hg from volatile Hg(0) were also seen in East Fork Poplar Creek in Tennessee, USA. This creek is a highly contaminated water body that exhibits a spatial and temporal trend of sediment Hg enriched in the light isotopes relative to its source (Thomas M. Johnson, unpublished data). Since reduction and subsequent volatilization of reduced Hg(0) preferentially leave behind the heavy isotopes of Hg to accumulate in sediments, these processes cannot be invoked to explain the observation of relatively isotopically light sediment Hg.

Mercury is known to enter the creek waters as Hg(0) and has been detected at concentrations as high as 60 µg/L (Brooks and Southworth, 2011). The conversion of this source Hg(0) to non-purgeable Hg, which is expected to enrich non-volatile Hg in the light isotopes, provides a potential explanation for the observed trend.

5.2. Reaction mechanism of Hg(0) oxidation and fractionating steps

Understanding the mechanism of non-purgeable Hg formation and the fractionating steps in this process are important to determining how these findings apply to pathways of oxidation by other Hg(0)-reactive agents. Our past work with *D. desulfuricans* ND132 suggests that the cell-associated non-purgeable Hg product consists primarily of oxidized Hg(II) and a smaller fraction of sorbed Hg(0) (Colombo et al., 2013). The presence of Hg(II) and Hg(0) in the non-purgeable product is consistent with the mechanism of Hg(0) oxidation by natural organic matter proposed by Gu *et al.* (2011), which is presented here in a modified form relevant to this study:

$$Hg(0) \rightarrow Hg(0)\text{-cell} \rightarrow Hg(II)\text{-cell} \qquad \text{(Reaction 1)}$$

Gu *et al.* (2011) postulated that the reaction proceeds via a two step process which consists of the physicochemical sorption of Hg(0) to thiol groups followed by the oxidation of Hg(0) to Hg(II). In light of our recent work showing that anaerobic bacteria oxidize mercury by a passive mechanism (Colombo et al., submitted), bacteria may also oxidize Hg(0) via reaction 1 since they contain thiol functional groups in their cell walls (Morris et al., 1984; Joe-Wong et al., 2012) and cytoplasms (Fahey, 2001). Possible

fractionating steps include the sorption of Hg(0) to cells and the oxidation of Hg(0) to Hg(II) and are considered in detail below.

Current knowledge does not allow us to unequivocally decide the fractionating step(s) in this non-purgeable Hg forming process. One possibility is that the oxidation of Hg(0) to Hg(II) causes fractionation. Generally, changes in oxidation state result in larger fractionations than non-redox processes for a given element due to significant changes in bonding environment (Schauble, 2004); experiments with many different elements have confirmed this notion (Johnson, 2011). For mercury, the isotope fractionation caused by Hg(II) reduction has been studied extensively, resulting in fractionation factors as large as 1.0020 (Kritee et al., 2007). In contrast, the largest fractionation factor determined for an environmentally relevant non-redox process was 1.0006 (Wiederhold et al., 2010). These examples show that redox changes for mercury, too, generally result in larger fractionations than those reactions in which the oxidation state does not change.

However, we cannot rule out the contributions of Hg(0) sorption to fractionation in these experiments, especially considering the apparently strong nature of the sorption that causes Hg(0) to become non-purgeable. The isotope fractionation produced by Hg(0) sorption has never been measured, though several studies have measured sorption kinetics and extent to various media (Fang, 1981; Krishnan et al., 1994; Bouffard and Amyot, 2009). The sorbed Hg(0) in our experiments cannot be purged from the sample at room temperature, and studies show that Hg(0) sorbed to sediments must be thermally desorbed at temperatures as high as 150°C (Bouffard and

Amyot, 2009). We currently understand the oxidation of Hg(0) by *D. desulfuricans* ND132 to be a stepwise process in which oxidation follows Hg(0) sorption (Reaction 1). Therefore, we argue that even if the Hg(0) sorption reaction is the dominant fractionating reaction and oxidation causes little to no fractionation, the oxidized Hg(II) product will express the δ^{202}Hg of the sorption process, as has been observed in other multi-step reactions of mercury (Jiskra et al., 2012).

5.3. Stable isotope fractionation modeling

Modeling of isotope data allows the calculation of a fractionation factor, which is directly useful for tracing Hg biogeochemical reactions in the environment (Gehrke et al., 2011b; Foucher et al., 2013). Our non-purgeable Hg data is plotted against the fraction of reactant remaining in Figure 4.4. The solid black lines are predicted based on a Rayleigh fractionation model, which we have drawn over our non-purgeable Hg data using the initial δ^{202}Hg value of -0.63‰ and assuming a fractionation factor of 1.0015. This fractionation factor is used as an approximation based on the difference between the initial δ^{202}Hg (-0.63‰) and the δ^{202}Hg at 45 min (-2.14‰), and is not intended to imply the exact fractionation factor. A closed system equilibrium fractionation model is also drawn in dotted lines using the same approximation. Though we do not have enough data at this stage to produce an accurate model, we consider below whether our fractionation data best fits the approximated Rayleigh fractionation model, consistent with a kinetic isotope effect, or closed system equilibrium model, consistent with an equilibrium isotope effect.

Analysis of our δ^{202}Hg data, which shows that isotopically light Hg preferentially accumulates in the non-purgeable product, suggests that the fractionation resulting from the oxidation pathway is caused by a kinetic isotope effect. We have drawn a Rayleigh fractionation model over our non-purgeable Hg data using an initial δ^{202}Hg of -0.63‰ and assuming a fractionation factor of 1.0015 (Figure 4.4, solid curves). Assuming reaction 1 proceeds with no back reaction, the data should follow the lower curved line, which represents the predicted δ^{202}Hg of the cumulative non-purgeable Hg product. 3 of the 10 data points plot on this line. The 3 seemingly "noisy" points (grey squares) must be assumed to be the result of sample alteration during shipment or pre-analysis preparation in this scenario, since they do not follow the consistent increasing δ^{202}Hg trend of the other data points. A reason for the remaining 4 grey circles at low 'f' being elevated could be the sampling method employed in these experiments. Since isotopically light Hg appears to have preferentially dissolved into the liquid phase relative to the starting $Hg(0)_{(g)}$ (Table 4.1), sampling the liquid phase represented a bias which made the δ^{202}Hg of reactor mercury higher on average. This preferential removal of light isotopes leaves 'artificially' higher δ^{202}Hg mercury for conversion to non-purgeable Hg, and potentially explains why the data appear to trend toward high δ^{202}Hg more quickly than the Rayleigh model predicts. This reaction model is plausible, but it does not sufficiently explain all of the data (grey squares in Figure 4.4).

An explanation that accounts for all of the data could be that simultaneous non-purgeable Hg forming reactions following reaction 1 are occurring intracellularly and on the cell surface. If this explanation is correct, our data suggest that these two reactions

result in a kinetic isotope effect whereby the lighter isotopes preferentially accumulate in the non-purgeable Hg products. However, if cell surface and cytoplasmic reactions are both driving isotope fractionation, their relative rates and isotope effects may result in a mixed fractionation signal. This competition between reactions potentially explains the 3 'off-trend' data points observed at 1.5 and 3 h of reaction (Table 4.2 and Figure 4.4, grey squares), even though non-purgeable Hg concentrations were increasing smoothly (Figure 4.1). For example, one of the oxidation reactions may cause greater fractionation than the other, resulting in the two seemingly low δ^{202}Hg grey squares that do not fit the Rayleigh model. Eventually, one of the reactions may dominate resulting in a steadying δ^{202}Hg in the last 4 grey circles. The sampling effect described above would still account for these last 4 points lying above the predicted cumulative product line. This multiple reaction model seems to best describe all of the data, but much further work is needed to test this hypothesis and sufficiently fit a Rayleigh fractionation model.

Though a closed system equilibrium model appears to provide a good fit to the data (Figure 4.4, dotted lines), we would not expect fractionation to be the result of an equilibrium isotope effect based upon equilibrium theory and experiments conducted with other metals such as aqueous iron (Johnson et al., 2002; Welch et al., 2003). If isotope exchange equilibration was occurring in either step of reaction 1, we would expect the non-purgeable Hg (Hg(0)-cell and Hg(II)-cell) to be enriched in the heavier isotopes, since both Hg(0)-cell and Hg(II)-cell bonds are stiffer and stronger bonds than relatively weak Hg(0) interactions with water molecules. Theoretical calculations have

also shown that Hg(II) should be enriched in the neutron-rich isotopes relative to Hg(0) at equilibrium (Schauble, 2007). In other words, we would expect all of the data points for non-purgeable Hg in Figure 4.4 to plot above -0.63‰ if fractionation were the result of an equilibrium isotope effect. Since no isotope experiments have been conducted with Hg(0) and Hg(II) remaining in contact, we cannot say for certain that the heavy isotopes of Hg will preferentially accumulate in the oxidized phase at isotopic equilibrium. However, based upon current knowledge, the preferential accumulation of light isotopes in the more stiffly bound non-purgeable Hg is unlikely to be the result of an equilibrium effect. Thus, our preliminary data suggests that over the 24 h time period of this reaction, there is negligible or no back reaction occurring in reaction 1.

5.4. Conclusions and future work

The results of our work demonstrate that (1) the fractionation of mercury stable isotopes during the oxidation of Hg(0) by *D. desulfuricans* ND132 results in the preferential accumulation of light isotopes in the non-purgeable Hg product, (2) fractionation is mass-dependent, and (3) fractionation is likely the result of a kinetic isotope effect. Since non-purgeable Hg primarily consists of Hg(II) which may be formed from sorbed Hg(0), we expect that oxidized mercury produced by bacteria will be isotopically light relative to purgeable reactant Hg(0).

We do not have sufficient data to justify a model of our observed isotope fractionation, though doing so is clearly a priority for future work. Quantifying the δ^{202}Hg values for both product non-purgeable Hg and reactant Hg(0) as the reaction(s)

proceed will better constrain the fractionation model by allowing data to be plotted on upper and lower model lines in Figure 4.4. δ^{202}Hg values at a greater extent of reaction (lower 'f') will be particularly useful in distinguishing between a Rayleigh fractionation model and a closed system equilibrium model, as well as determining a fractionation factor. Decoupling fractionation caused by Hg(0) volatilization/dissolution from non-purgeable Hg formation may be necessary, unless the data can be modeled with this partitioning included. Determining the kinetics of isotope exchange and associated fractionation factor between Hg(0) and Hg(II) is also essential for studies of Hg(0) oxidation, since it is not experimentally feasible to instantaneously separate reactant Hg(0) from product Hg(II) as the reaction proceeds. Our study seems to suggest negligible isotope exchange between reduced and oxidized Hg over the course of 1 day since the light isotopes accumulate in the oxidized product and there appears to be no radical shift in δ^{202}Hg between 5 and 24 h of reaction. However, a clearer demonstration could be accomplished by mixing Hg(0) and Hg(II) of the same δ^{202}Hg or by partially oxidizing or reducing one of the oxidation states and allowing the redox states to equilibrate for an extended period of time. Isotope exchange kinetics, even if slow, have important implications for the interpretation of isotope signatures in environments where Hg(0) and Hg(II) are confined in close proximity for extended periods of time.

Bacterial Hg(0) oxidation is currently the only known redox process that enriches non-volatile Hg in the light isotopes of Hg. Overall, the findings of this study and the subsequent determination of a fractionation factor for Hg(0) oxidation will provide isotope geochemists with an enhanced ability to explain current and yet-to-be observed

environmental Hg isotope ratios in terms of sources and biogeochemical reactions. Future work should focus on determining fractionation factors for this and other environmentally relevant Hg(0) oxidation processes.

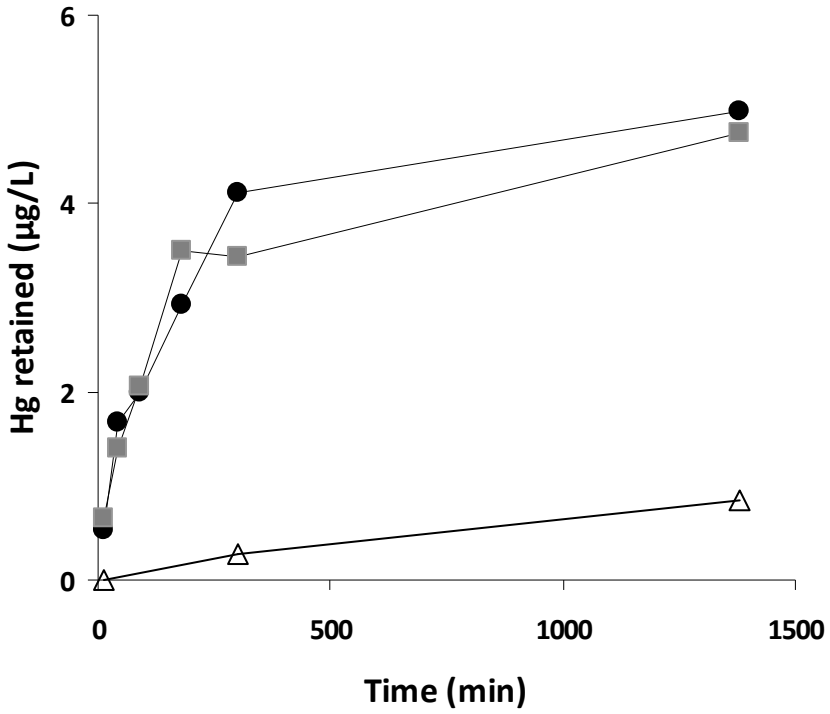

Figure 4.1. Formation of non-purgeable Hg by *D. desulfuricans* ND132. Duplicate bottles in black circles and gray squares, phosphate buffer controls in open triangles. 585 ng of Hg(0) was provided to reactors which resulted in an initial Hg(0) concentration of 9.45 ng/mL. Cell densities in experiments were 3 x 10^7 cells/mL. Points are single analyses of a single sample.

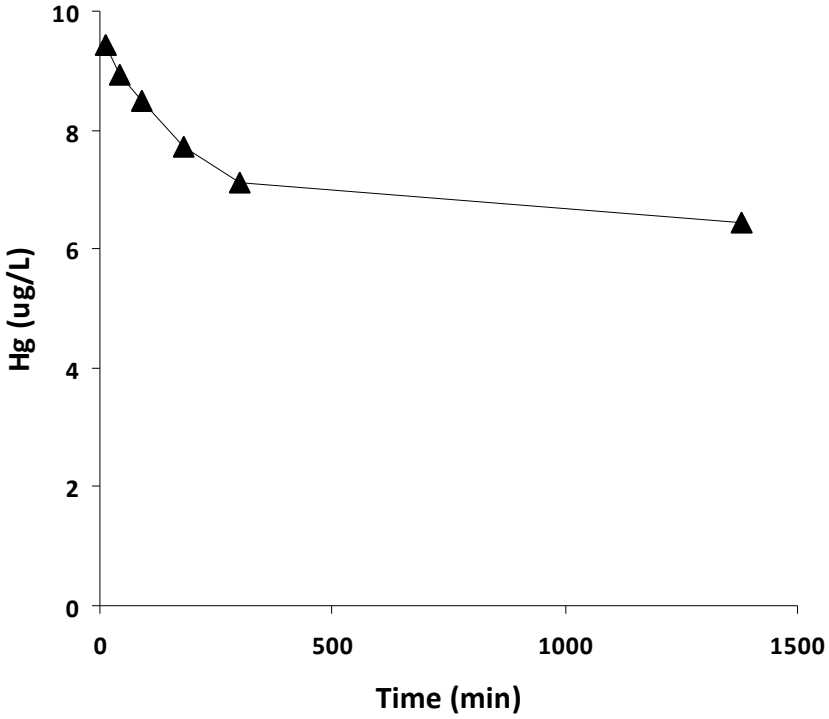

Figure 4.2. Concentration of Hg(0) in solution due to dissolution and sampling. 585 ng of Hg(0) was injected into the headspace of the 150 mL reactor containing 50 mL of buffer solution, and the solution phase was sampled over time for total mercury. Points are single analyses of a single sample.

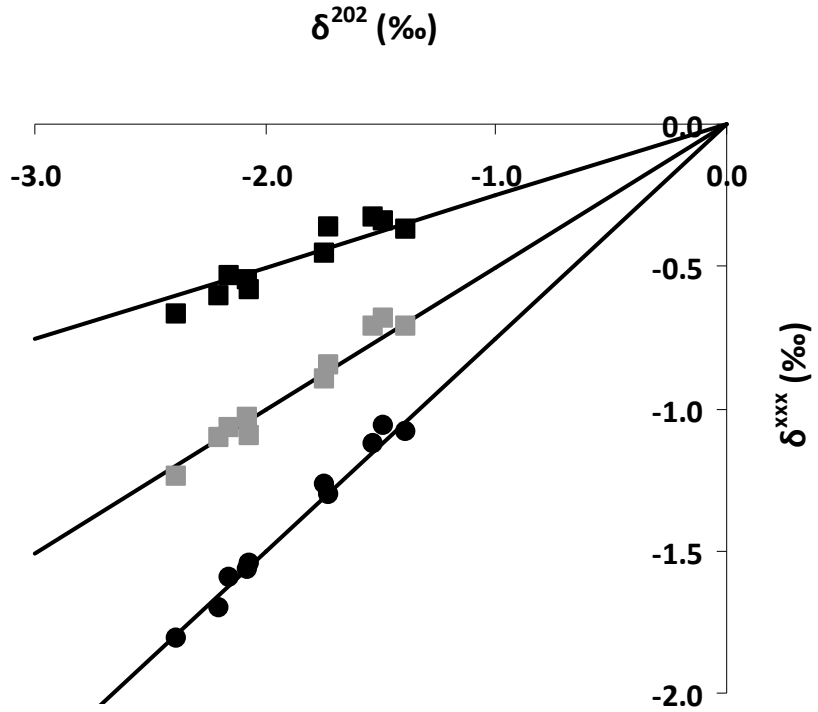

Figure 4.3. Mass dependence of isotope fractionation. Black squares δ^{199}Hg, gray squares δ^{200}Hg, black circles δ^{201}Hg. Theoretical lines are based on the constants calculated by Blum & Bergquist (2007), which were derived from transition state theory. The data lack odd isotope deviations from the predicted mass dependent lines, indicative of the absence of mass independent fractionation.

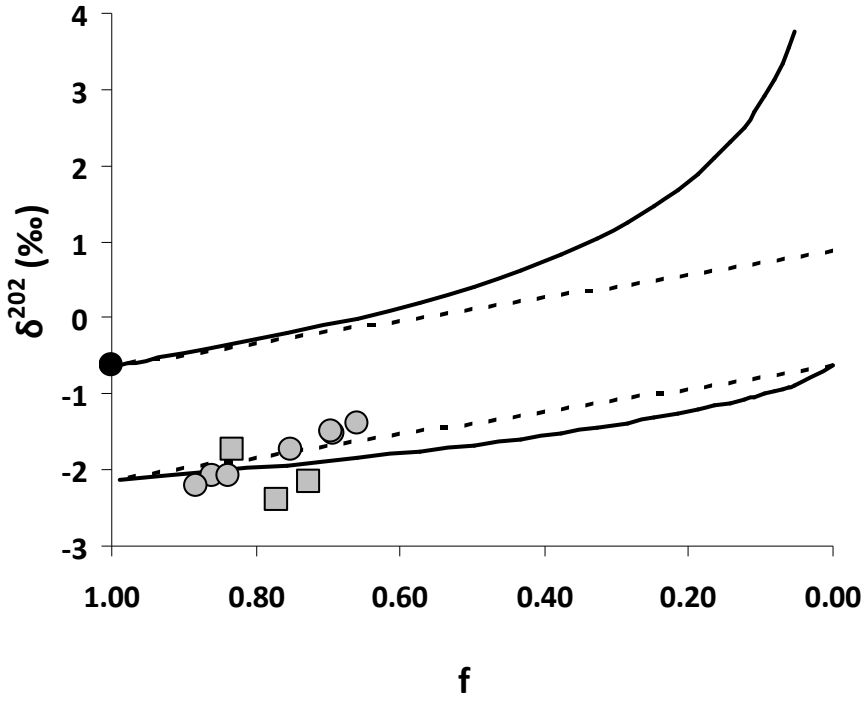

Figure 4.4. Non-purgeable δ^{202}Hg data with superimposed models. Rayleigh fractionation model (dark lines) and closed system equilibrium model (dotted lines). Black symbol is measurement of initial gaseous Hg(0) reactant, grey symbols are measured δ^{202}Hg values for non-purgeable Hg. Three symbols are marked as squares for clarity purposes in the text. Fractionation models are based on a fractionation factor of 1.0015 and an initial Hg(0) δ^{202}Hg of -0.63‰. Note that the value of 1.0015 is chosen as an approximation for illustrative purposes. Uncertainties in δ^{202}Hg data are the same size as symbols.

Table 4.1. δ^{202}Hg of aqueous Hg(0) during dissolution and sampling. 585 ng of Hg(0) was injected into the headspace of the 150 mL reactor containing 50 mL of buffer solution and sampled over time.

Sample	**δ^{202}Hg (‰)**	**[$Hg_{(aq)}$] (ng/ml)**
Source	-0.63‰	--
12 min	-0.91‰	9.45
45 min	-0.91‰	8.91
1.5 h	-0.82‰	8.50
3 h	-0.83‰	7.72

Table 4.2. δ^{202}Hg of non-purgeable Hg produced by *D. desulfuricans* ND132. A and B represent duplicate experiments. 12 min samples were not analyzed due to the low concentration/volume of samples.

Sample	δ^{202}Hg (‰)	Hg retained (ng/ml)
Source	-0.63	--
12 min A	--	0.53
45 min A	-2.07	1.67
1.5 h A	-2.08	2.00
3 h A	-2.39	2.93
5 h A	-1.53	4.12
23 h A	-1.39	4.99
12 min B	--	0.66
45 min B	-2.20	1.41
1.5 h B	-1.72	2.06
3 h B	-2.15	3.51
5 h B	-1.74	3.44
23 h B	-1.49	4.75

CHAPTER 5

CONCLUSION

The main conclusions of this dissertation are: (1) diverse anaerobic bacteria oxidize Hg(0) to Hg(II), (2) anaerobic mercury-methylating bacteria produce MeHg when provided with Hg(0) as their sole mercury source, (3) Hg oxidation by the anaerobic bacteria in this dissertation is mediated by a passive cellular mechanism, and (4) mass dependent stable isotope fractionation during Hg(0) oxidation by *D. desulfuricans* ND132 enriches Hg(II) in the light isotopes. Overall, our work calls into question the classification of Hg(0) as inert (Morel et al., 1998), since it is highly reactive toward anaerobic bacteria in pure culture. The results of this study also have several more specific environmental implications. First, the oxidation of Hg(0) by the diverse anaerobic bacteria in this dissertation suggests that Hg oxidation ability may be widespread among bacteria. Next, Hg(0) oxidation could be a competing reaction to Hg reduction that controls mercury transport and the pool of Hg available for methylation in anoxic environments. Our study with the anaerobic mercury-methylating bacterium *D. desulfuricans* ND132 points out that Hg(0) may be an unrecognized source of MeHg in the environment. Fourth, Hg(0) oxidation by anaerobic bacteria could be the prevailing Hg redox transformation in low nutrient environments inhabited by inactive or slowly metabolizing bacteria. Last, pools of Hg(II) with lower δ^{202}Hg than that of their sources could result from Hg(0) oxidation. The specific contributions of each dissertation chapter are highlighted below.

Chapter 2 documents the production of inorganic Hg(II) and MeHg from dissolved Hg(0) by *Desulfovibrio desulfuricans* ND132. By performing X-ray absorption spectroscopy (XAS) and ethylation experiments, we demonstrated that oxidized Hg(II) was unequivocally produced by the cells. Our data also shows that the oxidation reaction is mediated by the cells and not their extracellular exudates. XAS data suggests that the Hg(II) produced by *D. desulfuricans* ND132 was bound to cellular thiol functional groups, which highlights the potential role of these sulfhydryl moieties in the oxidation mechanism. Last, we showed that MeHg production from Hg(0) was positively correlated with cell growth and may have been related to the aggregation state of the cells. This chapter is the first work to demonstrate the oxidation, and subsequent methylation, of Hg(0) by an anaerobic bacterium, and highlights a potentially overlooked source of MeHg in the environment.

After demonstrating Hg(0) oxidation activity in one anaerobic strain, we then examined the Hg oxidation abilities of other diverse anaerobic bacteria in Chapter 3. The obligate anaerobic bacterium *Geothrix fermentans* H5 and the facultative anaerobic bacteria *Shewanella oneidensis* MR-1 and *Cupriavidus metallidurans* AE104 all oxidized Hg(0) to Hg(II). As in Chapter 2, we confirmed the presence of Hg(II) using XAS and ethylation experiments and also used the XAS data to demonstrate that oxidized mercury was covalently bound to the cells (likely to reduced sulfur). This study expands the list of bacteria that are known to oxidize Hg from catalase and non-catalase carrying aerobic bacteria in Smith *et al.* (1998) and the obligate anaerobic bacteria in Chapter 2, suggesting that Hg(0) oxidation activity may be widespread among bacteria.

Interestingly, we found that heat-inactivated cells and live cells oxidized Hg to similar extents, indicating that mercury oxidation occurs by a passive cellular mechanism in these bacteria. This discovery demonstrates that the oxidation of Hg(0) by bacteria occurs by at least two different pathways (catalase and non-catalase). Since mercury reduction by bacteria is an energy dependent process that requires active metabolism (Barkay et al., 2003; Wiatrowski et al., 2006), mercury oxidation may prove to be the prevailing redox transformation pathway in oligotrophic environments. These results also imply that some bacteria that can reduce Hg(II), such as *S. oneidensis* MR-1 (Wiatrowski et al., 2006), may play a dual role in the mercury cycle by both oxidizing and reducing Hg.

Chapter 4 provides preliminary insight into Hg stable isotope fractionation during the oxidation of Hg(0) to Hg(II) by *D. desulfuricans* ND132. The data shows that the oxidation pathway results in the preferential accumulation of the light isotopes of mercury in the Hg(II) product. No mass-independent fractionation was observed during this dark reaction, and fractionation appears to be the result of a kinetic isotope effect. This study is the first to demonstrate Hg stable isotope fractionation during Hg(0) oxidation, and these results have important implications for environmental Hg isotope signatures. Since Hg(0) is volatile and can partition into the gas phase, the oxidation of Hg(0) provides a means by which isotopically light Hg (relative to its source) can accumulate in aquatic or sedimentary environments. Equipped with this qualitative understanding of Hg stable isotope fractionation during Hg(0) oxidation by anaerobic

bacteria, isotope geochemists can now better interpret environmental Hg isotope signatures.

Suggestions for Future Research

The results of these experimental studies open up many new questions, but also guide future research. The next research question to be explored should be: how important is Hg(0) oxidation by anaerobic bacteria in the environment? A simultaneous two-pronged approach using chemical and stable isotope methods provides a potentially fruitful path forward.

Reacting dissolved Hg(0) with environmental materials from anoxic zones, such as groundwater, sediment, and microbial consortia, could provide initial insight into the importance of Hg(0) oxidation in these environments. Quantification of the rates of Hg(0) oxidation and Hg(II) reduction by pure cultures of bacteria and environmental samples could also lead to improved understanding regarding the dominant redox transformations under a given set of conditions. These studies are not likely to directly demonstrate that the oxidation of Hg(0) is caused by anaerobic bacteria, but mechanistic insights into bacterial oxidation would be useful to distinguish or determine similarities between this reaction and oxidation by other agents. We have suggested the potential role of reduced thiol moieties in Hg(0) oxidation by anaerobic bacteria in this dissertation. The use of 'thiol-blocking' agents, such as N-ethylmaleimide and monobromobimane, to perform Hg(0) oxidation experiments with bacteria, dissolved organic matter, and model thiol compounds will allow this hypothesis to be tested.

Quantification of thiol groups in bacteria using newly developed methods (Joe-Wong et al., 2012) also provides a means for developing correlations between oxidation activity and thiol content.

Solidifying an experimental fractionation factor for the anaerobic oxidation of Hg(0) observed in Chapter 4 should complement the above work. Doing so will require developing a method for trapping reactant Hg(0) separated from product non-purgeable Hg to attain a mass balance and accurately model the isotope data. Measuring the δ^{202}Hg of reactant and product will allow unequivocal modeling according to a Rayleigh fractionation or closed system equilibrium model. The experimental setup employed in Chapter 4 may need to be modified if Hg(0) dissolution/volatilization cannot be incorporated into the isotope fractionation modeling. Removal of gaseous Hg(0) phase could be accomplished using Cubitainers®, which would be filled completely with an Hg(0) saturated solution at the start of the experiment. Sub-sampling would not require the injection of N_2 gas and no headspace volume would be created since the walls of these containers are collapsible. Other approaches could include sacrificing no-headspace bottles at each time point or using a dual-syringe technique to inject fresh medium into a no-headspace bottle while simultaneously allowing the increase in pressure to take a liquid sample through the other syringe.

Performing experiments with other oxidizing agents will be important to explaining fractionation in a potentially complex microbial system and distinguishing oxidation by these agents from bacterial oxidation in the environment. Determination of fractionation factors for the abiotic oxidation of Hg(0) by strong oxidants like BrCl or

$KMnO_4$ should be straightforward and allow the isolation of Hg(0) oxidation from Hg(0) sorption. From there, the experiments of Zheng *et al.* (2012) showing the oxidation of Hg(0) by model thiol compounds could be repeated with isotopic analysis of reactant and product. These different reaction mechanisms will likely result in distinct fractionation factors, as have been observed for the biotic and abiotic reduction of Hg(II) (Kritee et al., 2013). Thus, fractionation of Hg isotopes during oxidation by various environmental media should be measured and compared to the fractionation factors for biotic and abiotic oxidation. Similarly, if Hg(0) concentrations and isotope composition in aquatic systems such as East Fork Poplar Creek (Brooks and Southworth, 2011) are measured with distance from their source, the role of Hg oxidation in these systems could potentially be determined.

In confined aquifer systems, Hg(0) and Hg(II) can remain in contact for extended periods of time. For this reason, and due to the potential influence of isotopic equilibrium on Hg oxidation experiments, equilibrium isotope exchange between Hg(0) and Hg(II) should be quantified, as has been done with Cr(III) / Cr(VI) (Zink et al., 2010) and Fe(II) / Fe(III) (Johnson et al., 2002; Welch et al., 2003). In these experiments, aqueous reduced and oxidized species with δ = 0‰ were mixed at different ratios and measured for isotope composition with time. The isotope exchange reaction between reduced and oxidized forms of iron occurs on the time-scale of seconds and overwhelms the kinetic isotope effects of iron redox changes (Kappler et al., 2010). For aqueous Cr(III) and Cr(VI), isotope exchange is slow, with neither species showing a change in δ over a period of 8 weeks (Zink et al., 2010). The rate of isotopic exchange and the

fractionation factor for isotopic equilibration between aqueous Hg(0) and Hg(II) is unknown.

This dissertation lays the groundwork for future studies of Hg(0) oxidation. Since Hg(0) oxidation and Hg(II) reduction play a key role in Hg transport and the availability of Hg for conversion to bioaccumulative MeHg, the quantification of rates of oxidation against rates of reduction and determination of the conditions that promote one redox change over the other are essential. A deeper understanding of oxidation processes in the environment is required not only for bacteria, but also for dissolved organic matter (Gu et al., 2011) and light (Lalonde et al., 2001), since all of these oxidizing agents play a dual role in both oxidizing and reducing Hg. The above outlined isotopic approaches to examining the oxidation of Hg(0) by bacteria could be readily applied to studies of oxidation by dissolved organic matter and light.

REFERENCES

Aakesson R., Persson I., Sandstroem M. and Wahlgren U. (1994) Structure and Bonding of Solvated Mercury(II) and Thallium(III) Dihalide and Dicyanide Complexes by XAFS Spectroscopic Measurements and Theoretical Calculations. *Inorg. Chem.* 33, 3715–3723.

Al-Abed S. R., Jegadeesan G., Scheckel K. G. and Tolaymat T. (2008) Speciation, characterization, and mobility of As, Se, and Hg in flue gas desulphurization residues. *Environ. Sci. Technol.* 42, 1693–1698.

Amyot, M., McQueen, D.J., Mierle, G., and Lean, D.R.S. (1994) Sunlight-Induced Formation of Dissolved Gaseous Mercury in Lake Waters. *Environ. Sci. Technol.* 28, 2366–2371.

Amyot M., Gill G. A. and Morel F. M. M. (1997) Production and loss of dissolved gaseous mercury in coastal seawater. *Environ. Sci. Technol.* 31, 3606–3611.

Amyot M., Lean D. R. S., Poissant L. and Doyon M. R. (2000) Distribution and transformation of elemental mercury in the St. Lawrence River and Lake Ontario. *Can. J. Fish Aquat. Sci.* 57, 155–163.

Amyot M., Morel F. M. M. and Ariya P. A. (2005) Dark oxidation of dissolved and liquid elemental mercury in aquatic environments. *Environ. Sci. Technol.* 39, 110–114.

Andersson M. E., Sommar J., Gardfeldt K. and Lindqvist O. (2008) Enhanced concentrations of dissolved gaseous mercury in the surface waters of the Arctic Ocean. *Mar. Chem.* 110, 190–194.

Balch W. E., Fox G. E., Magrum L. J., Woese C. R. and Wolfe R. S. (1979) Methanogens: reevaluation of a unique biological group. *Microbiol. Rev.* 43, 260–296.

Barkay T., Gillman M. and Turner R. R. (1997) Effects of dissolved organic carbon and salinity on bioavailability of mercury. *Appl. Environ. Microb.* 63, 4267–4271.

Barkay T., Miller S. M. and Summers A. O. (2003) Bacterial mercury resistance from atoms to ecosystems. *FEMS Microbiol. Rev.* 27, 355–384.

Barkay, T., Wagner-Dobler, I., 2005. Microbial transformations of mercury: Potentials, challenges, and achievements in controlling mercury toxicity in the environment. Advances in Applied Microbiology 57, 1–52.

Barringer, J.B., Szabo, Z., and Reilly, P.A. (2013). Occurrence and Mobility of Mercury in Groundwater. In Current Perspectives in Contaminant Hydrology and Water Resources Sustainability, InTech.

Bartov, G., Deonarine, A., Johnson, T.M., Ruhl, L., Vengosh, A., and Hsu-Kim, H. (2013). Environmental Impacts of the Tennessee Valley Authority Kingston Coal Ash Spill. 1. Source Apportionment Using Mercury Stable Isotopes. Environ. Sci. Technol. *47*, 2092–2099.

Benoit J. M., Gilmour C. C., Mason R. P. and Heyes A. (1999) Sulfide controls on mercury speciation and bioavailability to methylating bacteria in sediment pore waters. *Environ. Sci. Technol.* 33, 951–957.

Benoit J. M., Gilmour C. C. and Mason R. P. (2001) The influence of sulfide on solid phase mercury bioavailability for methylation by pure cultures of *Desulfobulbus propionicus* (1pr3). *Environ. Sci. Technol.* 35, 127–132.

Bergquist, B.A., and Blum, J.D. (2007). Mass-dependent and -independent fractionation of Hg isotopes by photoreduction in aquatic systems. Science *318*, 417–420.

Biester, H., Gosar, M., Covelli, S., 2000. Mercury speciation in sediments affected by dumped mining residues in the drainage area of the Idrija mercury mine, Slovenia. Environmental Science & Technology 34 (16), 3330–3336.

Bigeleisen, J., and Mayer, M.G. (1947). Calculation of equilibrium constants for isotopic exchange reactions. J. Chem. Phys. *15*, 261–267.

Bigeleisen, J., and Wolfsberg, M. (1958). Theoretical and experimental aspects of isotope effects in chemical kinetics. Advances in Chem. Phys. *1*, 15–76.

Biswas A., Brooks S. C., Miller C. L., Mosher J. J., Yin X. L. and Drake M. M. (2011) Bacterial growth phase influences methylmercury production by the sulfate-reducing bacterium *Desulfovibrio desulfuricans* ND132. *Sci. Total Environ.* 409, 3943-3948.

Bloom N. (1989) Determination of Picogram Levels of Methylmercury by Aqueous Phase Ethylation, Followed by Cryogenic Gas Chromatography with Cold Vapour Atomic Fluorescence Detection. *Can. J. Fish Aquat. Sci.* 46, 1131–1140.

Blum, J.D., and Bergquist, B.A. (2007). Reporting of variations in the natural isotopic composition of mercury. Anal. Bioanal. Chem. *388*, 353–359.

Bone S. E., Charette M. A., Lamborg C. H. and Gonneea M. E. (2007) Has submarine groundwater discharge been overlooked as a source of mercury to coastal waters? *Environ. Sci. Technol.* 41, 3090–3095.

Bouffard, A., and Amyot, M. (2009). Importance of elemental mercury in lake sediments. Chemosphere *74*, 1098–1103.

Brigatti M. F., Colonna S., Malferrari D., Medici L. and Poppi L. (2005) Mercury adsorption by montmorillonite and vermiculite: a combined XRD, TG-MS, and EXAFS study. *Appl. Clay Sci.* 28, 1–8.

Brooks, S.C., Southworth, G.R., 2011. History of mercury use and environmental contamination at the Oak Ridge Y-12 Plant. Environmental Pollution 159 (1), 219–228.

Campbell K. R., Ford C. J. and Levine D. A. (1998) Mercury distribution in Poplar Creek, Oak Ridge, Tennessee, USA. *Environ. Toxicol. Chem.* 17, 1191–1198.

Charlet L., Bosbach D. and Peretyashko T. (2002) Natural attenuation of TCE, As, Hg linked to the heterogeneous oxidation of Fe(II): an AFM study. *Chem. Geol.* 190, 303–319.

Choi S. C., Chase T. and Bartha R. (1994) Metabolic Pathways Leading to Mercury Methylation in *Desulfovibrio desulfuricans* LS. *Appl. Environ. Microb.* 60, 4072–4077.

Cline, J.D. (1969) Spectrophotometric determination of hydrogen sulfide in natural waters. *Limnol. Oceonogr.* 14, 454-458.

Coates, J.D., Ellis, D.J., Gaw, C.V., Lovley, D.R., 1999. *Geothrix fermentans* gen. nov., sp nov., a novel Fe(III)-reducing bacterium from a hydrocarbon-contaminated aquifer. International Journal of Systematic Bacteriology 49, 1615–1622.

Cohen-Atiya M. and Mandler D. (2003) Studying thiol adsorption on Au, Ag and Hg surfaces by potentiometric measurements. *J. Electroanal. Chem.* 550-551, 267–276.

Colombo, M.J., Ha, J., Reinfelder, J.R., Barkay, T., Yee, N., 2013. Anaerobic oxidation of Hg(0) and methylmercury formation by *Desulfovibrio desulfuricans* ND132. Geochimica et Cosmochimica Acta 112, 166–177.

Colombo, M.J., Ha, J., Reinfelder, J.R., Barkay, T., Yee, N. Oxidation of Hg(0) to Hg(II) by Diverse Anaerobic Bacteria. Chemical Geology, submitted.

Compeau G. C. and Bartha R. (1985) Sulfate-Reducing Bacteria: Principal Methylators of Mercury in Anoxic Estuarine Sediment. *Appl. Environ. Microb.* 50, 498–502.

Craft, D., Fields, J., Yoder, N., 2005. Mercury in the Carson River Basin, California and Nevada. U.S. Department of the Interior.

Daughney C. J., Siciliano S. D., Rencz A. N., Lean D. and Fortin D. (2002) Hg(II) adsorption by bacteria: A surface complexation model and its application to shallow acidic lakes and wetlands in Kejimkujik National Park, Nova Scotia, Canada. *Environ. Sci. Technol.* 36, 1546–1553.

Demagalhaes M. E. A. and Tubino M. (1995) A possible path for mercury in biological systems: the oxidation of metallic mercury by molecular oxygen in aqueous solutions. *Sci. Total Environ.* 170, 229–239.

Dominique, Y., Muresan, B., Duran, R., Richard, S., and Boudou, A. (2007). Simulation of the chemical fate and bioavailability of liquid elemental mercury drops from gold mining in amazonian freshwater systems. Environmental Science & Technology *41*, 7322–7329.

Drott A., Lambertsson L., Bjorn E. and Skyllberg U. (2007) Importance of dissolved neutral mercury sulfides for methyl mercury production in contaminated sediments. *Environ. Sci. Technol.* 41, 2270–2276.

Ekstrom E. B. and Morel F. M. M. (2008) Cobalt limitation of growth and mercury methylation in sulfate-reducing bacteria. *Environ. Sci. Technol.* 42, 93–99.

Ekstrom E. B., Morel F. M. M. and Benoit J. M. (2003) Mercury methylation independent of the acetyl-coenzyme a pathway in sulfate-reducing bacteria. *Appl. Environ. Microb.* 69, 5414–5422.

Estrade, N., Carignan, J., Sonke, J.E., and Donard, O.F.X. (2009). Mercury isotope fractionation during liquid-vapor evaporation experiments. Geochimica Et Cosmochimica Acta *73*, 2693–2711.

Estrade, N., Carignan, J., and Donard, O.F.X. (2011). Tracing and Quantifying Anthropogenic Mercury Sources in Soils of Northern France Using Isotopic Signatures. Environ. Sci. Technol. *45*, 1235–1242.

Eyster, H.C., 1950. Effect of temperature on catalase activity. The Ohio Journal of Science 50 (6), 273–277.

Fahey, R.C., 2001. Novel thiols of prokaryotes. Annual Review of Microbiology 55, 333–356.

Fang, S.C. (1981). Studies on the sorption of elemental mercury vapor by soils. Arch. Environ. Contam. Toxicol. *10*, 193–201.

Feng, X., Foucher, D., Hintelmann, H., Yan, H., He, T., and Qiu, G. (2010). Tracing Mercury Contamination Sources in Sediments Using Mercury Isotope Compositions. Environ. Sci. Technol. *44*, 3363–3368.

Finneran, K.T., Housewright, M.E., Lovley, D.R., 2002. Multiple influences of nitrate on uranium solubility during bioremediation of uranium-contaminated subsurface sediments. Environmental Microbiology 4 (9), 510–516.

Fitzgerald W. F., Mason R. P. and Vandal G. M. (1991) Atmospheric cycling and air-water exchange of mercury over mid-continental lacustrine regions. *Water Air Soil Poll.* 56, 745–767.

Fitzgerald, W.F., Engstrom, D.R., Mason, R.P., and Nater, E.A. (1998). The case for atmospheric mercury contamination in remote areas. Environ. Sci. Technol. *32*, 1–7.

Fitzgerald, W.F., Lamborg, C.H., and Hammerschmidt, C.R. (2007). Marine biogeochemical cycling of mercury. Chem. Rev. *107*, 641–662.

Fleming, E.J., Mack, E.E., Green, P.G., and Nelson, D.C. (2006). Mercury methylation from unexpected sources: Molybdate-inhibited freshwater sediments and an iron-reducing bacterium. Applied and Environmental Microbiology *72*, 457–464.

Foucher, D., Ogrinc, N., and Hintelmann, H. (2009). Tracing Mercury Contamination from the Idrija Mining Region (Slovenia) to the Gulf of Trieste Using Hg Isotope Ratio Measurements. Environmental Science & Technology *43*, 33–39.

Foucher, D., Hintelmann, H., Al, T.A., and MacQuarrie, K.T. (2013). Mercury isotope fractionation in waters and sediments of the Murray Brook mine watershed (New Brunswick, Canada): Tracing mercury contamination and transformation. Chem. Geol. *336*, 87–95.

Gehrke, G.E., Blum, J.D., and Marvin-DiPasquale, M. (2011a). Sources of mercury to San Francisco Bay surface sediment as revealed by mercury stable isotopes. Geochim. Cosmochim. Acta *75*, 691–705.

Gehrke, G.E., Blum, J.D., Slotton, D.G., and Greenfield, B.K. (2011b). Mercury Isotopes Link Mercury in San Francisco Bay Forage Fish to Surface Sediments. Environ. Sci. Technol. *45*, 1264–1270.

Gihring T. M., Zhang G., Brandt C. C., Brooks S. C., Campbell J. H., Carroll S., Criddle C. S., Green S. J., Jardine P., Kostka J. E., Lowe K., Mehlhorn T. L., Overholt W., Watson D. B., Yang Z., Wu W.-M. and Schadt Christopher W. (2011) A limited microbial consortium is responsible for extended bioreduction of uranium in a contaminated aquifer. *Appl. Environ. Microbiol.* 77, 5955–5965.

Gilmour C. C., Henry E. A. and Mitchell R. (1992) Sulfate stimulation of mercury methylation in freshwater sediments. *Environ. Sci. Technol.* 26, 2281–2287.

Gilmour C. C., Elias D. A., Kucken A. M., Brown S. D., Palumbo A. V., Schadt C. W. and Wall J. D. (2011) Sulfate-Reducing Bacterium *Desulfovibrio desulfuricans* ND132 as a Model for Understanding Bacterial Mercury Methylation. *Appl. Environ. Microb.* 77, 3938–3951.

Gray, J.E., Hines, M.E., Higueras, P.L., Adatto, I., Lasorsa, B.K., 2004. Mercury speciation and microbial transformations in mine wastes, stream sediments, and surface waters at the Almaden Mining District, Spain. Environmental Science & Technology 38 (16), 4285–4292.

Gu B. H., Bian Y. R., Miller C. L., Dong W. M., Jiang X. and Liang L. Y. (2011) Mercury reduction and complexation by natural organic matter in anoxic environments. *P. Natl. Acad. Sci. USA* 108, 1479–1483.

Harada, M. (1995). Minamata Disease - Methylmercury Poisoning in Japan Caused by Environmental-Pollution. Crit. Rev. Toxicol. *25*, 1–24.

Harris H. H., Pickering I. and George G. N. (2003) The chemical form of mercury in fish. *Science* 301, 1203.

Hoefs, J. (2009). Stable Isotope Geochemistry (Springer).

Horvat M., Bloom N. S. and Liang L. (1993) Comparison of distillation with other current isolation methods for the determination of methyl mercury compounds in low level environmental samples: Part 1. Sediments. *Anal. Chim. Acta* 281, 135–152.

Hsu-Kim, H., Kucharzyk, K.H., Zhang, T., and Deshusses, M.A. (2013). Mechanisms Regulating Mercury Bioavailability for Methylating Microorganisms in the Aquatic Environment: A Critical Review. Environ. Sci. Technol. *47*, 2441–2456.

Huggins F. E., Huffman G. P., Dunham G. E. and Senior C. L. (1998) XAFS Examination of Mercury Sorption on Three Activated Carbons. *Energ. Fuel.* 13, 114–121.

Hwang C., Wu W., Gentry T. J., Carley J., Corbin G. A., Carroll S. L., Watson D. B., Jardine P. M., Zhou J., Criddle C. S. and Fields M. W. (2009) Bacterial community succession during in situ uranium bioremediation: spatial similarities along controlled flow paths. *ISME J.* 3, 47–64.

Jackson, T.A., Whittle, D.M., Evans, M.S., and Muir, D.C.G. (2008). Evidence for mass-independent and mass-dependent fractionation of the stable isotopes of mercury by natural processes in aquatic ecosystems. Appl. Geochem. *23*, 547–571.

Jew A. D., Kim C. S., Rytuba J. J., Gustin M. S. and Brown G. E. (2011) New Technique for Quantification of Elemental Hg in Mine Wastes and Its Implications for Mercury Evasion Into the Atmosphere. *Environ. Sci. Technol.* 45, 412–417.

Jiskra, M., Wiederhold, J.G., Bourdon, B., and Kretzschmar, R. (2012). Solution Speciation Controls Mercury Isotope Fractionation of Hg(II) Sorption to Goethite. Environ. Sci. Technol. *46*, 6654–6662.

Joe-Wong, C., Shoenfelt, E., Hauser, E.J., Crompton, N., Myneni, S.C.B., 2012. Estimation of Reactive Thiol Concentrations in Dissolved Organic Matter and Bacterial Cell Membranes in Aquatic Systems. Environmental Science & Technology 46 (18), 9854–9861.

Johnson, T.M. (2011). Stable Isotopes of Cr and Se as Tracers of Redox Processes in Earth Surface Environments. In Handbook of Environmental Isotope Geochemistry, (New York: Springer), pp. 155–176.

Johnson, C.M., Skulan, J.L., Beard, B.L., Sun, H., Nealson, K.H., and Braterman, P.S. (2002). Isotopic fractionation between Fe(III) and Fe(II) in aqueous solutions. Earth and Planetary Science Letters *195*, 141–153.

Johnson, C.M., Beard, B.L., and Albarede, F. (2004). Overview and General Concepts. Reviews in Mineralogy and Geochemistry *55*, 1–24.

Jonas R. B., Gilmour Cynthia C., Stoner D. L., Weir M. M. and Tuttle J. H. (1984) Comparison of methods to measure acute metal and organometal toxicity to natural aquatic microbial communities. *Appl. Environ. Microbiol.* 47, 1005–11.

Kappler, A., Johnson, C.M., Crosby, H.A., Beard, B.L., and Newman, D.K. (2010). Evidence for equilibrium iron isotope fractionation by nitrate-reducing iron(II)-oxidizing bacteria. Geochim. Cosmochim. Acta *74*, 2826–2842.

Kerin, E.J., Gilmour, C.C., Roden, E., Suzuki, M.T., Coates, J.D., and Mason, R.P. (2006). Mercury methylation by dissimilatory iron-reducing bacteria. Applied and Environmental Microbiology *72*, 7919–7921.

Khwaja A. R., Bloom Paul R. and Brezonik P. L. (2006) Binding Constants of Divalent Mercury (Hg^{2+}) in Soil Humic Acids and Soil Organic Matter. *Environ. Sci. Technol.* 40, 844–849.

Kim C. S., Brown G. E., and Rytuba J. J. (2000) Characterization and speciation of mercury-bearing mine wastes using X-ray absorption spectroscopy. *Sci. Total Environ.* 261, 157-168.

Kim, C.S., Rytube, J.J., Brown G.E., 2004a. EXAFS study of mercury(II) sorption to Fe- and Al-(hydr)oxides - II. Effects of chloride and sulfate. Journal of Colloid and Interface Science 270 (1), 9-20.

Kim C. S., Rytuba J. J. and Brown G. E. (2004b) EXAFS study of mercury(II) sorption to Fe- and Al-(hydr)oxides I. Effects of pH. *J. Colloid Interf. Sci.* 271, 1–15.

Krishnan, S., Gullett, B., and Jozewicz, W. (1994). Sorption of Elemental Mercury by Activated Carbons. Environ. Sci. Technol. *28*, 1506–1512.

Kritee, K., Blum, J.D., Johnson, M.W., Bergquist, B.A., and Barkay, T. (2007). Mercury stable isotope fractionation during reduction of Hg(II) to Hg(0) by mercury resistant microorganisms. Environmental Science & Technology *41*, 1889–1895.

Kritee, K., Blum, J.D., and Barkay, T. (2008). Mercury Stable Isotope Fractionation during Reduction of Hg(II) by Different Microbial Pathways. Environmental Science & Technology *42*, 9171–9177.

Kritee, K., Barkay, T., and Blum, J.D. (2009). Mass dependent stable isotope fractionation of mercury during mer mediated microbial degradation of monomethylmercury. Geochimica Et Cosmochimica Acta *73*, 1285–1296.

Kritee, K., Blum, J.D., Reinfelder, J.R., and Barkay, T. (2013). Microbial stable isotope fractionation of mercury: A synthesis of present understanding and future directions. Chem. Geol. *336*, 13–25.

Lalonde J. D., Amyot M., Kraepiel A. M. L. and Morel F. M. M. (2001) Photooxidation of Hg(0) in artificial and natural waters. *Environ. Sci. Technol.* 35, 1367–1372.

Lalonde J. D., Amyot M., Orvoine J., Morel F. M. M., Auclair J. C. and Ariya P. A. (2004) Photoinduced Oxidation of Hg^0(aq) in the Waters from the St. Lawrence Estuary. *Environ. Sci. Technol.* 38, 508–514.

Lamborg, C.H., Tseng, C.M., Fitzgerald, W.F., Balcom, P.H., Hammerschmidt, C.R, 2003. Determination of the Mercury Complexation Characteristics of Dissolved Organic Matter in Natural Waters with “Reducible Hg” Titrations. Environmental Science & Technology 37 (15), 3316-3322.

Liang L., Watson D., Miller C., Howe J., He F. and Pierce E. (2012) The fate of mercury at a contaminated site. Goldschmidt Conference, Montreal, Canada.

Lin C. and Jay J.A. (2007) Mercury Methylation by Planktonic and Biofilm Cultures of *Desulfovibrio desulfuricans*. *Environ. Sci. Technol.* 41, 6691-6697.

Lin, C.J., and Pehkonen, S.O. (1999). The chemistry of atmospheric mercury: a review. Atmos. Environ. *33*, 2067–2079.

Lin, C.-C., Yee, N., and Barkay, T. (2011). Microbial Transformations in the Mercury Cycle. In Environmental Chemistry and Toxicology of Mercury, G. Liu, Y. Cai, and N. O’Driscoll, eds. John Wiley & Sons, pp. 155–191.

Liu, J., Feng, X., Yin, R., Zhu, W., and Li, Z. (2011). Mercury distributions and mercury isotope signatures in sediments of Dongjiang, the Pearl River Delta, China. Chem. Geol. *287*, 81–89.

Lockwood, R.A., Chen, K.Y., 1974. Adsorption of Hg (II) by ferric hydroxide. Environmental Letters 6 (3), 151–166.

Lovley, D.R., Chapelle, F.H., 1995. Deep Subsurface Microbial Processes. Reviews of Geophysics 33 (3), 365–381.

MacNaughton, M.G., James, R.O., 1974. Adsorption of aqueous mercury (II) complexes on the oxide/water interface. Journal of Colloid and Interface Science 46 (2), 431-440.

Mason, R.P., Reinfelder, J.R., Morel, F.M.M., 1995. Bioaccumulation of mercury and methylmercury. Water Air and Soil Pollution 80 (1-4), 915–921.

Mergeay, M., Nies, D., Schlegel, H.G., Gerits, J., Charles, P., Vangijsegem, F., 1985. *Alcaligenes eutrophus* CH34 is a Facultative Chemolithotroph with Plasmid-bound Resistance to Heavy Metals. Journal of Bacteriology 162 (1), 328–334.

Mierle, G., Ingram, R., 1991. The role of humic substances in the mobilization of mercury from watersheds. Water Air and Soil Pollution 56 (1), 349-357.

Mishra B., O'Loughlin E. J., Boyanov M. I. and Kemner K. M. (2011) Binding of Hg^{II} to High-Affinity Sites on Bacteria Inhibits Reduction to Hg^{0} by Mixed $Fe^{II/III}$ Phases. *Environ. Sci. Technol.* 45, 9597–9603.

Morel F. M. M., Kraepiel A. M. L. and Amyot M. (1998) The chemical cycle and bioaccumulation of mercury. *Annu. Rev. Ecol. Syst.* 29, 543–566.

Morris, S.L., Walsh, R.C., Hansen, J.N., 1984. Identification and characterization of some bacterial membrane sulfhydryl groups which are targets of bacteriostatic and antibiotic action. The Journal of Biological Chemistry 259 (21), 13590–13594.

Murphy E. A., Dooley J., Windom H. L. and Smith R. G. (1994) Mercury species in potable ground water in southern New Jersey. *Water Air Soil Poll.* 78, 61–72.

Myers, C., Nealson, K., 1988. Bacterial Manganese Reduction and Growth with Manganese Oxide as the Sole Electron-Acceptor. Science 240 (4857), 1319–1321.

Newton, D.W., Ellis, R., Paulsen, G.M., 1976. Effect of pH and complex formation on mercury (II) adsorption by bentonite. Journal of Environmental Quality 5 (3), 251–254.

Newville M. (2001) IFEFFIT: interactive XAFS analysis and FEFF fitting. *J. Synchrotron Radiat.* 8, 322–324.

Osborne, F.H., Ehrlich, H.L., 1976. Oxidation of arsenite by a soil isolate of *Alcaligenes*. Journal of Applied Microbiology 41 (2), 295–305.

Parks, J.M., Johs, A., Podar, M., Bridou, R., Hurt, R.A., Smith, S.D., Tomanicek, S.J., Qian, Y., Brown, S.D., Brandt, C.C., et al. (2013). The Genetic Basis for Bacterial Mercury Methylation. Science *339*, 1332–1335.

Pecora, W.T. (1970) Mercury in the Environment. Washington, D.C., U.S. Geological Survey, p. 62.

Point, D., Sonke, J.E., Day, R.D., Roseneau, D.G., Hobson, K.A., Vander Pol, S.S., Moors, A.J., Pugh, R.S., Donard, O.F.X., and Becker, P.R. (2011). Methylmercury photodegradation influenced by sea-ice cover in Arctic marine ecosystems. Nat. Geosci. *4*, 188–194.

Poulain A. J., Garcia E., Amyot M., Campbell P. G. C., Raofie F. and Ariya P. A. (2007) Biological and chemical redox transformations of mercury in fresh and salt waters of the high arctic during spring and summer. *Environ. Sci. Technol.* 41, 1883–1888.

Powers L. (1982) X-ray absorption spectroscopy Application to biological molecules. *BBA-Rev. Bioenergetics* 683, 1–38.

Rajan M., Darrow J., Hua M., Barnett B., Mendoza M., Greenfield B. K. and Andrews J. C. (2008) Hg L_3 XANES Study of Mercury Methylation in Shredded *Eichhornia crassipes*. *Environ. Sci. Technol.* 42, 5568–5573.

Rapsomanikis, S., Donard, O.F.X. and Weber, J.H. (1986) Speciation of Lead and Methyllead Ions in Water by Chromatography/Atomic Absorption Spectrometry after Ethylation with Sodium Tetraethylborate. *Anal. Chem.* 58, 35-38.

Riddle S. G., Tran H. H., Dewitt J. G. and Andrews J. C. (2002) Field, Laboratory, and X-ray Absorption Spectroscopic Studies of Mercury Accumulation by Water Hyacinths. *Environ. Sci. Technol.* 36, 1965–1970.

Riley R.G., Zachara J.M., and Wobber F.J. (1992) Chemical contaminants on DOE lands and selection of contaminant mixtures for subsurface science research. Washington, D.C., U.S. Department of Energy, p. 77.

Rimondi, V., Gray, J.E., Costagliola, P., Vaselli, O., Lattanzi, P., 2012. Concentration, distribution, and translocation of mercury and methylmercury in mine-waste, sediment, soil, water, and fish collected near the Abbadia San Salvatore mercury mine, Monte Amiata district, Italy. Science of the Total Environment 414, 318–327.

Rodriguez-Gonzalez, P., Epov, V.N., Bridou, R., Tessier, E., Guyoneaud, R., Monperrus, M., and Amouroux, D. (2009). Species-Specific Stable Isotope Fractionation of Mercury during Hg(II) Methylation by an Anaerobic Bacteria (*Desulfobulbus propionicus*) under Dark Conditions. Environmental Science & Technology *43*, 9183–9188.

Schaefer J. K. and Morel F. M. M. (2009) High methylation rates of mercury bound to cysteine by *Geobacter sulfurreducens*. *Nat. Geosci.* 2, 123–126.

Schaefer, J.K., Yagi, J., Reinfelder, J.R., Cardona, T., Ellickson, K.M., Tel-Or, S., and Barkay, T. (2004). Role of the bacterial organomercury lyase (MerB) in controlling methylmercury accumulation in mercury-contaminated natural waters. Environmental Science & Technology *38*, 4304–4311.

Schaefer J. K., Rocks S. S., Zheng W., Liang L. Y., Gu B. H. and Morel F. M. M. (2011) Active transport, substrate specificity, and methylation of Hg(II) in anaerobic bacteria. *P. Natl. Acad. Sci. USA* 108, 8714–8719.

Schauble, E.A. (2004). Applying stable isotope fractionation theory to new systems. Rev. Mineral. Geochem. *55*, 65–111.

Schauble, E.A. (2007). Role of nuclear volume in driving equilibrium stable isotope fractionation of mercury, thallium, and other very heavy elements. Geochimica et Cosmochimica Acta. *71*, 2170-2189.

Schuster, E., 1991. The behavior of mercury in the soil with special emphasis on complexation and adsorption processes – a review of the literature. Water Air and Soil Pollution 56, 667-680.

Selin N. E. (2009) Global Biogeochemical Cycling of Mercury: A Review. *Annu. Rev. Env. Resour.* 34, 43–63.

Selvendiran P., Driscoll C. T., Montesdeoca M. R. and Bushey J. T. (2008) Inputs, storage, and transport of total and methyl mercury in two temperate forest wetlands. *J. Geophys. Res-Biogeo.* 113. Available at: ://WOS:000261145200001.

Siciliano S. D., O'Driscoll N. J. and Lean D. R. S. (2002) Microbial reduction and oxidation of mercury in freshwater lakes. *Environ. Sci. Technol.* 36, 3064–3068.

Silver S. (1996) Bacterial resistances to toxic metal ions - a review. *Gene* 179, 9–19.

Skerfving, S.B., and Copplestone, J.F. (1976). Poisoning caused by the consumption of organomercury-dressed seed in Iraq. Bull World Health Organ *54*, 101–112.

Skogerboe R. K. and Wilson S. A. (1981) Reduction of ionic species by fulvic acid. *Anal. Chem.* 53, 228–32.

Skyllberg U., Bloom P. R., Qian J., Lin C.-M. and Bleam W. F. (2006) Complexation of Mercury(II) in Soil Organic Matter: EXAFS Evidence for Linear Two-Coordination with Reduced Sulfur Groups. *Environ. Sci. Technol.* 40, 4174–4180.

Smith T., Pitts K., McGarvey J. A. and Summers A. O. (1998) Bacterial oxidation of mercury metal vapor, Hg(0). *Appl. Environ. Microb.* 64, 1328–1332.

Sonke, J.E., and Blum, J.D. (2013). Advances in mercury stable isotope biogeochemistry Preface. Chem. Geol. *336*, 1–4.

Southworth G. R., Turner R. R., Peterson M. J. and Bogle M. A. (1995) Form of mercury in stream fish exposed to high concentrations of dissolved inorganic mercury. *Chemosphere* 30, 779–787.

Southworth G. R., Peterson M. J. and Bogle M. A. (2002) Effect of point source removal on mercury bioaccumulation in an industrial pond. *Chemosphere* 49, 455–460.

Southworth G. R., Turner R. R., Peterson M. J., Bogle M. A. and Ryon M. G. (2000) Response of mercury contamination in fish to decreased aqueous concentrations and loading of inorganic mercury in a small stream. *Environ. Monit. Assess.* 63, 481–494.

Southworth, G.R., Peterson, M.J., and Bogle, M.A. (2002). Effect of point source removal on mercury bioaccumulation in an industrial pond. Chemosphere *49*, 455–460.

Spangler, W.J., Spigarelli, J.L., Rose, J.M., and Miller, H.M. (1973). Methylmercury: Bacterial Degradation in Lake Sediments. Science *180*, 192–193.

Stoffers, P., Hannington, M., Wright, I., Herzig, P., and de Ronde, C. (1999). Elemental mercury at submarine hydrothermal vents in the Bay of Plenty, Taupo volcanic zone, New Zealand. Geology *27*, 931–934.

Stoor R. W., Hurley J. P., Babiarz C. L. and Armstrong D. E. (2006) Subsurface sources of methyl mercury to Lake Superior from a wetland-forested watershed. *Sci. Total Environ.* 368, 99–110.

Stumm W. and Morgan J.J. (1996) *Aquatic Chemistry: Chemical Equilibria and Rates in Natural Waters*. Wiley-Interscience, New York.

Suchanek, T.H., Richerson, P.J., Holts, L.J., Lamphere, B.A., Woodmansee, C.E., Slotton, D.G., Harner, E.J., Woodward, L.A., 1995. Impacts of mercury on benthic invertebrate populations and communities within the aquatic ecosystem of Clear Lake, California. Water Air and Soil Pollution 80, 951–960.

Turner R. R., Olsen C. R. and Wilcox W. J. (1984) Environmental fate of mercury and cesium-137 discharged from Oak Ridge facilities. *Trace Subst. Environ. Health* 18, 329–338.

Urey, H.C. (1947). Thermodynamic properties of isotopic substances. Journal of the Chemical Society 562–581.

Walvoord M. A., Andraski B. J., Krabbenhoft D. P. and Striegl R. G. (2008) Transport of elemental mercury in the unsaturated zone from a waste disposal site in an and region. *Appl. Geochem.* 23, 572–583.

Webb S. M. (2005) SIXpack: a graphical user interface for XAS analysis using IFEFFIT. *Phys. Scripta* T115, 1011–1014.

Welch, S.A., Beard, B.L., Johnson, C.M., and Braterman, P.S. (2003). Kinetic and equilibrium Fe isotope fractionation between aqueous Fe(II) and Fe(III). Geochimica Et Cosmochimica Acta *67*, 4231–4250.

Wiatrowski H. A., Das S., Kukkadapu R., Ilton E. S., Barkay T. and Yee N. (2009) Reduction of Hg(II) to Hg(0) by Magnetite. *Environ. Sci. Technol.* 43, 5307–5313.

Widdel, F., Schnell, S., Heising, S., Ehrenreich, A., Assmus, B., Schink, B., 1993. Ferrous Iron Oxidation by Anoxygenic Phototrophic Bacteria. Nature 362 (6423), 834–836.

Wiederhold, J.G., Cramer, C.J., Daniel, K., Infante, I., Bourdon, B., and Kretzschmar, R. (2010). Equilibrium Mercury Isotope Fractionation between Dissolved Hg(II) Species and Thiol-Bound Hg. Environ. Sci. Technol. *44*, 4191–4197.

Xia K., Skyllberg U. L., Bleam W. F., Bloom P. R., Nater E. A. and Helmke P. A. (1999) X-ray Absorption Spectroscopic Evidence for the Complexation of Hg(II) by Reduced Sulfur in Soil Humic Substances. *Environ. Sci. Technol.* 33, 257–261.

Yamamoto M. (1995) Possible mechanism of elemental mercury oxidation in the presence of SH compounds in aqueous solution. *Chemosphere* 31, 2791–2798.

Yamamoto M. (1996) Stimulation of elemental mercury oxidation in the presence of chloride ion in aquatic environments. *Chemosphere* 32, 1217–1224.

Yamamoto, M., Hou, H., Nakamura, K., Yasutake, A., Fujisaki, T., and Nakano, A. (1995). Stimulation of elemental mercury oxidation by SH compounds. Bulletin of Environmental Contamination and Toxicology *54*, 409–413.

Zhang H., Lindberg S. E., Marsik F. J. and Keeler G. J. (2001) Mercury air/surface exchange kinetics of background soils of the Tahquamenon River watershed in the Michigan Upper Peninsula. *Water Air Soil Poll.* 126, 151–169.

Zhang, T., Kim, B., Leyard, C., Reinsch, B.C., Lowry, G.V., Deshusses, M.A., and Hsu-Kim, H. (2012). Methylation of Mercury by Bacteria Exposed to Dissolved, Nanoparticulate, and Microparticulate Mercuric Sulfides. Environ. Sci. Technol. *46*, 6950–6958.

Zheng, W., and Hintelmann, H. (2010a). Nuclear Field Shift Effect in Isotope Fractionation of Mercury during Abiotic Reduction in the Absence of Light. Journal of Physical Chemistry A *114*, 4238–4245.

Zheng, W., and Hintelmann, H. (2010b). Isotope Fractionation of Mercury during Its Photochemical Reduction by Low-Molecular-Weight Organic Compounds. J. Phys. Chem. A *114*, 4246–4253.

Zheng, W., Foucher, D., and Hintelmann, H. (2007). Mercury isotope fractionation during volatilization of Hg(0) from solution into the gas phase. Journal of Analytical Atomic Spectrometry *22*, 1097–1104.

Zheng, W., Liang, L., and Gu, B. (2012). Mercury Reduction and Oxidation by Reduced Natural Organic Matter in Anoxic Environments. Environ. Sci. Technol. *46*, 292–299.

Zink, S., Schoenberg, R., and Staubwasser, M. (2010). Isotopic fractionation and reaction kinetics between Cr(III) and Cr(VI) in aqueous media. Geochimica Et Cosmochimica Acta *74*, 5729–5745.